Light Water Reactor Sustainability Program

Demonstration of External Hazards Analysis

Carlo Parisi
Steven R Prescott
Ronaldo H Szilard
Justin L Coleman
Robert E Spears
Abhinav Gupta

July 2016

U.S. Department of Energy Office of Nuclear Energy

Light Water Reactor Sustainability Program

Demonstration of External Hazards Analysis

Carlo Parisi
Steven R Prescott
Ronaldo H Szilard
Justin L Coleman
Robert E Spears
Abinav Gupta

July 2016

Idaho National Laboratory
Idaho Falls, Idaho 83415

http://www.inl.gov

EXECUTIVE SUMMARY

The scope of this Light Water Reactor Sustainability Risk-Informed Safety Margin Characterization (LWRS-RISMC) industry application task is to perform an advanced risk analysis of accident events at a nuclear power plant caused by a combination of natural external hazards, i.e. earthquake and flooding. A combined deterministic and probabilistic methodology is applied to a realistic nuclear power plant model of a Pressurized Water Reactor (PWR).

The rationale for these activities, the RISMC methodology, and the industry application baseline toolkit are developed for this demonstration. The initial results of a combined deterministic-probabilistic analysis of an earthquake-induced Station Black-Out (SBO) scenario with internal flooding for a generic PWR are shown.

These results are obtained by coupling a set of state-of-the-art tools and by developing realistic models of the Nuclear Power Plant (NPP) and of its Structure, Systems and Components (SSCs).

The following analyses are performed:

- Earthquake propagation and Non-Linear Soil-Structure Interaction

- Determination of the Response Spectra for the NPP Auxiliary Building and for the sprinkler system

- Determination of the earthquake-induced stresses on the sprinkler system

- Deterministic flooding analysis of the battery rooms

- Long-Term SBO and Short-Term SBO system thermal-hydraulic analyses (bounding events)

- Uncertainty Quantification for the Long-Term and Short-Term SBO scenarios, determination of Figure-of-Merits and of relevant independent variables

- Integration of the structural mechanics, flooding and system thermal-hydraulic calculations in a dynamic Probabilistic Risk Assessment (PRA) model

With the above formulation, one of several PRA-determined SBO scenarios is analyzed.

This initial demonstration shows the capabilities of the baseline RISMC toolkit and better quantification of the safety margins of the analyzed nuclear power plant model.

ACKNOWLEDGMENTS

CONTENTS

FIGURES

TABLES

ACRONYMS

3D	Three Dimensional
AC	Alternating Current
AFW	Auxiliary Feed-Water
A-SPRA	Advanced Seismic PRA
ATWS	Anticipated Transients Without Scram
BDBA	Beyond Design Basis Accident
BEPU	Best Estimate Plus Uncertainty
BOP	Balance of Plant
BWR	Boiling Water Reactor
CCW	Component Cooling Water System
CDF	Core Damage Frequency
CFR	Code of Federal Regulation
CHF	Critical Heat Flux
CSAU	Code Scaling, Applicability and Uncertainty Evaluation
CST	Condensate Storage Tank
DBA	Design Basis Accident
DC	Direct Current
DG	Diesel Generator
DOE	Department of Energy
DNB	Departure from Nuclear Boiling
ECC	Emergency Core Cooling
ECCS	Emergency Core Cooling System
ECST	Emergency Condensate Storage Tank
EE	External Events
EEVE-A	External Events Project – Advanced
EEVE-B	External Events Project – Baseline
EDG	Emergency Diesel Generator
EPRI	Electric Power Research Institute
EQ	Earthquake
ESF	Engineered Safeguards

FOM	Figure Of Merit
FSF	Fundamental Safety Functions
FTE	Full Time Equivalent
FY	Fiscal Year
HPC	High Performance Computing
HPI	High Pressure Injection
HPIS	High Pressure Injection System
IA2	Industry Application 2
IGBWR	INL Generic BWR
IGPWR	INL Generic PWR
INL	Idaho National Laboratory
LB-LOCA	Large Break LOCA
LOCA	Loss of Coolant Accident
LOOP	Loss Of Offsite Power
LPIS	Low Pressure Injection System
LTSBO	Long Term Station Black-Out
LWR	Light Water Reactor
LWRS	Light Water Reactor Sustainability
MCC	Main Circulation Circuit
MCP	Main Coolant Pump
MFW	Main Feed-Water
MOOSE	Multi-Physics Object-Oriented Simulation Environment
MSIV	Main Steam Isolation Valve
MSLB	Main Steam Line Break
NC	Natural Circulation
NLSSI	Non-linear Soil-Structure Interaction
NPP	Nuclear Power Plant
NRC	Nuclear Regulatory Commission
NUREG	Nuclear Regulatory Report
PCT	Peak Clad Temperature
PIRT	Phenomena Identification and Ranking Table
PORV	Pilot-Operated Relief Valve
PRA	Probabilistic Risk Assessment

PRZ	Pressurizer
PWR	Pressurized Water Reactor
RA	Risk Assessment
RAVEN	Risk Analysis and Virtual Control Environment
RCP	Reactor Coolant Pump
RCS	Reactor Cooling System
R&D	Research and Development
RELAP5-3D	Reactor Excursion and Leak Analysis Program 5 – 3D
RHR	Residual Heat Removal System
RIMM	Risk-Informed Margin Management
RISMC	Risk Informed Safety Margin Characterization
ROM	Reduced Order Model
RPV	Reactor Pressure Vessel
RWST	Refueling Water Storage Tank
TAF	Top of Active Fuel
TD-AFW	Turbine Driven AFW
TH	Thermal-Hydraulics
SA	Severe Accident
SBO	Station Black-Out
SG	Steam Generator
SOARCA	State-Of-the-Art Reactor Consequence Analyses
SPH	Smooth Particle Hydrodynamics
SPRA	Seismic PRA
SRV	Steam Relief Valve
SSCs	Structures, Systems, and Components
SSI	Soil-Structure Interaction
STSBO	Short Term Station Black-Out
SV	Safety Valve
TH	Thermal-hydraulic
UP	Upper Plenum
UQ	Uncertainty Quantification
US	United States

1. INTRODUCTION

1.1   Background

Design of nuclear power plant (NPP) facilities to resist external hazards has been a part of the regulatory process since the beginning of the NPP industry in the United States (US), but has evolved substantially over time. The original set of approaches and methods were entirely deterministic in nature and focused on a traditional engineering margins-based approach. In this approach, design is undertaken for each structure, system, and component (SSC) individually based on achieving a capacity that is expected to provide a minimum margin over some specific design load of interest. Neither the risk significance of the SSC nor its role within the facility is considered. The traditional approach also does not account for operator action, redundancy and other risk-related element.

Deterministic and probabilistic approaches were developed and included over time by the US Nuclear Regulatory Commission (US NRC) in its guidance and regulation. In response to the 2011 Fukushima nuclear accident in Japan, new emphasis has been put on severe accidents studies and on the risk assessment of scenarios involving extreme external events (e.g., see Fukushima NTTF recommendations, [1]).

Although the US regulatory framework has continued to evolve over time, the tools, methods and data available to the US nuclear industry to meet the changing requirements have largely remained static. Notably, there is room for improvement in the tools and methods available for external event probabilistic risk assessment (PRA), which is the principal assessment approach used in risk-informed regulations and risk-informed decision-making [2]. This is particularly true if PRA is applied to natural hazards other than seismic loading.

Development of a new set of tools and methods that incorporate current knowledge, modern best practice, and state-of-the-art computational resources would lead to more reliable assessment of facility risk and risk insights (e.g., the SSCs and accident sequences that are most risk-significant), with less uncertainty, and reduced potential conservatisms. New tools would also benefit risk-informed approaches to assessing and managing margin. In the framework of the US-DOE Light Water Reactor Sustainability (LWRS) program, a research effort for developing advanced tools, data and methods has been launched. The ongoing activities are part of the LWRS-Risk Informed Margin Characterization (RISMC) program, [3]. In particular, activities devoted to the study of external events are part of the Industry Application 2 (IA2) [4].

A brief description of the LWRS/RISMC approach is provided in Section 1 of this document (see below). Section 2 describes the IA2 problem, including methods, tools, data and scenarios. Section 3 presents the demo of the IA2 analysis, reporting seismic, flooding, PRA, thermal-hydraulic (TH) and uncertainty quantification (UQ) results. Section 4 reports the results of one set of coupled codes calculations. Section 5 outlines the path forward for the IA2.

1.2   The Risk-Informed Margin Management (RIMM) Approach

The new tools and methods being developed have a number of applications that support the nuclear industry including, a risk-informed margins management approach. The key-point of RIMM approach is that it will calculate risk by considering all applicable external hazards together (as shown on the right side of Figure 1). Instead the current approach calculates separately the risk from external hazards.

The focus on RIMM provides a technical basis to understand and manage hazards. At a nuclear facility, a hazard is a condition that is or causes a deviation in normal operation.

Examples of the types of hazards that may exist at a nuclear power plant (NPP) include different types of kinetic energy (e.g., motion from a seismic event, from tornado winds, etc.) and potential energy (e.g., energy release by shorted equipment during a flood). These types of hazards complicate the determination of safety in any complex facility. However, in IA2, we propose advanced methods to represent these potential impacts to safety by developing the technology to incorporate physics (via probabilistic and mechanistic modeling) into scenarios (see Section 2 of this report).

Evolution of Nuclear Power Plant External Hazards Risk Assessment and Management
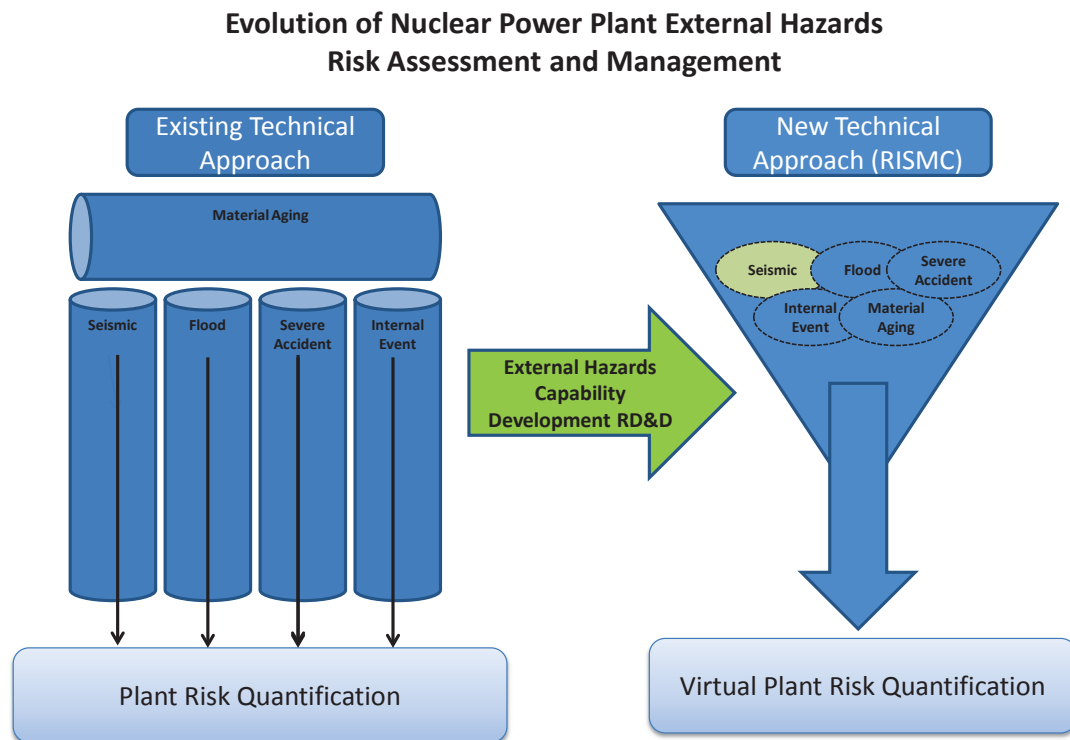
Figure 1   – Current Risk Calculation Approach that Generally Considers External Hazards in a Silo versus the Advanced RIMM Approach that Considers External Hazards Together. [4]

2.   INDUSTRY APPLICATION PROBLEM DEFINITION

Over the past years, a series of US NRC documents, e.g. [1], [2], recommended to move NPP safety evaluations towards the so-called "Risk Informed" policies. Moreover, a new reevaluation of the external hazards was requested before [5] and after the Fukushima accident [1], [6]. The review of the activities performed so far has highlighted a large number of technical challenges and shortcomings in the current set of tools and methods available for assessment of NPP safety in light of natural hazards.

Therefore, improved tools and methods have to be developed. These could be beneficial for the nuclear industry and for the safety authority by better demonstrating NPP safety and increasing regulatory assurance.

2.1   Goal

The scope of LWRS-RISMC IA2 is to perform an advanced risk analysis of accidental events caused at a NPP by a combination of natural external hazards, i.e. earthquake and flooding [4]. Therefore combined deterministic and probabilistic methods have to be developed and applied to a realistic NPP model of a PWR and of a BWR.

For achieving such goal, two detailed roadmaps (a baseline and an advanced) have been identified [7]. The so-called EEVE-A and EEVE-B projects (External EVEnts - Advanced/Baseline) and their respective tools are shown in Figure 2.
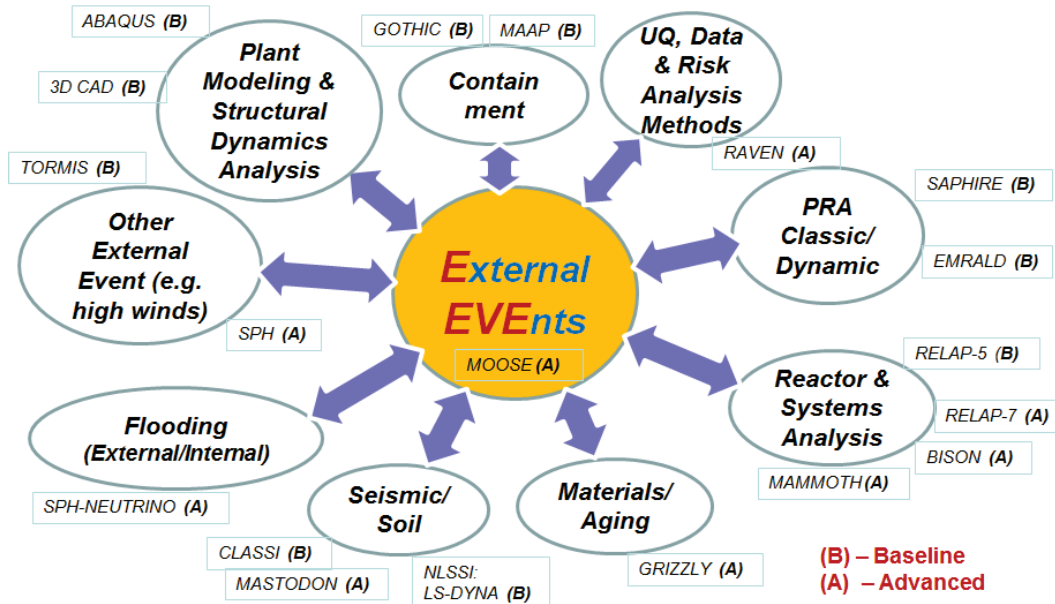
Figure 2 – Schematic illustration of EEVE-A and EEVE-B. [7]

2.2   Methods and Tools Definition

2.2.1   Methodology

This section includes a brief discussion on the types of tools and methods used for simulating soil, structures (containment and auxiliary buildings), nuclear island and the Balance of Plant (BOP), internal flooding, and PRA. The seismically induced flooding demonstration includes the following:

- Effects of an EQ on a NPP and on corresponding SSCs (System, Structure, Component) using advanced non-linear soil-structure interaction (NLSSI) analysis and including NLSSI in seismic probabilistic risk analysis (SPRA). The NLSSI analysis includes two nonlinear effects: 1) soil nonlinearity, and 2) gapping and sliding. The EQ is propagated through a heterogeneous soil site and into the relevant buildings. The accelerations are then input into a secondary piping analysis that calculates stresses and strains and thus if a pipe is significantly cracked. The NLSSI analysis is performed using LS-DYNA [8] and the secondary piping analysis uses OPENSEES [9]. LS-DYNA is a commercially available finite element code that performs both implicit and explicit finite element analysis. LS-DYNA explicit is used for the NLSSI analysis. OPENSEES is an open source finite element analysis code and has capability to simulate nonlinear moment curvature piping analysis. OPENSEES is used for the piping analysis.

- NPP flooding scenario caused by EQ-induced pipe rupture. This part of the analysis is performed using the SPH-based NEUTRINO code [10]. After locating the possible pipeline breaks by combining the fragility curves and the seismic loads, a flooding analysis is performed taking into account the three-dimensional (3D) configuration of the flooded room and the positions of the selected SSC. The SSC possible faults are determined depending on the type/position of the break.

- NPP dynamic by a system thermal-hydraulic (TH) code (RELAP5-3D [11]). A Station Black Out (SBO) scenario is assumed (total loss of onsite and offsite AC power). Simulation of a PWR primary circuit and of part of BOP. The timing and the type of faults are determined by the combined deterministic-PRA analysis driven by EMRALD code (see below). The figure of merit (FOM) that is being considered by RELAP5-3D is the core peak clad temperature (PCT);

- S/U analysis. The effects of different input uncertainty parameters are addressed in order to evaluate a realistic safety margins. For S/U analysis of the RELAP5-3D model, RAVEN tool [12] is used. The first step is to identify the different phenomena happening during a SBO scenario. Then, relevant parameters and their uncertainty distribution are selected. The uncertainties are then propagated through the code using forward samplers like Monte Carlo, grid based, etc.

- For the PRA part, an event tree for the SBO scenario is developed. EMRALD tool [13] is used for performing dynamic PRA. The code is coupled to NEUTRINO for investigating the different patterns of flooding and to RELAP5-3D for investigating the final core damage frequency (CDF).

The tools identified for the IA2 analysis are provided in the Table 1.

Table 1 – Tools for the analysis

Tools	Task
LS-DYNA	EQ Analysis
OPENSEES	Piping Analysis
NEUTRINO	3D Flooding Simulation
EMRALD	Dynamic PRA
RELAP5-3D	System TH
RAVEN	S/U for RELAP5-3D sim.

The workflow of the IA2 analysis and tools is provided in Figure 3.
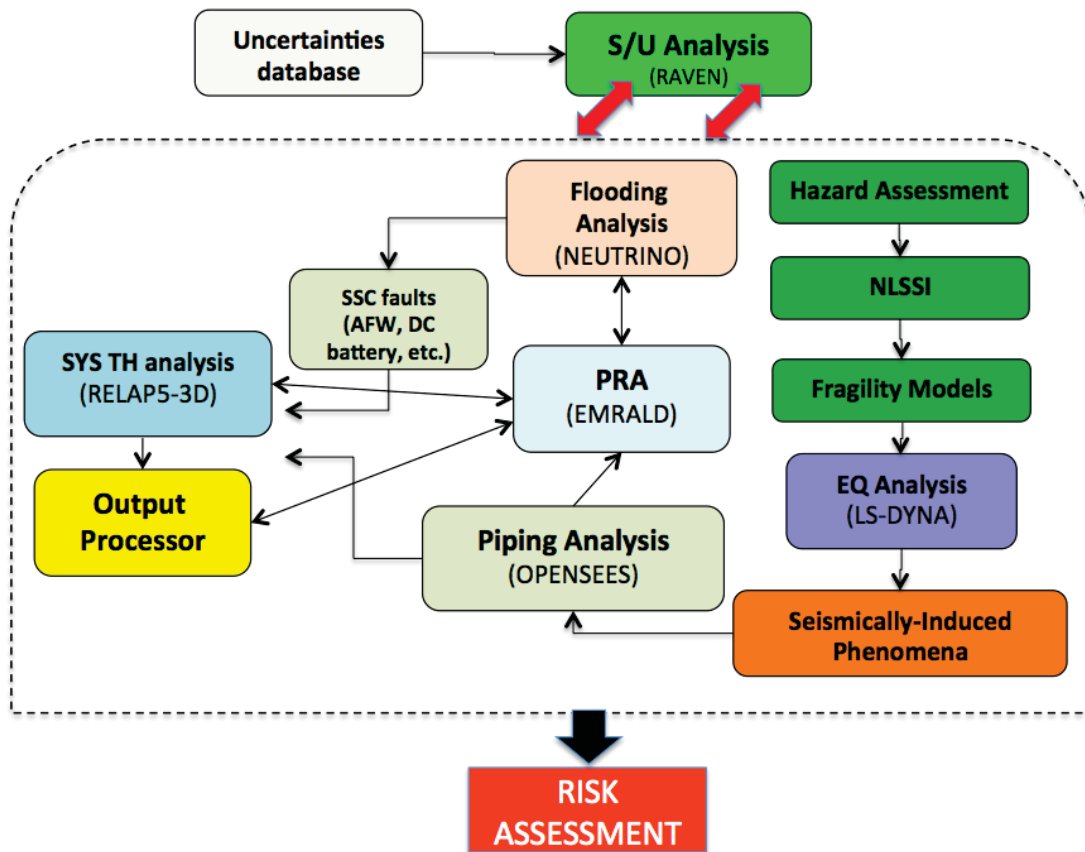
Figure 3 – Workflow and tools for IA2.

2.2.2   Structural Mechanics Tools

LS-DYNA is a commercially available finite element code that performs both implicit and explicit finite element analysis. LS-DYNA explicit is used for the NLSSI analysis. OPENSEES is an open source finite element analysis code and has capability to simulate nonlinear moment curvature piping analysis. OPENSEES is used for the piping analysis.

2.2.3   Flooding Analysis Tool

Physics based simulation tools can be used to predict the behavior of water in a 3D environment. For this demonstration, NEUTRINO was used because of its advanced tool set and capabilities develop for other similar simulation tasks. The NEUTRINO software uses an IISPH solve engine which is faster than many similar tools, and still acceptably accurate. An advanced "Z Sorted Compact Hashing" method is used to accomplish quick nearest neighbor lookup when computing particle interactions [18].
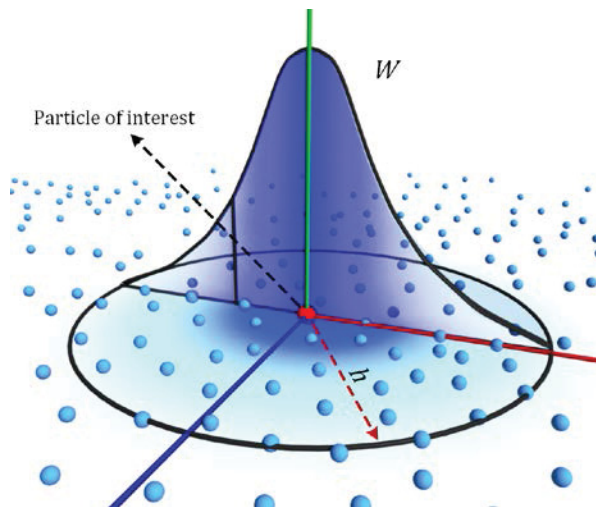
Figure 4 – Illustration of the SPH interpolation. W denotes a Gaussian-like shape kernel function and h is the support radius.

The setup for these simulations consists of a 3D polygon model of a floor of the facility. The model contains the room layouts and several critical components that are susceptible to water damage, including four battery units, two 4kV switchgear units, two 125V DC distribution panels and four UPS units. Dynamic particle emitters are used to simulate a rupture from the water based fire suppression system. The simulation monitors fluid interaction with the rigid bodies and component measurement fields, if a component's failure criteria are met, a failure message is sent to the parent application. Water contact, height, and pressure can be used as criteria for failure.
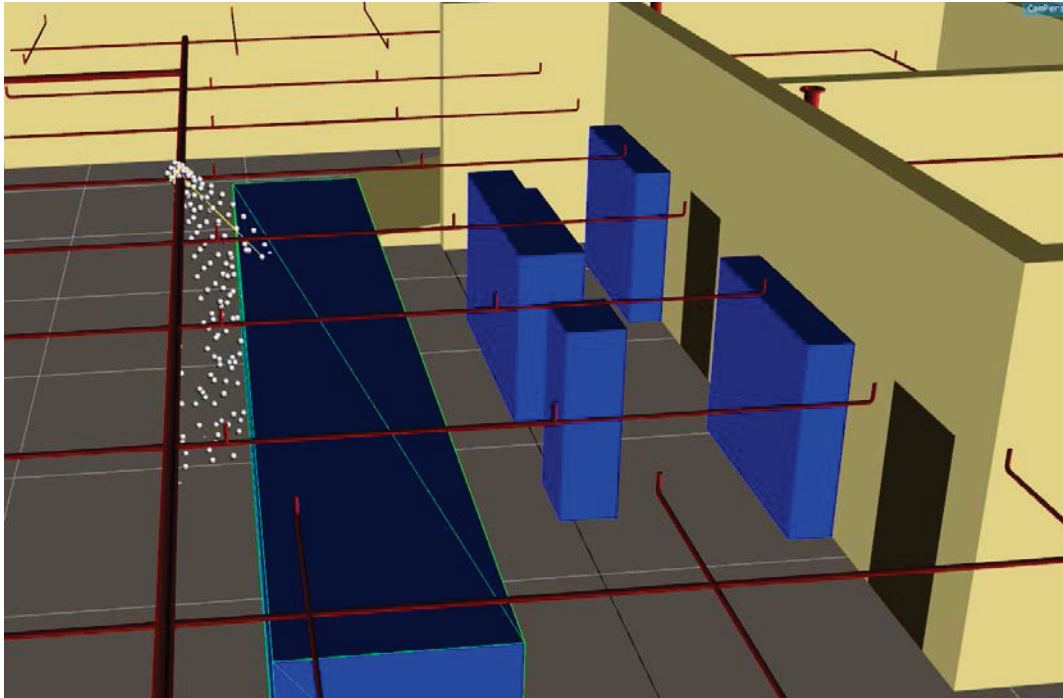
Figure 5 – Example of pipe fracture using NEUTRINO.

2.2.4   PRA Tools

Two PRA tools are used for this demonstration. First, SAPHIRE is a traditional PRA modeling tool using of Basic Events, Fault Trees and Event Trees. These models can determine the failure probability for complex system but they are static, not able to deal with changes over time. Initial scoping system modeling was done in SAPHIRE to represent the component dependencies and failure rates.
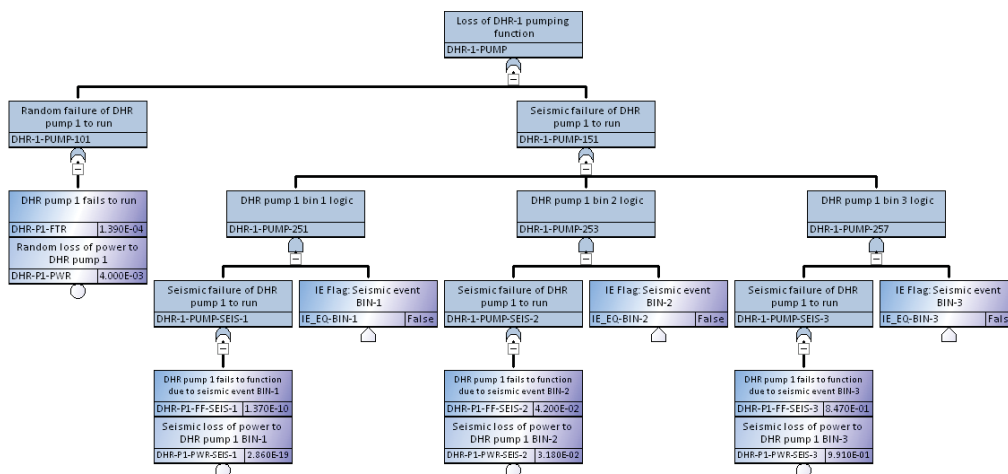
Figure 6 – An Example of a Fault Tree for a Pump with Affected by Several Failure Methods Including Seismically Induced Failures.

The second, EMRALD, is a state-based code for discrete event simulation. States in the code include the following.

0. Setup – Add initial start states.
1. If sifted to a new state do the following, else go to step 2.
    a. If terminal state then quit.
    b. Execute the state's immediate actions.
    c. Process the state's event actions by adding conditional events to the lookup list or calculating the next occurrence of a probabilistic item and add it to the next event Que.
2. Execute any conditional events that have their criteria met, go to step 1 if any states changed.
3. Jump to the next event in the chronological event queue and process the events actions. Then go to step 1.
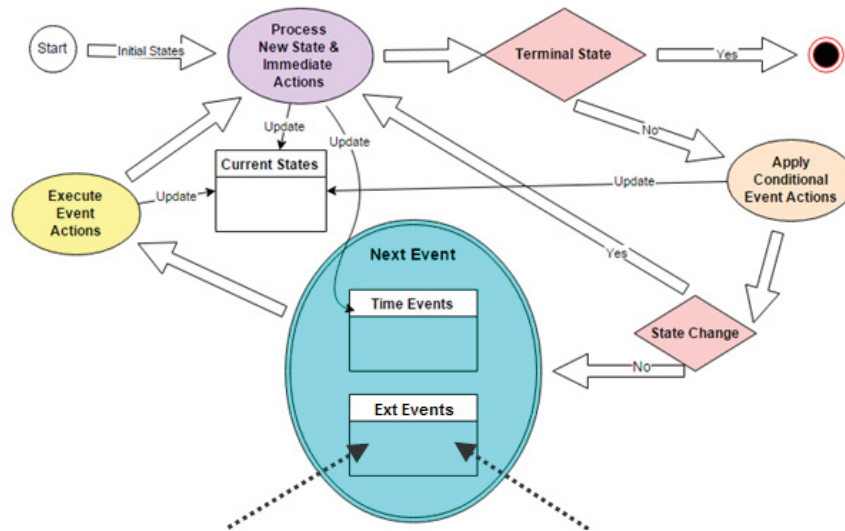
Figure 7 – Flow Diagram for Processing and EMRALD Model.

A model for EMRALD consists of States with immediate actions, and conditional event actions. Many different types of events and actions can be evaluated or executed, designed in a way for easy equivalents to items in traditional PRA such as basic events and fault trees. States can also be tagged as "key states" and are noted if a simulation run ends on that state. Through multiple runs of the simulation model, probabilities of each key state are derived, these are similar to end states results in SAPHIRE. In addition, heuristics can be made to show the path or cause of the key state and the times of those events. Some traditional PRA models can be converted into an equivalent EMRALD model with statistically equivalent results [13].
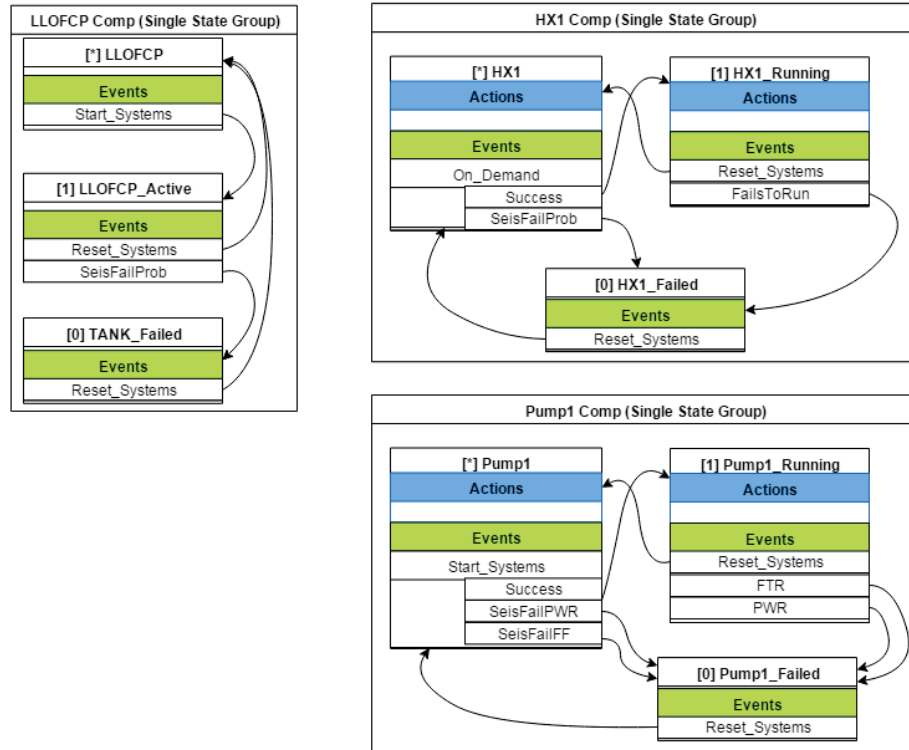
Figure 8 – Example of EMRALD State Diagrams for Several Components and their State Changes.

In addition to the dynamic PRA, EMRALD is being used to couple the PRA with the piping failure analysis, the flooding simulation, and the RELAP5-3D simulations for this demonstration. Because it is time based, it can be coupled with other time based simulation methods. User defined and other specialized events and actions allow it to input and select defined piping failures, read component failures from NEUTRINO, and run RELAP5-3D then retrieve its results; using the data from the various tools to determine a final answer. See section 4 for more details on EMRALD calling other analysis methods.

2.2.5   System Thermal-hydraulic Tool

The system TH code RELAP5-3D is used for analyzing the dynamic of the primary and secondary side parameters of a NPP. RELAP5-3D is capable of performing best-estimate transient simulations of LWR coolant systems during normal and accidental conditions (LOCA, ATWS, etc.). One-dimensional and three-dimensional volumes, zero-dimensional components, heat structures and reactor control logics model the reactor coolant systems. NPP is discretized in several hundred/thousand nodes and a two-phase TH solution is achieved for the analyzed transient. The code is capable of analyzing several DBA and BDBA scenarios until the occurring of the fuel clad damage.

The SBO type of transient has been thoroughly analyzed by RELAP5-type codes during the years, e.g. [20], [21], [22]. The sequence of events requires:

- operator actions (e.g., AFW actuation, SG depressurization, feed & bleed, etc.), which can be modeled by the RELAP5-3D control system;

- the detailed description of the primary system components like PRZ, SG and RPV or faults like a MCP seal LOCA (see further).

Transient can be run until clad overheating occurs (2200 F), so calculations should analyze scenario for a period up to ~8-16 hrs., depending of number of failed components. Thus, coping time (i.e. the capability for a certain time to not exceed a safety threshold, e.g. fuel clad temperature limit) can be evaluated. After clad/fuel failures, severe accident codes like MAAP [23] or RELAP/SCDAP [24] are needed for continuing the analysis in the Emergency Response domain (see Figure 9).
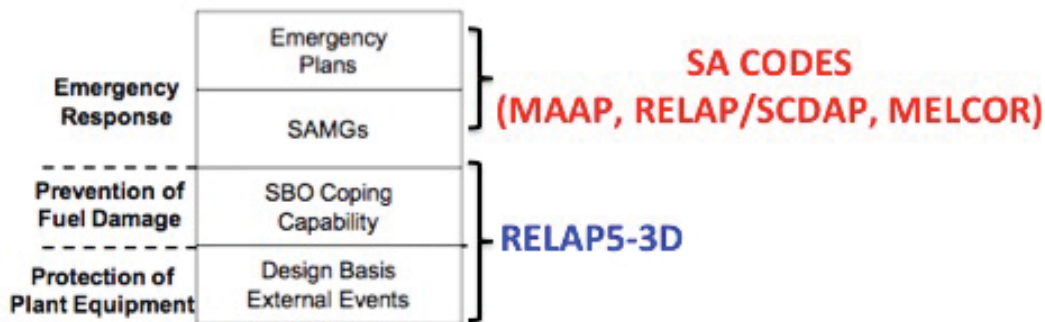
Figure 9 – RELAP5-3D role in SBO-BDBA calculations.

2.2.6   Sensitivity Uncertainty Tool

Sensitivity/uncertainty analysis is performed by coupling RELAP5-3D system TH code to the RAVEN code. RAVEN code is a generic software framework to perform parametric and probabilistic analysis based on the response of complex system codes. RAVEN is coupled to RELAP5-3D via a special software interface, which allows the analyst to perform input space sampling using Monte Carlo, Grid or Latin Hyper Cube sampling schemes. RAVEN has the capability to run on HPC, which allows the execution of hundreds of parallel serial runs for uncertainty propagations.

For IA2, RELAP5-3D relevant input parameters and their uncertainty distributions are selected, considering the main phases (e.g. reactor scram, SG depressurization, etc.) and the main phenomena involved during a SBO scenario (e.g., natural circulation in the RCS, critical flow on PRZ and SG PORV/SRV, heat transfer in the SGs).

The effect of the variation of these parameters (independent variables) on the RELAP5-3D output (dependent variable, in this case the clad temperature) will then be assessed, providing an indication of the calculation uncertainty.

2.3   Scenario Description

As described earlier, many external events can cause multiple hazards over duration of time. This scenario demonstrates a possible relation between a seismic event and internal flooding caused by fractures in the water based fire suppression system from that seismic event. Several different tools are used to evaluate the flow and effects of events through the facility. For this demonstration we will test each of the areas by forcing one specific sequence of events through the set of codes. In a subsequent report multiple runs will be used to calculate a probability of fuel damage.

2.3.1   Seismic Event

Sampling of a seismic event begins the evaluation process. The EMRALD model samples for various levels of an earthquake. This information is then used in two areas. First, the example site seismic analysis and piping simulation failure data, described in Section 2.2, is used to sample on internal piping failures. This piping failure model determines if there are any leaks to cause internal flooding. Second the sampled seismic event is used to determine LOOP and probabilistic sampling of susceptible component failures.

2.3.2   Internal Flooding

If the seismic event is preceded by pipe failure, then NEUTRINO us used to simulate this internal flooding. Component failures detected from the flooding simulation are returned throughout the simulation to EMRALD.

2.3.3   Cooling Systems

If in a state of SBO, the component failures directly caused by the seismic event and proceeding flooding failures are used to execute RELAP5-3D. RELAP5-3D then simulates the cooling systems and determines the temperature/failure of the fuel. These results are then logged by EMRALD for the given run of the simulation.

3.   ANALYSIS DEMONSTRATION

To model an initiating earthquake it is important to consider nonlinear effects that will potential change the response of SSCs. Two specific effects modeled are cyclic soil nonlinearity and gapping and sliding

Physics based simulation tools can be used to predict 3D NLSSI behavior of an EQ on a NPP. For this demonstration, LS-DYNA was used because of its nonlinear soil modeling capabilities and its ability to efficiently solve large finite element problems. Figure 10 to Figure 21 show the finite element model used to perform the NLSSI analysis. The full model (shown in Figure 10) consists of 766 beam elements, 3128 shell elements, and 1,492,000 solid elements.

3.1   Seismic

The soil (shown in Figure 11) consists of 37 nonlinear layers with unique material properties. There is an added 38th soil layer at the bottom of the soil that is elastic and used to bring the seismic waves into the model. The bottom of the elastic soil layer has non-reflective boundary conditions and the top of the elastic soil layer has an applied seismic load time history. On the horizontal boundary of all of the soil, constraints are added to mimic an infinite horizontal continuum. The constraints are used to constrain each set of boundary nodes at a given elevation so that they translate the same in all directions. The top surface of the soil is free.
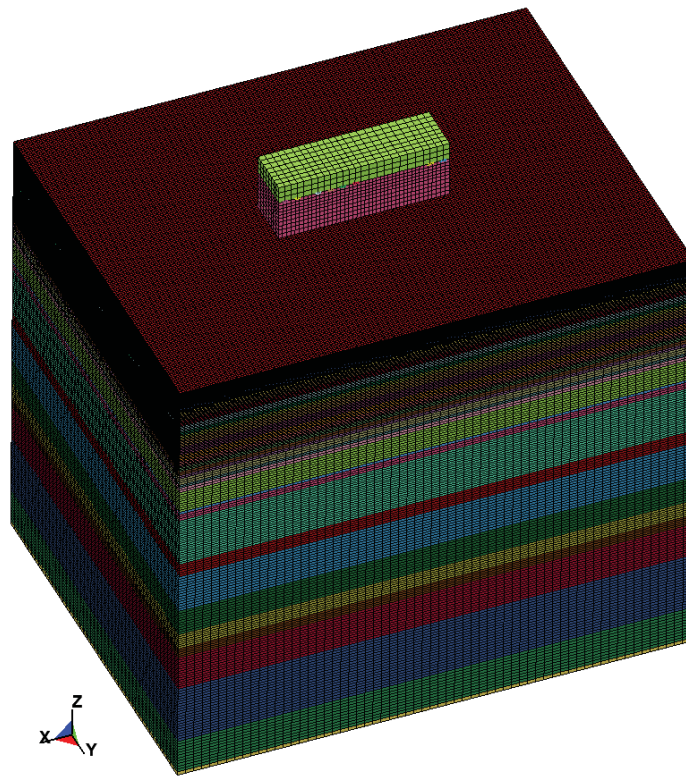
Figure 10 – NLSSI finite element model.

To produce contact between the soil and the structure, elements (shown in Figure 11) are joined to the soil and constrained to the structure. These elements are defined using the nonlinear soil constitutive model with the plastic shear stress set to mimic a 0.5 friction coefficient and a hydrostatic stress dependency set to provide stress free gapping. Defining contact in this manner virtually eliminates contact chatter.
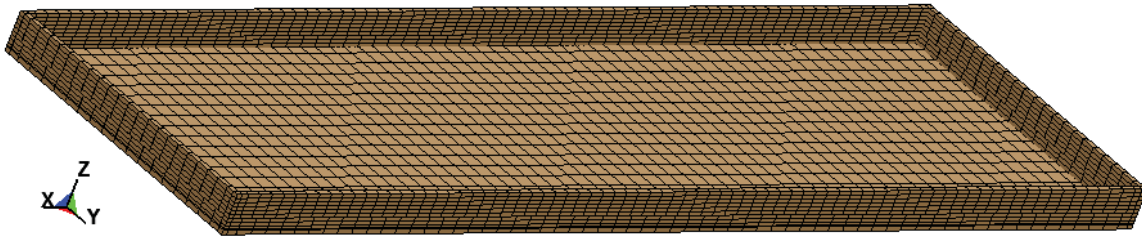
Figure 11 – Elements used for soil-structure contact.

The drawings used to generate the structural are from Figures 3.8-44 to 3.8-46 of the Beaver Valley Power Station – Unit 2, Final Safety Analysis Report [14]. Approximations and simplifications were used to generate a reasonable structural mesh given the available information. The soil layer geometry and material properties are from [15]. The units used in both of these references are feet (or inches), kips, and seconds. Consequently, the finite element model was generated and run with feet, kips, and seconds units. The output acceleration time histories are given in g's. This report is documented in SI units. Consequently, the dimensions given in Figure 12 to Figure 21 are converted to meters.

The soil mesh (shown in Figure 13) is 168 m by 130 m by 149 m with a 2 m deep excavation for the structure. The element sizes are set to pass vertically propagating, planer shear and normal seismic waves up to 50 Hz with at least 10 elements per wavelength. Horizontally, the elements are sized to pass up to 15 Hz reflected waves with at least 10 elements per wavelength. A likely source of horizontal wave propagation is structural rocking and that does not produce significant high frequency content (unless it becomes severe enough to produce impact which can excite all frequencies).

All of the soil elements are rectangular parallelepiped in shape. Consequently, when there is a significant stiffness change between soil layers, the soil layer meshes do not align. To attach these soil layers, tied contact is used.

Rayleigh damping is applied to the soil and structure. The Rayleigh damping in the soil is minimal and is just defined to ensure that some damping occurs even at very low strains. The material properties defined in [15] are adjusted to accommodate the Rayleigh damping. This damping is set so that there is 1% damping at 0.6 Hz and 1/2% at 100 Hz. The structural damping is set to best approximate 4% damping for the frequencies where the structure responds. This damping is set so that there is exactly 4% damping at 5.3 Hz and 15.1 Hz.

The structural mesh (shown in Figure 14 to Figure 21) is 56.1 m by 16.3 m by 21.9 m. It consists of shells and beams with material properties of concrete and steel. The element sizes are based on being small enough to capture the significant structural modes but large enough so that

the model run time step is most influence by the soil elements. Because the steel is much stiffer than the concrete, the mesh size is increased where the steel is present. Some rigid constraints are added to connect the mesh together where the mesh size change causes a mismatch in the mesh. In particular, the rigid elements create a continuous mesh connection (shown in Figure 14) between the 0.152•m thick shells (identified in Figure 16) and the 0.610•m shells (identified in Figure 18).
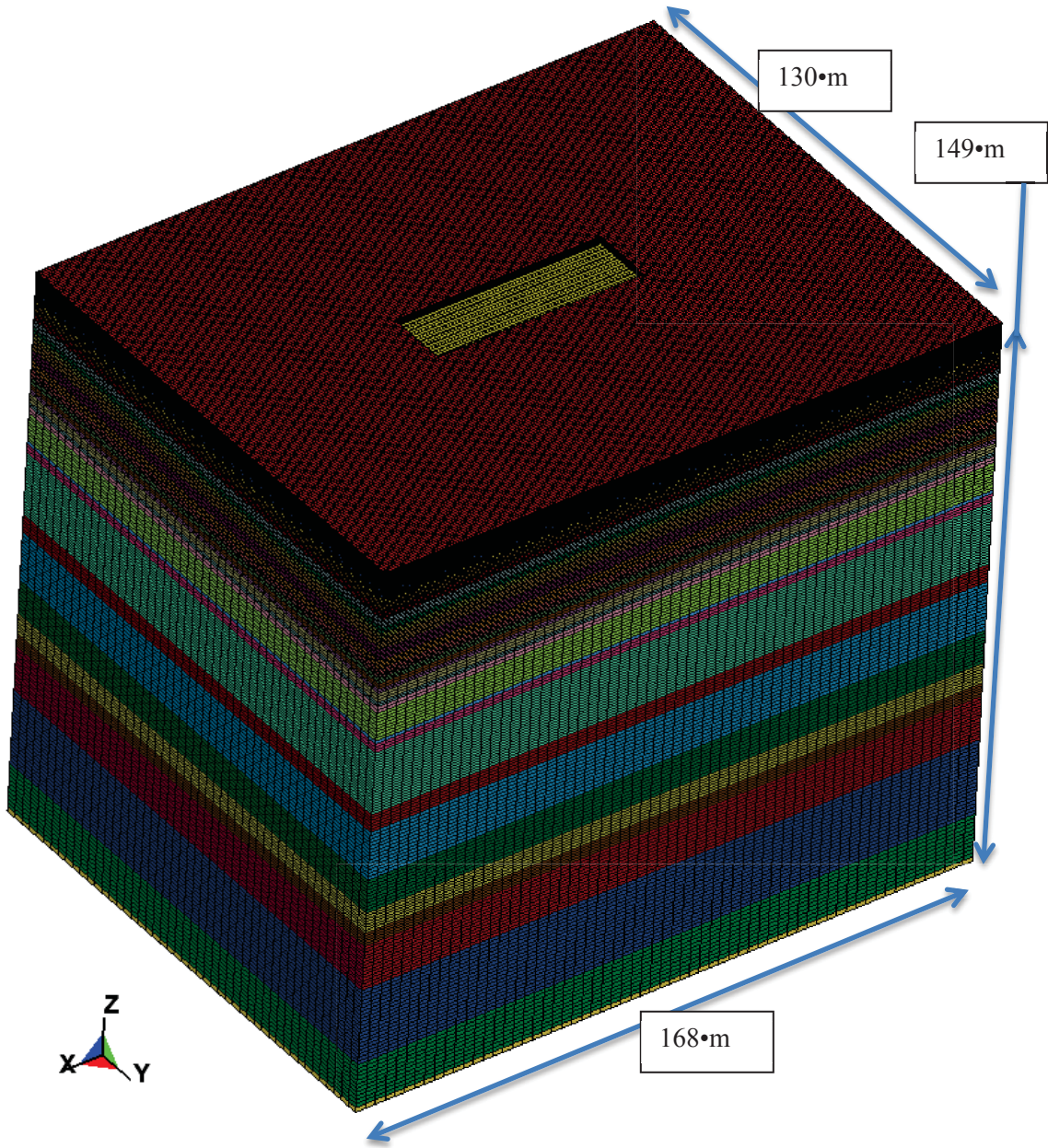
Figure 12 – NLSSI finite element soil mesh.
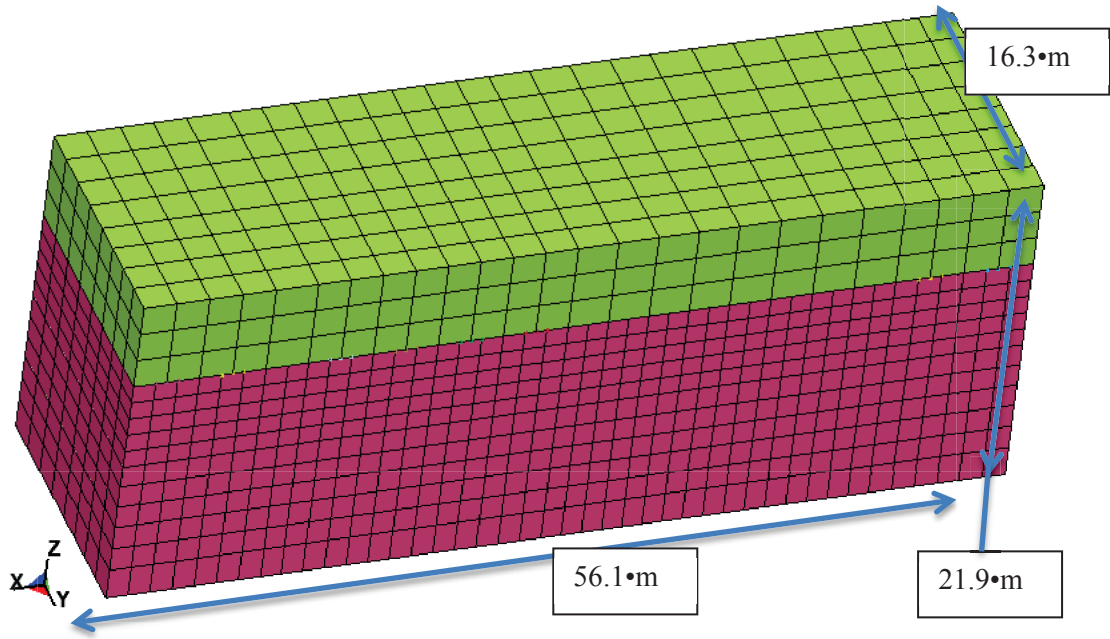
Figure 13 – NLSSI finite element structural mesh.
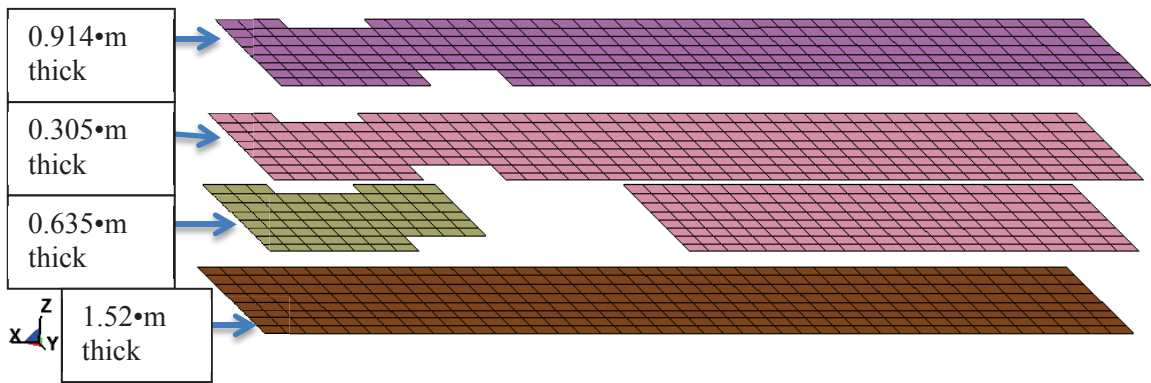
Figure 14 – Concrete shell elements in the floors.
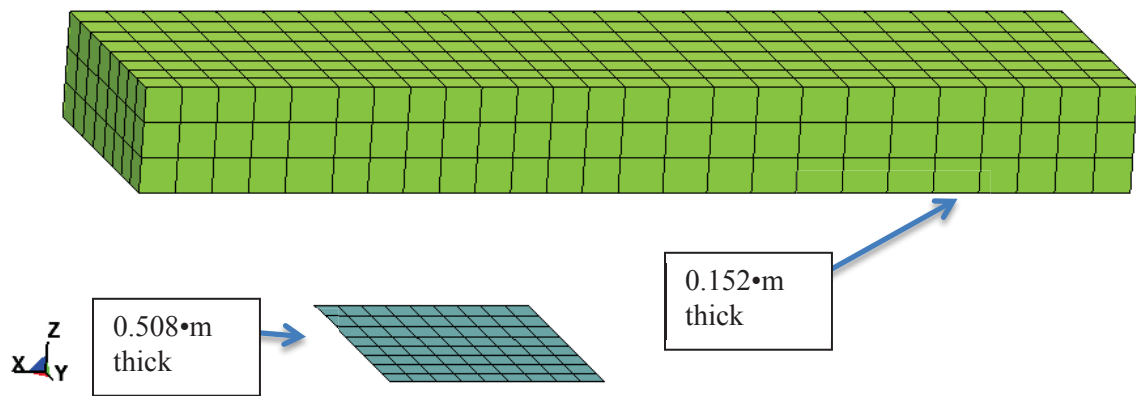
Figure 15 – Concrete shell elements in a floor and roof vicinity.
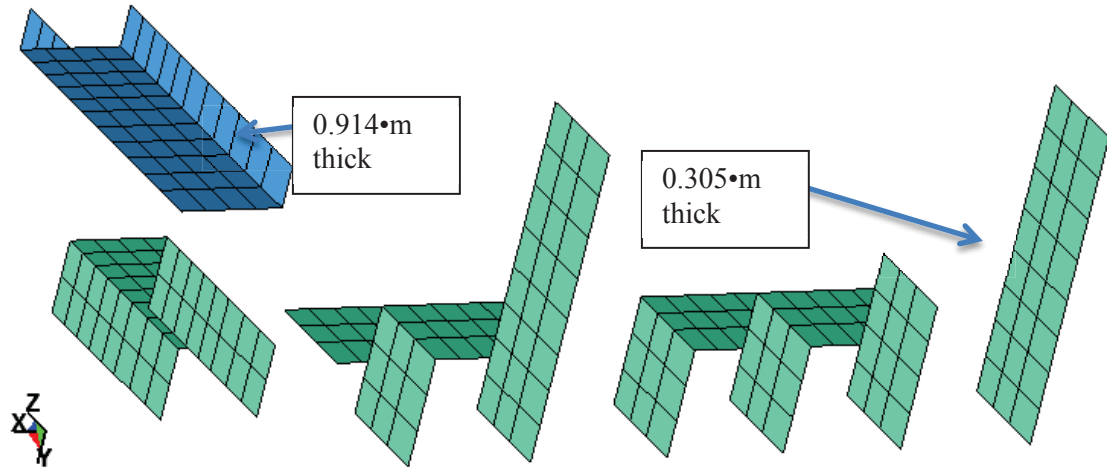
Figure 16 – Concrete shell elements in most of the interior of the walls.
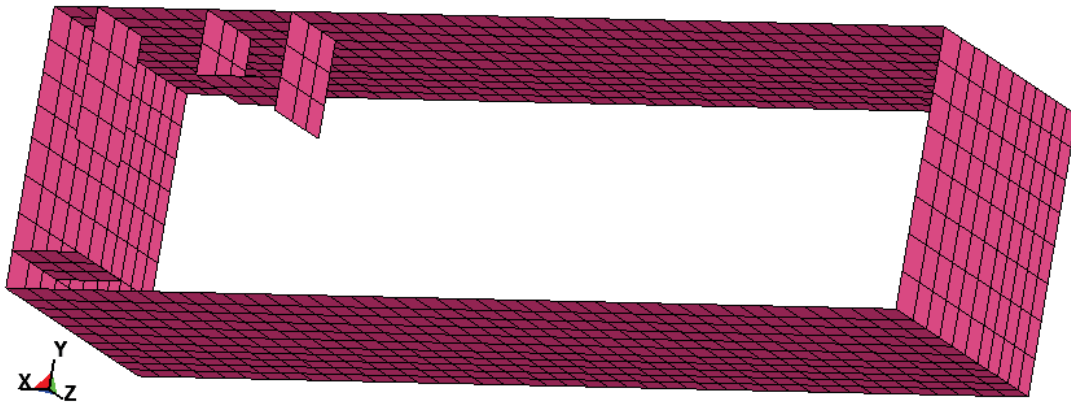
Figure 17 – Concrete shell elements in the 0.610•m walls.
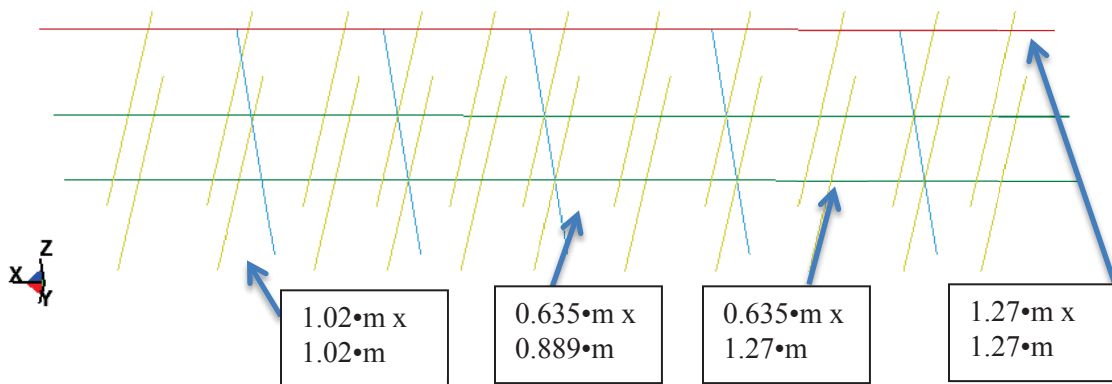
Figure 18 – Concrete beam elements.
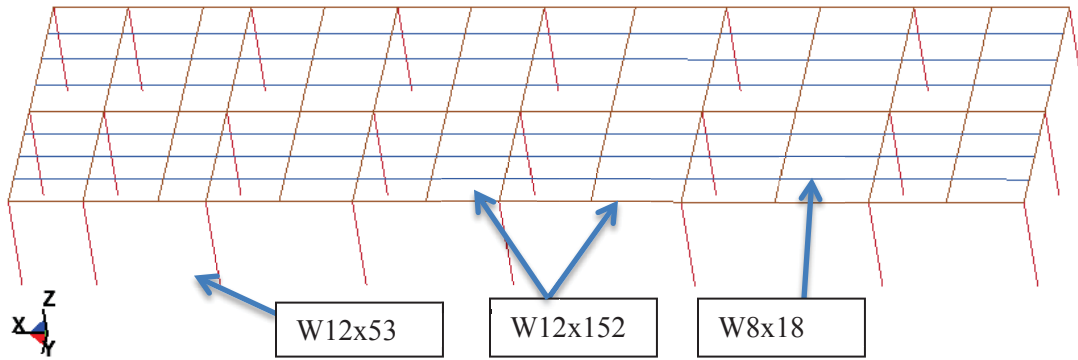
Figure 19 – Steel beam elements.

3.1.1 Seismic results

The initial model run for this finite element model uses the seismic, rock outcrop time histories shown in Figure 21. These time histories are taken from [15]. To produce load time histories applied to the top of the elastic soil layer, the acceleration time histories are integrated to velocity time histories and then scaled with the stiffness and density properties of the elastic soil layer.
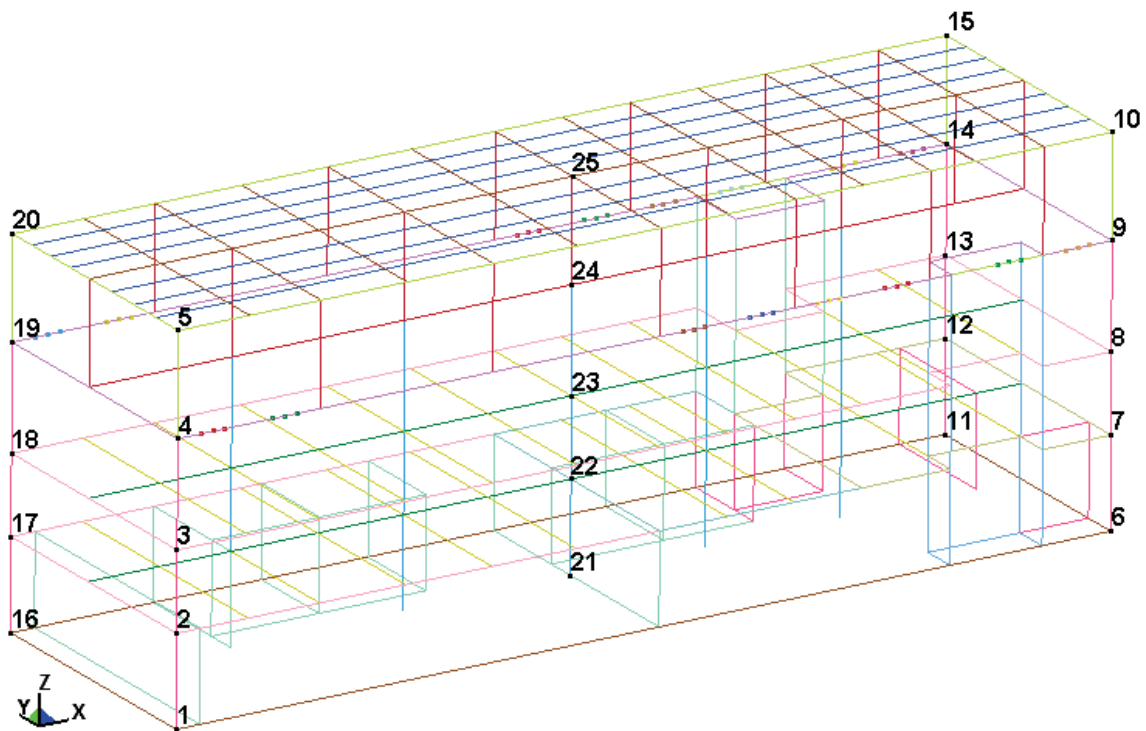
Figure 20 – Structural nodes where output is given.

Acceleration output (Figure 21) is reported for all three translational directions at 25 nodes (as shown in Figure 20). The nodal locations include the corners of each floor and roof and the intersection of the floors and roof with the column nearest the center of the structure.
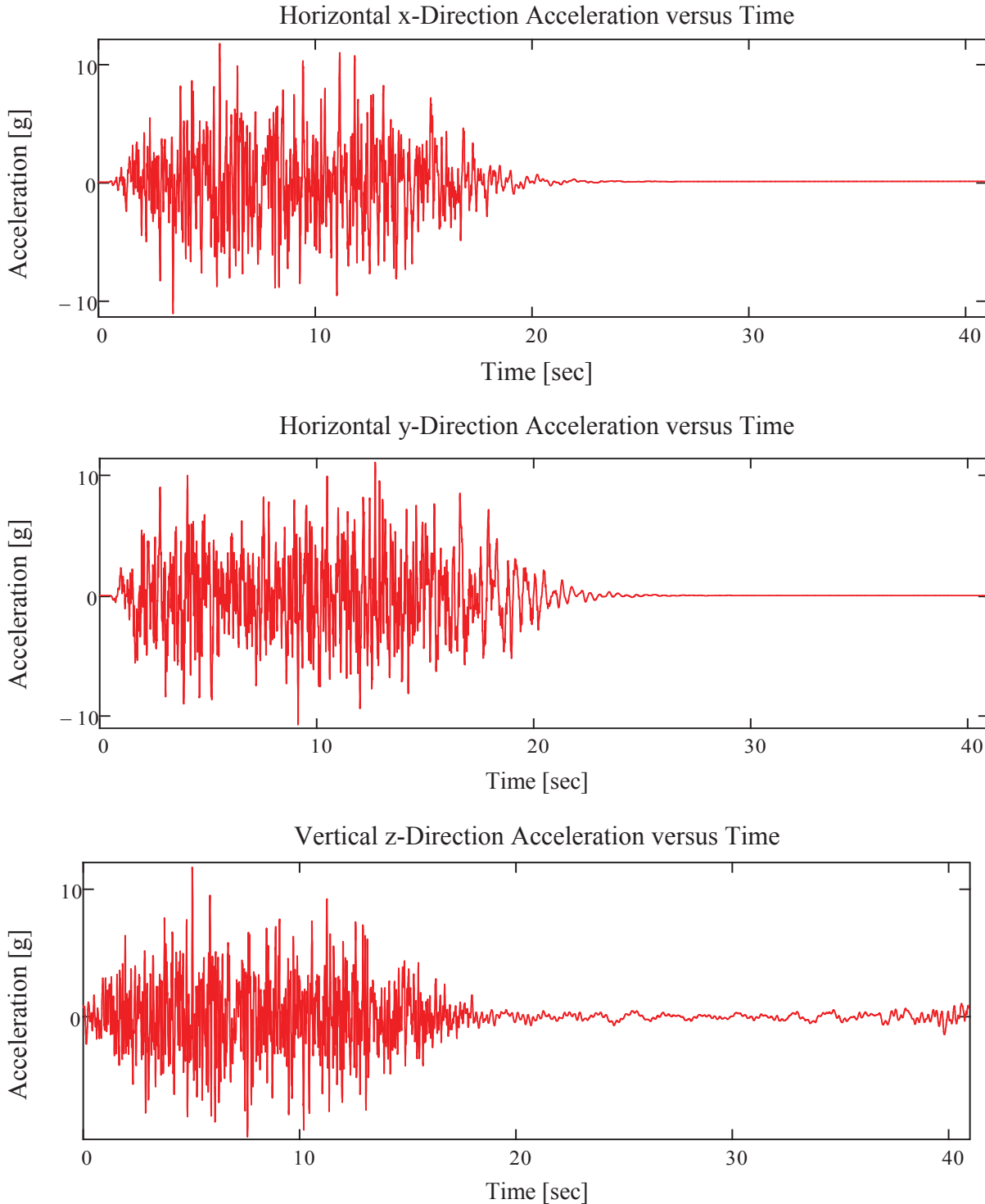
Figure 21 – Horizontal and vertical seismic time histories.

Initial acceleration time history results for nodal location shown in Figure 20 are then passed on to the piping subsystem model as described in Section 3.1.2.

3.1.2   Piping Modeling

3.1.2.1   Introduction

SC Solutions LLC developed a three dimensional (3D) spatial model of the fire suppression system in a sample plant service building. This model was developed to allow evaluation of seismically induced piping failures for assessment of internal flooding scenarios. The spatial model was developed in SolidWorks software.

The spatial model of the building represents two switchgear rooms and adjacent battery rooms in the service building of a representative/generic 3-loop pressurized water reactor (PWR). The switchgear rooms and adjacent battery rooms contain critical and sensitive electrical equipment that provides DC power to safety systems required for safe shutdown following a seismic event. This critical equipment may be affected by either direct spray or water accumulation.

Center for Nuclear Energy Facilities and Structures (CNEFS) at NC State University converted the spatial model of fire suppression system provided by SC Solutions to an analytical nonlinear FE model in Open System for Earthquake Engineering Simulation [9] in order to perform the seismic fragility analysis of the fire suppression system.

A key component of the model is the modeling of the threaded joints as nonlinear rotational springs. The moment -rotation relationships at these joints are available from existing experimental data. Previous research at CNEFS in conjunction with MCEER-Buffalo had focused on conducting experimental tests on piping T-Joint components of different diameters. The T-joints were observed to undergo cyclic degradation in strength and stiffness under cyclic loading.

3.1.2.2   Fire Suppression Piping System

The spatial model for the fire suppression system provided by SC Solutions consisted of piping in the switchgear and battery rooms for the service building. These systems together comprises of 6 inch vertical water supply standpipes, overhead 4-inch main lines that convey water to the smaller 1.5 inch and 1.25 inch branch lines. The sprinkler-heads are located on the branch lines. The fire suppression system for the two adjacent switchgear rooms is an integrated system and is supplied by three standpipes.

The fire suppression system is supported by 3ft. long hanger supports attached to the ceiling slab. The placement of the hangar supports are generally at every 16 ft. along the 4 inch main line, at the location of each sprinkler-head unless sufficiently close to hangers on the main line, and where intersecting lines or long unsupported spans warrant additional hanger supports.

The pipes are of varying schedules – Schedule 40, Schedule 80 and Schedule 160. For the switchgear rooms, there is one main 4-inch line running along their length. The span length of the smaller branch lines coming off the main 4-inch line is between 8 – 18 ft.

3.1.2.3   Key Observations/Points in Modeling of the Fire Suppression System

- Each of the battery rooms has its own standpipe and piping and sprinkler system. This system is not connected to the main fire suppression system in any way, and thus, is essentially decoupled. Thus, the main piping system and battery room piping system are modeled separately.

- Since the experimental data (moment-rotation relationships at the threaded T – Joints) is available for only the 1, 2 and 4 inch Schedule 40 pipes, all the 1.25 inch and 1.5-inch pipes are converted to 1 inch and 2 inch respectively.

- The 3 vertical water supply standpipes are connected at the top as well as the bottom floor slabs. Hence, they are considered to be anchored – fixed in all 6 degrees of freedom, at these locations.

- Connections at the joints have been modeled as nonlinear rotational springs. Thus, connections at every T-Joint have been modeled by 3 nonlinear rotational springs and the connections at every 4-way cross have been modeled by 4 nonlinear rotational springs. This model is valid for bending of the pipes in the horizontal plane only.

- The rotational springs for hysteretic behavior are characterized by models in *OpenSees*. The hysteretic behavior of nonlinear springs for 1 inch piping is characterized by yield strength M_y, initial stiffness K_1, hardening stiffness K_2, and parameter R, which controls the transition from elastic to plastic branches as shown, in Figure 22. The isotropic hardening parameter defines the increase of the compression or tension yield envelope as a proportion of yield strength after a plastic strain. The material model used is *Giuffré-Menegotto-Pinto Model.* [16]

- The hysteretic behavior of T-joint connections in 2 inch and 4 inch piping is characterized by a material that represents a "pinched" moment-rotation response which is modeled using a moment-rotation envelope [17]. Figure 23 shows the experimental v/s analytical results under cyclic loading condition, for a 2 inch T-joint, exhibiting the "pinched" behavior. The cyclic strength and stiffness degradation properties are determined in this model by considering stiffness degradation during unloading and reloading and strength degradation from the test data.
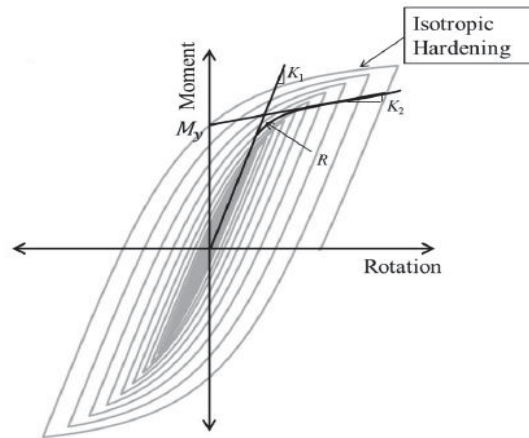
Figure 22 – 1 inch Rotational Spring Model.
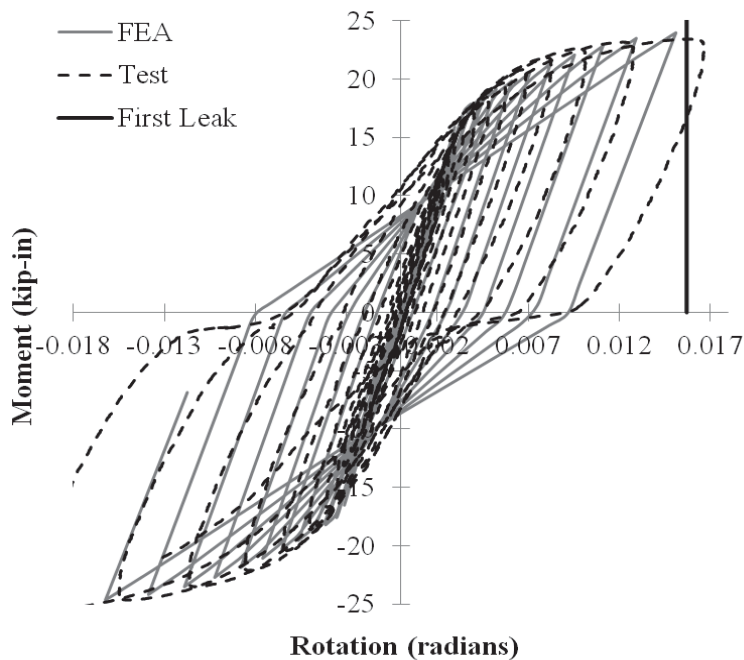
Figure 23 – Experimental v/s Analytical Results under cyclic loading condition.

- The pipe connections to walls are modeled as anchors (fixed in all 6 degrees of freedom).

- Modal analysis after the completion of the modeling indicates that the piping system is very flexible. This is due to the absence of any lateral restraints at the locations where the

hangers are meeting the piping system. Usually, the braces in a piping system offer lateral restraints, but this piping system is not braced at any location as provided in the spatial model. The frequencies of the first 10 modes of the piping system are given in Table 2 which shows that the natural frequencies are relatively very small and the piping is extremely flexible which is unlike typical piping in nuclear plants.

Table 2 – Frequencies of the Piping System – Without Lateral Restraints

Mode	Frequency (Hertz)
1	0.122
2	0.1255
3	0.4521
4	0.4803
5	0.635
6	0.677
7	0.77126
8	0.787
9	1.09
10	1.14

Table 3 – Frequencies of Piping System with Lateral Restraints

Mode	Frequency (Hertz)
1	2.415
2	3.413
3	3.433
4	3.472
5	3.631
6	4.144
7	4.979
8	5.076
9	5.385
10	5.896

- Lateral restraints are added in the piping system as an improvement of the spatial model which in turn helps to increase the natural frequencies and bring them closer to the typical values observed in nuclear plants. These lateral restraints are added at all the hanger locations. In principle, each hanger is replaced by a bracing that provides lateral as well as vertical restraint. Figure 24shows the location of these lateral restraints.

- As expected, the piping system becomes stiffer after the addition of these lateral restraints and thus similar to piping placed in NPPs. The natural frequencies are given in Table 2 and Table 3.
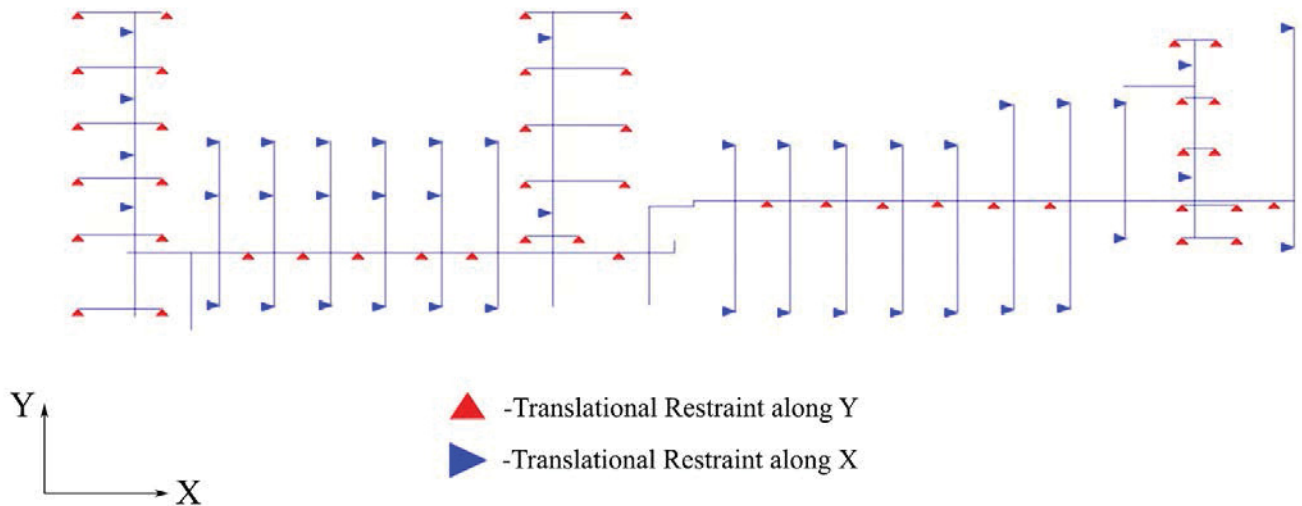
Figure 24 – Lateral Restraints on the Piping System.

3.1.2.4 Leakage Locations on Piping System for Sample Runs

The piping system is analyzed for earthquake time history runs normalized to increasing values of PGA in the X direction, to determine the leakage locations. The details of the earthquake record chosen are as follows:

- Location: "Parkfield"
- Date: 6/28/1966
- Station: "Cholame - Shandon Array #12"
- Direction: Horizontal, 50 degrees
- Units of acceleration: g = 9.81 m/s2
- Number of points: 4430
- Time interval: 0.01 s

The locations of damages at different PGA levels are indicated form Figure 25 to Figure 27 of this section and from Figure 97 to Figure 123 of Appendix A.

Figure 25 – Damage Locations for "Parkfield" Earthquake – 0.3 g.
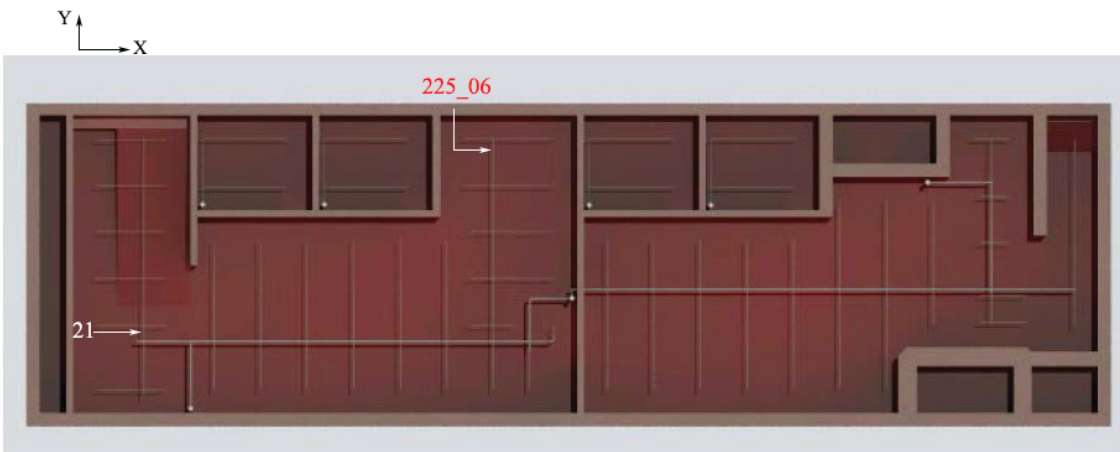
Figure 26 – Damage Locations for "Parkfield" Earthquake – 0.5 g.
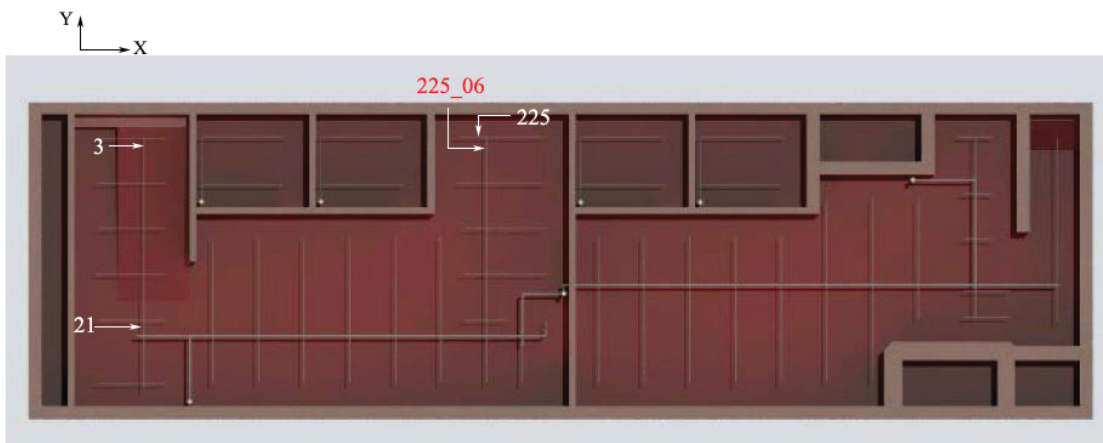
Figure 27 – Damage Locations for "Parkfield" Earthquake – 1.0 g.

3.1.2.5 Leakage Locations on Piping System for Evaluated Time History Sets

After the completion of the sample runs, the piping system is analyzed for the first 5 time histories provided by INL, both in the X and Y direction. The PGA's are normalized to levels of – 0.3 g, 0.6 g, 0.9 g, 1.2 g and 1.5 g, implying a total of 50 runs, 25 each in X and Y directions.

For the first time history in the X direction, the first damage is observed at a PGA of 0.297 g. The locations of damage are increasing in number with the increasing values of PGA. All the damages are for 1-inch pipes.

For the time history runs in the Y direction, two locations of damage are identified for a PGA level up to 1.5 g. The damages are for 2-inch pipes. Details are provided in Appendix A.

3.1.2.6 Explanation of Failures

The response spectra of the first 5 time histories in the X direction are given in the Figure 28.
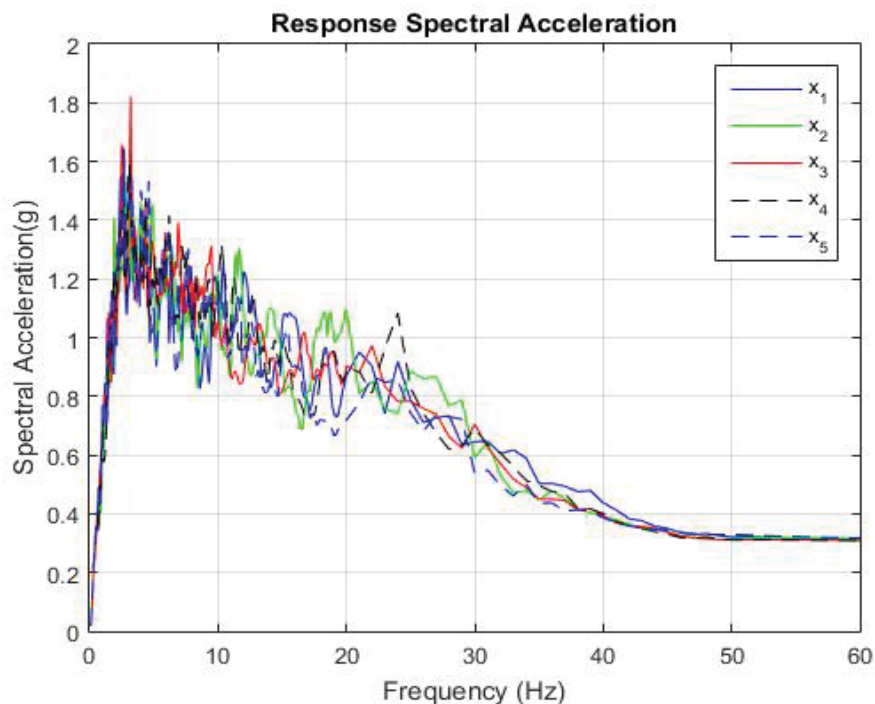
Figure 28 – Response Spectra of the first 5 time histories in the X Direction.

The peak of the spectra for the first 5 time histories occurs in the range of 2.5 – 3.2 Hertz. The first two modes of the piping system occur at 2.415 and 3.413 Hertz respectively – in the vicinity of the peak of response spectra. The modal participation factor in the X direction for first two modes is also high – 0.28 and 0.369 respectively. It is in these first two modes that we observe the excitation of the branch containing the maximum amount of failure locations (Figure 29 and Figure 30).
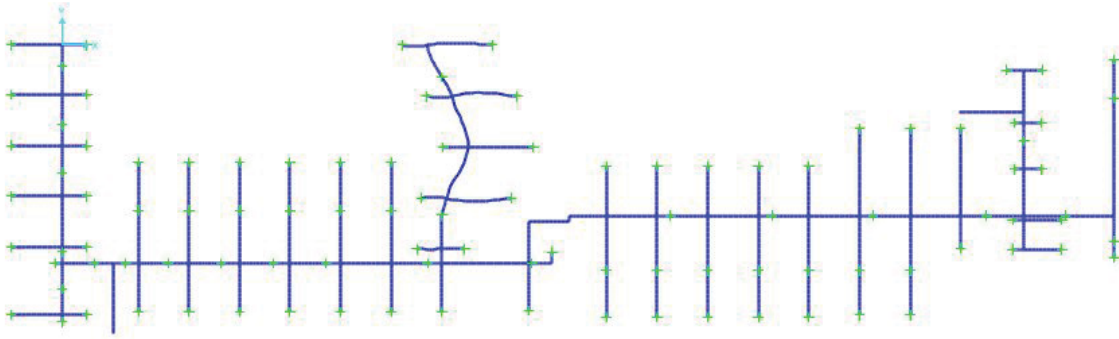
Figure 29 – Mode 1 of Piping System – Excitation of Branch Containing the maximum amount of failure locations.
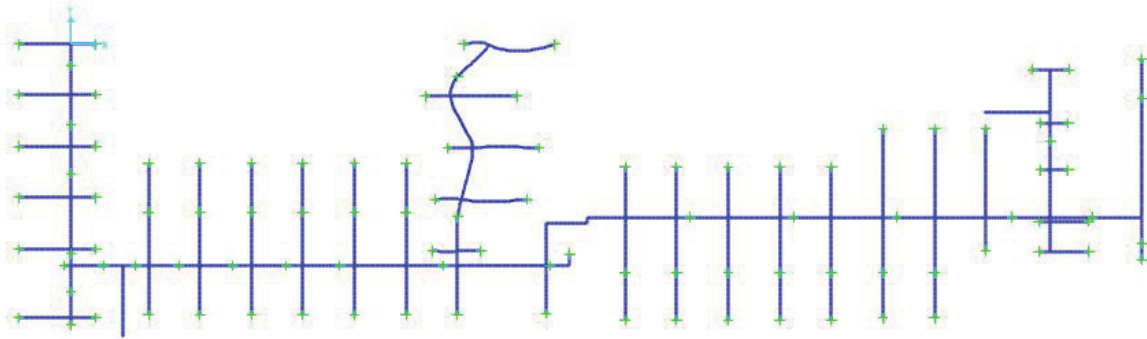
Figure 30 – Mode 2 of Piping System – Excitation of Branch Containing the maximum amount of failure locations.

The failure at the joints 225_06, 222_06, 222_06, 222_08, 216_06 & 216_08 (refer Figure 102 - Figure 120 in Appendix A of this document) can be attributed to bending of the pipe branch in the X direction, which is causing high rotations at the joints.

3.2 Flooding

In order to simulate flooding events, a semi dynamic model, capable of adjusting parameters for an event, must be used. The format or content of this model is dependent upon the tool that will be used to simulate the flooding event. Most simulation packages can import rigid body structures using many common formats. However, currently there is no standard toolset of capabilities needed to simulate real world scenarios and thus no common format can be used for adjusting parameters of the various simulation software packages.

For flooding events in the generic model are using NEUTRINO, a Smooth Particle Hydrodynamics (SPH) physics based tool. Although NEUTRINO has custom tools for things like particle emitters and measurement fields, it uses common 3D formats for the rigid body

structures. The 3D model of the two switchgear rooms constructed for the generic PWR are used as the rigid body structures for the NEUTRINO flooding model.
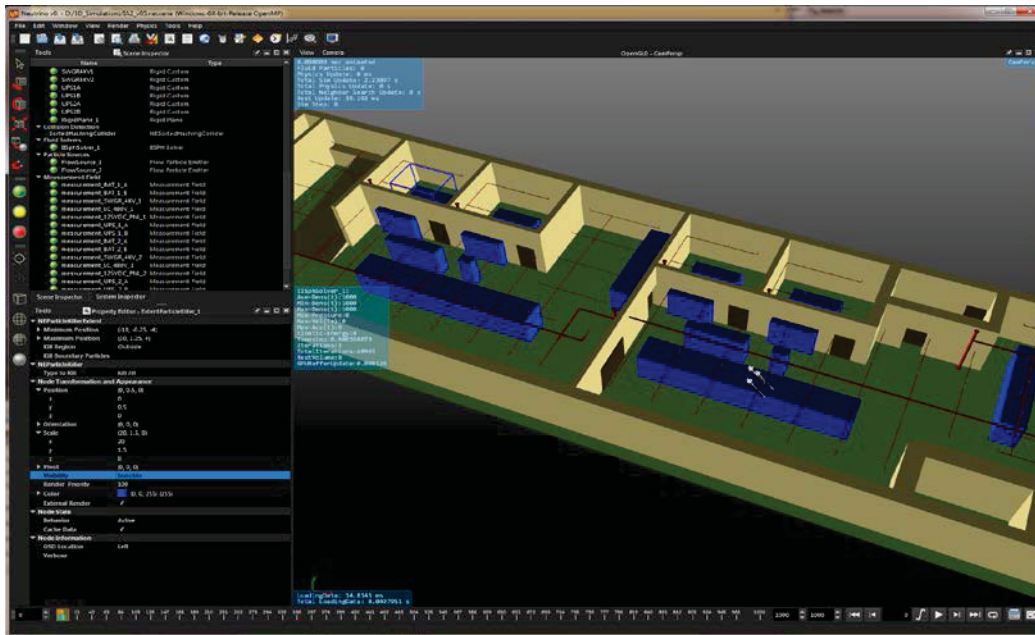
Figure 31 – User Interface for NEUTRINO and the IA2 switchgear rooms.

In addition to the physical structures, the flooding model contains different types of particle emitters. To simulate pipe failures variable flow particle emitters can be set with a specified location, orientation, and flow rate; corresponding to the location and the failure data of the pipe break (Figure 32). Each key component is also encompassed with a measurement field capable of measuring water contact, height, or pressure. A data file loaded at the beginning of the simulation indicates which items and what events to detect and send messages back on.
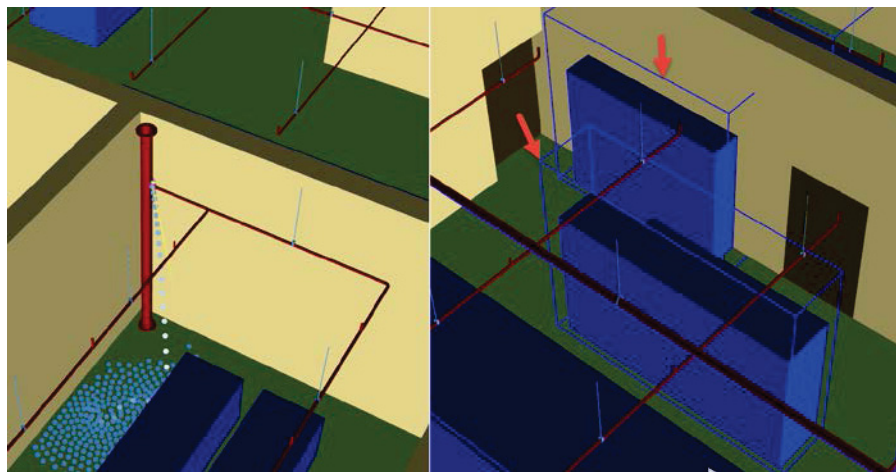
Figure 32 – NEUTRINO Tools (Left- Variable flow particle emitter. Right – Measurement Fields).

3.3   Probabilistic Risk Assessment

A basic generic PRA model was developed using SAPHIRE. This model contains only a few systems necessary for analyzing those areas affected by the seismic or flooding scenario and the main components/systems analyzed in the TH simulation. Other required systems are stubbed out with a general overall failure rate that can be expanded to full systems in the future. This model contains the failure methods and rates for key components and results provide a baseline to verify the dynamic model.

The following fault trees listed in Table 4 are the main systems in the SAPHIRE model.

Table 4 – SAPHIRE model for the main systems.

NAME	DESCRIPTION
AFW	Loss of AFW
DGEN	Loss of diesel power
FAB	Feed and bleed
HPI	HPI flow insufficient
LOOP-LOCA	Conditional loss of offsite power given LOCA
MFW	Loss of MFW
NLOSP	Seismic Loss of Site Power
OEP	Loss of offsite power
OPR-8HR	Operator fails to recover offsite power in 8 hours
PASS	Pass-through for transients
QLLOCA	Seismic Large LOCA
QSLOCA	Seismic Small LOCA
RHR	Residual heat removal
RHR-L	Long-term RHR flow - large LOCA
RHR-S	Long-term RHR flow - small LOCA
RPS	Reactor S/D
SEC	Secondary cool-down SG_PORV
SVC	Safety valves close
SVO	Safety valves open
UDC-CTRLPWR-1	DC control power train 1
UDC-CTRLPWR-2	DC control power train 2
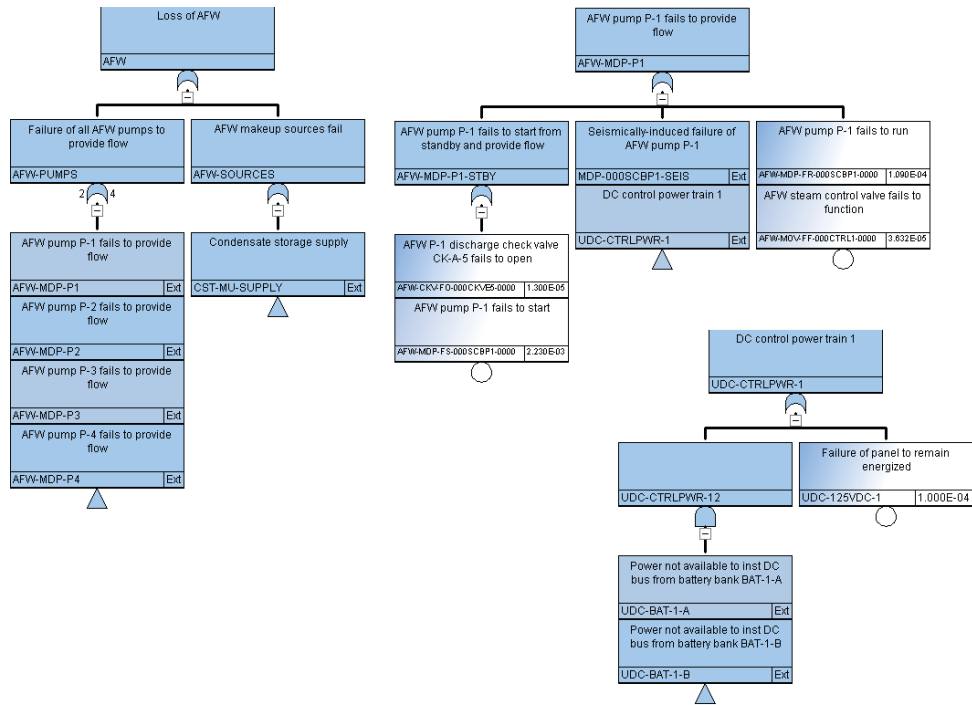
Figure 33 – Main Fault Trees in the SAPHIRE model.

Seismic capabilities for susceptible components have been added using a sub tree containing bin and flag set combinations. For each seismic bin, a basic event with an appropriate failure rate is combined with a house event that is triggered by a flag set (see Figure 34). When solving for a given EQ, the correct failure rate propagates up the sub tree, contributing to the overall failure rate. The SAPHIRE model contains 10 different seismic bins, other pieces of this test only contain 3 bins, so for this test bins 2, 5, and 8 will be used for calculations.
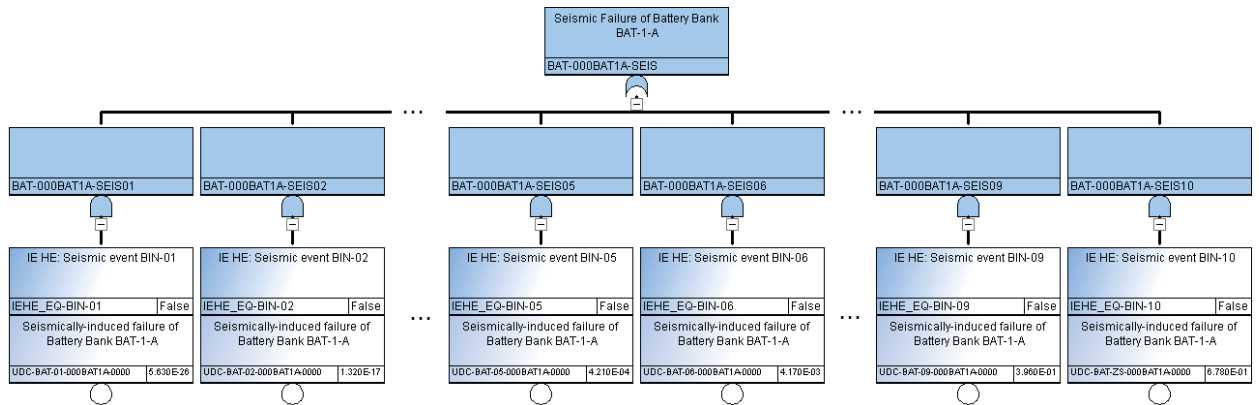
Figure 34 – Example of varying seismic failure rates by using a flagset

Since there is very little empirical data for component failure rates due to seismic events, arbitrary but logical values are used. This will due for demonstration purposes, and as more data is compiled, more accurate values can be applied.

29

Three main event trees are modeled including loss of off-site power (LOOP), Station Blackout (SBO) and Transient. Sequences are either OK or lead to core damage (CD). In most cases if CD is reached then RELAP5-3D will be used for further calculations. A combination LOOP and SBO are used to develop the plant response diagram for the dynamic PRA model.

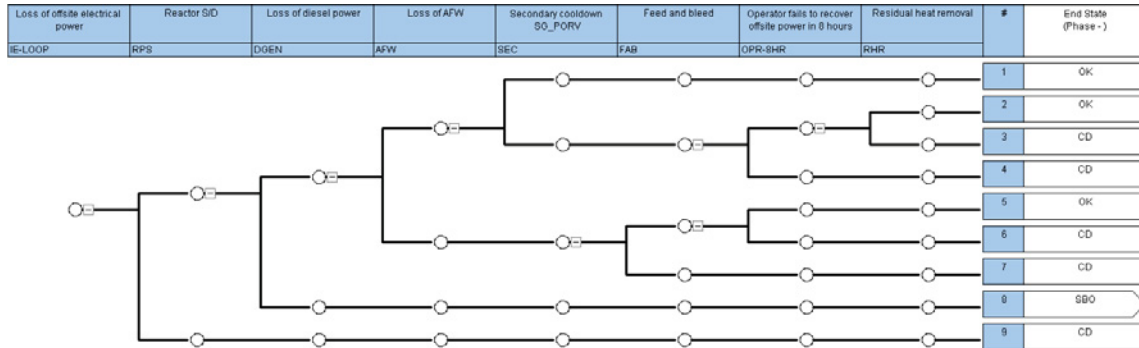| Loss of offsite electrical power	Reactor S/D	Loss of diesel power	Loss of AFW	Secondary cooldown SG_PORV	Feed and bleed	Operator fails to recover offsite power in 8 hours	Residual heat removal	#	End State (Phase -)
IE-LOOP	RPS	DGEN	AFW	SEC	FAB	OPR-8HR	RHR		
								1	OK
								2	OK
								3	CD
								4	CD
								5	OK
								6	CD
								7	CD
								8	SBO
								9	CD

Figure 35 – Loss of off-site power event tree.

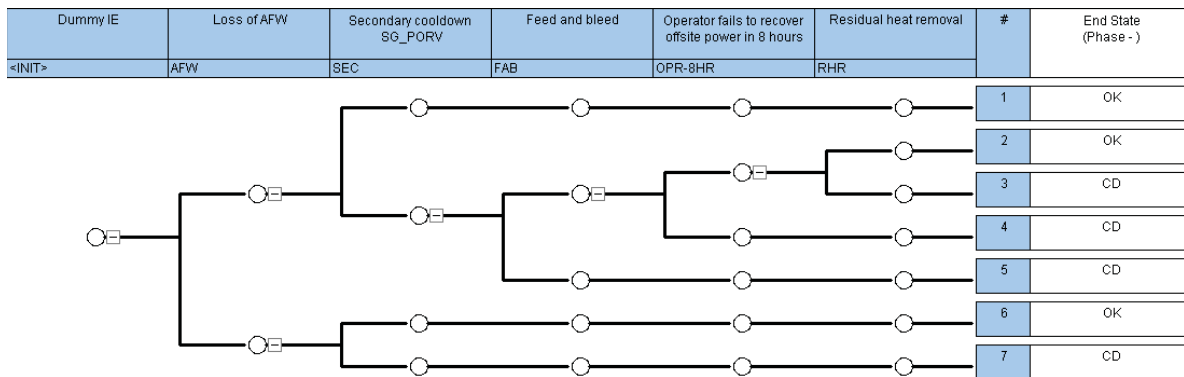| Dummy IE	Loss of AFW	Secondary cooldown SG_PORV	Feed and bleed	Operator fails to recover offsite power in 8 hours	Residual heat removal	#	End State (Phase -)
<INIT>	AFW	SEC	FAB	OPR-8HR	RHR		
						1	OK
						2	OK
						3	CD
						4	CD
						5	CD
						6	OK
						7	CD

Figure 36 – Station blackout event tree.

The dynamic PRA model was developed using EMRALD and is based on the SAPHIRE model. The core of the model is equivalent to the SAPHIRE model with additions to handle dynamic changes depending on results from the seismic event on the piping structure or events in the 3D flooding simulation.

An equivalent to fault tree evaluation is done in EMRALD, by evaluating logic when the state of any inputs to that logic changes. Unlike traditional PRA model, which uses event tree to graphically represent accident sequences, there is no such explicit measure in the EMRALD state-based PRA model to sequentially depict the responses of the systems and operator actions to an initiating event. Instead, the accident sequences are implicitly represented in the plant state diagram with the flow paths between the start state, initiating event states, system or component states, and key/end states.

In order reduce the number of 3D simulations and still get an accurate failure rate from Monty Carlo sampling, the model is designed so it can repeatedly sample and re-evaluate the rest of the systems after a SBO. This is done by marking the time before running the 3D simulation and saving any events. Then once a "Fuel Damage" or "OK" state is reached in the subsequent state evaluation, a counter is incremented, and the time is reset. The events are applied with the same timing, without running the 3D simulation, with the sampling and evaluation proceeding again. Once the prescribed number of iterations is achieved, the overall EMRALD run can continue to completion and the result will include accurate random failures.

The EMRALD model starts in normal operations the only event being tested, from this state, is an earthquake driven LOOP event. The following possible transitions then take place as show in Figure 37:

1. Normal_Op – The normal operation of the plant.

   Immediate Actions

   a. Reset the systems back to initial conditions.

   Conditional Events

   a. 24HrMission_Time – After 24 hours, terminate this run, no imitating event occurred.

   b. IE_LOOP_EQ – The earthquake that triggered a LOOP occurred so set the PGA and move to LOOP_EQ_OCCURED.

2. LOOP_EQ_OCCURED – An earthquake that triggered a LOOP occurred.

   Immediate Actions

   a. Eval_Pipe_Failures – Sample on the EQ and determine if any.

   b. Start_SBO_Eval – Start evaluating any systems related to SBO.

   Conditional Events

   a. OSP_REC – Offsite power is recovered return to Normal_OP.

   b. RPS – If Reactor S/D equipment fails to initiate move to Core_Damage.

   c. DGEN_Fail – If the diesel generators fail, move to SBO.

3. SBO – (Key State) Station black out, the only power is battery backup.

   Immediate Actions - None

   Conditional Events

   a. Pipe_Rupture – If there is a pipe rupture then move to Running_3D_Sim.

   b. No_Pipe_Ruptures – There are no pipe ruptures move to Loop_Eval.

4. Running_3D_Sim – 3D simulation is needed to evaluate components due to possible flooding.

Immediate Actions

    a. Save_Loop_Time – Save the time so that we can revert back to the time after the 3D simulation has started for multiple evaluations of the rest of the systems.

    b. Start_3D_Sim – Start the 3D simulation.

    c. Set_Pipe_Fail_Vals – Set the location, and flow rate of the any pipe failures that occurred.

Conditional Events

    c. OP_FW_Rec – Operator shuts down the fire water system so stop the 3D simulation by going to Stopping_3D_Sim.

    d. AFW & SG_PORV – The system that are affected by the simulation have failed, no more 3D simulation is needed, so move to Stoping_3D_Sim.

5. Stopping_3D_Sim – (Key State) The 3D simulation is no longer needed, so shut it down.

Immediate Actions

    a. Stop_3D_Sim – Send a message to stop the 3D simulation.

    b. Goto_Loop_Eval – Move to the Loop_Eval state.

Conditional Events - None

6. Loop_Eval – The starting point for repeatedly evaluating the rest of the systems.

Immediate Actions

    a. Start_Sys_Eval – Start sampling and evaluation of the main systems.

    b. Inc_Loop_Cnt – Increment the loop counter.

Conditional Events

    a. AC_Recover & No_Key_Sys_Failures – AC power from offsite power or the diesel generators is recovered and there are no key system failures, so move to Rerun_Loop.

    b. 8Hrs & AC_Recovery & Key_Sys_Failures – After 8 hours if the AC power is recovered but there are key system failures then move to Running_RELAP5-3D.

    c. 8Hrs & No_AC_Recover – After 8 hours if there is no AC power recovery then move to Fuel_Damage.

7. Running_RELAP5-3D – Conditions are met where there is possible fuel damage but further calculations are needed using RELAP5-3D.

Immediate Actions

    a. Run&Process_RELAP5-3D – Modify the RELAP5-3D input deck with the failure time of any components or systems and run RELAP5-3D. If RELAP5-3D indicates damage then move to Fuel Damage, otherwise move to Rerun_Loop.

Conditional Events - None

8. Fuel_Damage – Fuel damage has occurred.

   Immediate Actions

   a. Inc_Fuel_Damage – Increment the fuel damage variable to keep track of how many time fuel damage occurs in the multiple runs for a given initiating event and 3D simulation.

   b. Goto_Rerun_Loop – Move to Rerun_Loop.

   Conditional Events – None

9. Rerun_Loop – Reset and prepare for a new sampling of the main systems for the current Initiating event and possible 3D simulation.

   Immediate Actions

   a. Stop_Sys_Eval – Stops the main system evaluation and resets it for future sampling.

   Conditional Events

   a. Loop_Cnt_LT_n – The Loop count is less than the desired number so reset the time back to right after the start of the 3D simulation. All 3D simulation events will remain in the queue.

   b. Loop_Cnt_EQ_n – The loop count is equal to the desired number so move to Normal_Op.

10. Core_Damage – (Key State) There has been core damage.

    Immediate Actions

    c. Goto_Done – Add the Done state to the set of current states.

    Conditional Events – None

11. Done – (Terminal State) Exit this run of the EMRALD simulation.

    Immediate Actions - None

    Conditional Events – None

The EMRALD is simulated numerous times for each run, if a "Key State" occurs; it is recorded along with and desired variable Fuel_Damage_Cnt. Thus the probability of station blackout occurring is the number of times SBO occurred divided by the total number of runs. The probability of fuel damage is calculated by following:

$$Fuel\ Damage\ Probability = \frac{\sum Fuel\_Damage\_Cnt}{(SBO\ \text{Occurrences} * Loop\ run\ count)} * \frac{SBO\ Occurrences}{Total\ Runs}$$

Each EMRALD system was tested against the SAPHIRE main or sub fault tree result for validation before being used in the overall plant response diagram.   Detailed information on EMRALD operations and options are not covered in depth, but can be obtained [13].
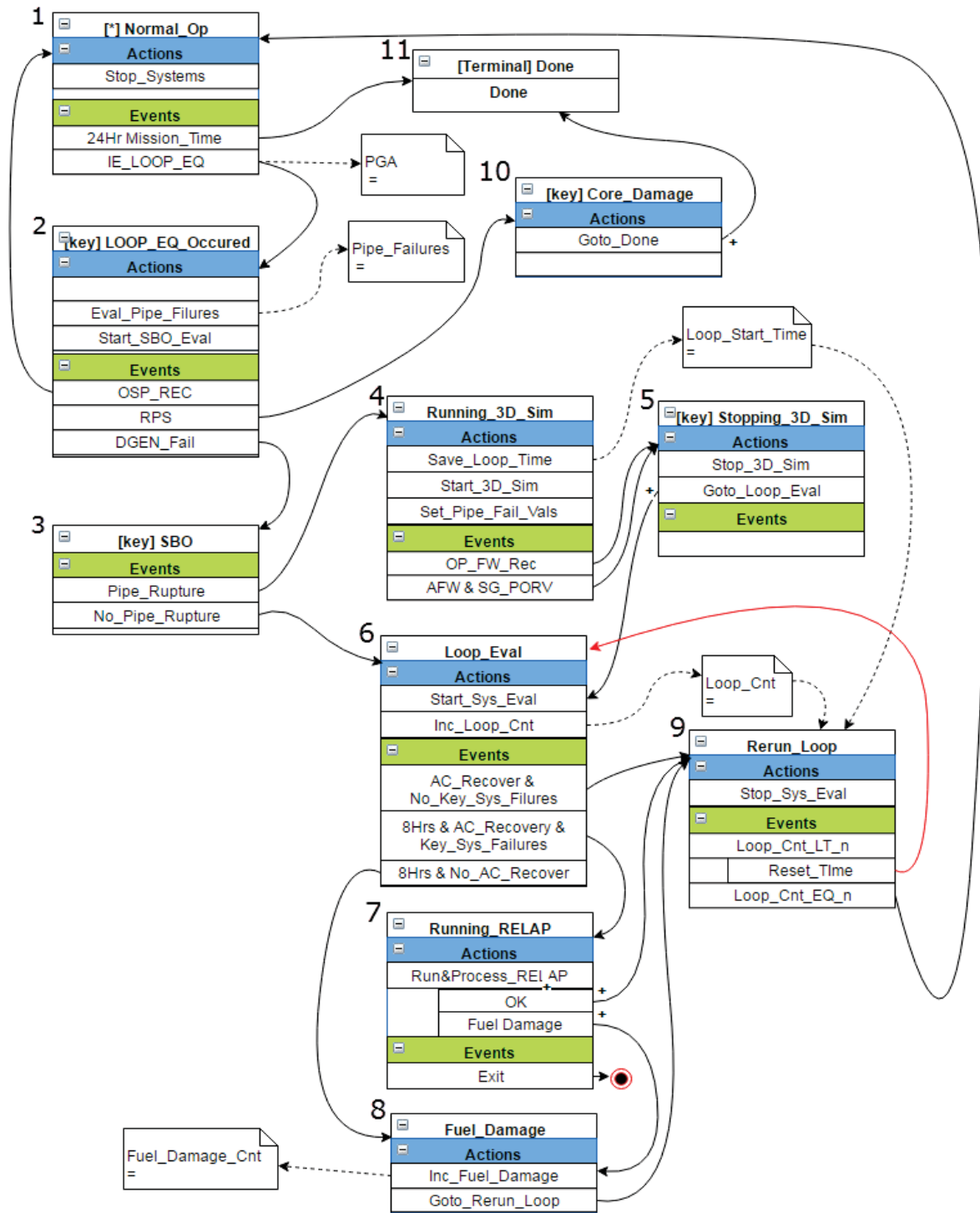

Figure 37 – The Plant Response Diagram to calculate failure probabilities by coupling seismic analysis, dynamic PRA, 3D simulation, and RELAP5-3D.

3.4   Thermal-hydraulic

3.4.1   Station Blackout Event Sequence Description

According to the US NRC 10 CFR 50.2, a Station Black-Out (SBO) event is defined as a the complete loss of alternating current (AC) electric power to the essential and nonessential switchgear buses in a nuclear power plant (i.e., loss of offsite electric power system concurrent with turbine trip and unavailability of the onsite emergency AC power system).

SBO does not include the loss of available AC power to buses fed by station batteries through inverters or by alternate AC sources, nor does it assume a concurrent single failure or design basis accident. Thus, loss of all AC power results in unavailability of all normal electrical equipment and most of the safety electrical equipment.

For the IA2 test case, an EQ-induced loss-of-offsite and on-site AC power occurs at time t=0, resulting in a SBO event. Two cases are considered and they are described hereafter: the Long Term SBO (LTSBO) and the Short Term SBO (STSBO). In the first case, it is assumed that no DC power is lost and the operator is able to perform reactor cool-down using feed-and-bleed procedure on the secondary side. The first 8 hours of the event (until battery depletion) are considered. On the last case (STSBO), more EQ-induced failures on the site are assumed: all DC power is lost and no water source is available for the actuation of the TD-AFW. Because of the unavailability of heat sinks, the reactor core rapidly overheat and fuel damage (PCT>1500 K) occurs in ~2.5 hours.

3.4.1.1   Long Term Station Blackout Event Sequence Description

The reactor is scrammed at t=0 and the cool down of the reactor is automatically performed by the start-up of the turbine-driven Auxiliary Feed Water (TD-AFW) pump at t=1 min. Use of motor-driven AFW pump and of high and low pressure injection systems (HPIS and LPIS) is prevented by the loss of AC power.

The SBO event causes the run-down of the all reactor coolant pumps (RCP) and a loss of the RCP seal injection. As a consequence, at t=0 a RCP seal LOCA of 1 Kg/s (21 gpm) is assumed.

The SG are isolated by the MSIV closures and the SG pressure is relieved via the Safety Relief Valves (SRV) or the pilot-operated relief valves (PORV). Actuation of the PORV and of the TD-AFW is guaranteed by the batteries and by the nitrogen gas or alternative compressed air supply.

During the first fifteen minutes of the transient, the TD-AFW is at full flow. After t=15 min., operator is assumed to take control of the TD-AFW pump for maintain the SG water level, preventing TD-AFW pump overflow or SG dry-out.

At t=1.5 hour, the operator performs a primary side cool down by SG depressurization. The cool down rate is restricted to ~55.5 C/hr (100 F/hr). The SG depressurization is achieved by a feed & bleed procedure, injecting Emergency Condensate Storage Tank (ECST) water in the

SG using the TD-AFW pump. Steam is released to the atmosphere through the actuation of the SG PORVs. The ECST water reservoir is eventually depleted in ~6 hours.

The primary side pressures and temperatures decrease after 2 hours from the beginning of the transient, causing a water level decrease in the upper plenum of the RPV and in the pressurizer. The MCP seals LOCA also contribute to reduce primary side pressure. A further cool down of the core is achieved by the passive injection of the accumulators water when the primary pressure decrease below 4.59 MPa (665 psig) at t= 2.5 hours. Then the water level in the RPV starts to increase again.

The operator stops SG cool-down when the SG pressure reaches 9.29 MPa (120 psig) for maintaining the minimum pressure for the TD-AFW pump operation.

At t = +8 hours, the batteries are depleted, and both pressurizer and SG PORV are not anymore available. TD-AFW pump, without any flow control, can run until ECST water inventory is depleted. After t=+8 hours, fuel temperature and RPV pressure start to increase, causing pressurizer SRV to open and an eventual failure of the pressurizer relief tank. Around t=~14 hours, fuel damage starts to occur.

3.4.1.2 Short-Term Station Blackout Event Sequence Description

The reactor is scrammed at t=0 and the cool down of the reactor is automatically performed by the start-up of the turbine-driven Auxiliary Feed Water (TD-AFW) pump at t=1 min. Use of motor-driven AFW pump and of high and low pressure injection systems (HPIS and LPIS) is prevented by the loss of AC power.

The SBO event causes the run-down of the all reactor coolant pumps (RCP) and a loss of the RCP seal injection. As a consequence, at t=0 a RCP seal LOCA of 1 Kg/s (21 gpm) is assumed.

The SG are isolated by the MSIV closures and the SG pressure is relieved via the Safety Relief Valves (SRV) or the pilot-operated relief valves (PORV). Actuation of the PORV and of the TD-AFW is guaranteed by the batteries and by the nitrogen gas or alternative compressed air supply.

At t=1 min 40 s, EQ induced damages, cause a break of the ECST and a loss of DC power (e.g., because of internal flooding, see paragraph 4). Consequently, TD-AFW stops to supply water to the SG and no SG or PRZ PORVs can be actuated by the operator.

The reactor core start to heat-up and primary and secondary pressures increase. The SG and PRZ SRV periodically discharge in the containment and in the atmosphere primary and secondary mass and energy. The fuel clad overheats and it reaches the safety threshold of 2200 F (~1500 K) in ~2.5 hrs.

3.4.2　RELAP5-3D Model Description

As detailed in [7], the reference NPP for IA2 is the INL Generic PWR (IGPWR). Using publicly available information, we created the IGPWR, which is based on a 2546 MWth Westinghouse 3-loop PWR [19]. The main characteristics are reported in Table 5.

Table 5 – Design Parameters of the IGPWR.

Parameter	Value (SI units)	Value (British units)
Core Power [MW_{th}]	2,546	
Reactor Inlet / Outlet Temperature [^oC / ^oF]	282 / 319	540 / 606
Number of Fuel Assemblies	157	
Rod Array	15x15	
RCS Coolant Flow [kg/s / lb_m/hr]	12,738	101.6E+8
Nominal RCS Pressure [MPa /psia]	15.5	2,250
MCP seal water injection [m^3/s / gpm]	3.78E-3	8
MCP seal water return [m^3/s / gpm]	1.42E-3	3
MCP Power [MW / hp]	4.00	5,364
Number of SG	3	
PRZ PORV set points op./clos. [MPa / psig]	16.2 / 15.7	2,350 / 2,280
PRZ PORV capacity [kg/s / lb_m/hr]	2 x 22.5	2 x 179,000
PRZ SV set points op./clos. [MPa / psig]	16.4 / 17.7	2,375 / 2,575
PRZ SV capacity [kg/s / lb_m/hr]	3 x 37.0	3 x 293,330
Relief Tank Rupture Disc capacity [kg/s / lb_m/hr]	113.4	9.0E+5
Relief Tank Rupture Disc set point op. [MPa / psid]	6.89	1000
Relief Tank Total Volume [m^3 / ft^3]	36.8	1300
Relief Tank Water Volume [m^3 / ft^3]	25.5	900
SG PORV capacity [kg/s / lb_m/hr]	1 x 47.0	1 x 3.73E+5
SG PORV set points op./clos. [MPa / psig]	7.24 / 6.89	1,050 / 1,000
SG SV capacity [kg/s / lb_m/hr]	5 x 94.0	5 x 7.46E+5
SG SV set points op./clos. [MPa / psig]	8.16 / 7.53	1,184 / 1,092
Secondary Pressure [MPa / psia]	5.405	785

Secondary Side Water Mass @ HFP [kg / lb$_m$]	41,639	91,798
SG Volume [m^3 / ft^3]	166	5,868
SG Steam Flow rate @ HFP [kg/s / lb$_m$/hr]	473.0	3.756E+6
FW Temperature [^{o}C / ^{o}F]	228	443
Main FW pump [m^3/s / gpm]	2 x 6.513 (at 518 m)	2 x 13,800 (at 1,700 feet)
Turbine-driven AFW pump [m^3/s / gpm]	1 x 0.3304 (at 832 m)	1 x 700 (at 2,730 feet)
Motor-driven AFW pump [m^3/s / gpm]	2 x 0.1625 (at 832 m)	2 x 350 (at 2,730 feet)
Emergency Condensate Storage Tank [m^3 / ft^3]	416	14,691
Accumulator Water Volume [m^3 / ft^3]	3 x 27.61	3 x 975
Accumulator Pressure [MPa /psig]	4.14-4.59	600-665
High Head Safety Injection [m^3/s /gpm]	3 x 0.0708 (at 1,767 m)	3 x 150 (at 5,800 ft)
Low Head Safety Injection [m^3/s /gpm]	2 x 1.416 (at 68.6 m)	2 x 3,000 (at 225 ft)
Containment Volume [m^3 / ft^3]	50,970	1,800,000
Containment Design Pressure [MPa /psig]	0.31	45
Containment Operating Pressure [MPa /psia]	0.062 to 0.071	9 to 10.3
Containment Operating Temperature [^{o}C / ^{o}F]	24 to 52	75 to 125
RHR Pump capacity [m^3/s /gpm]	2 x 1.888 (at 70.1 m)	2 x 4,000 (at 230 ft)
CCW Pump capacity [m^3/s /gpm]	2 x 4.248 (at 61.0 m)	2 x 9,000 (at 200 ft)

The RELAP5-3D model developed for analyzing SBO-like events is based on an input-deck describing:

- reactor pressure vessel (RPV);
- three main circulation circuits (MCC), including the main coolant pumps (MCP) and the steam generators (SG);
- pressurizer (PRZ), and its main valves (PORV and SV);
- connections for the emergency core cooling system (ECCS) and the auxiliary feed-water (AFW);

- secondary part of the SGs up to the SG outlet, including the main valves (PORV and SV);
- main feed-water (MFW).

The sketches of the RPV and of the MCC, including the secondary side of the SGs, are given in Figure 38 and Figure 39.

Three independent TH channels representing the central, the middle and the periphery of the core are used. A sketch of the three-channel core region subdivision is given in Figure 40, together with the number of the fuel assemblies and their relative radial power. Passive and active heat structures simulate the heat transfer between the coolant and fuel, the structures and the secondary side of the IGPWR. No heat losses toward the containment are included in the model.

214 hydraulic volumes connected by 257 junctions and coupled to 240 heat structures compose the nodalization. The total number of mesh points, discretizing the heat structures, is 1312. The model is based on a nodalization developed for the RELAP/SCDAP code for SBO analyses [18].
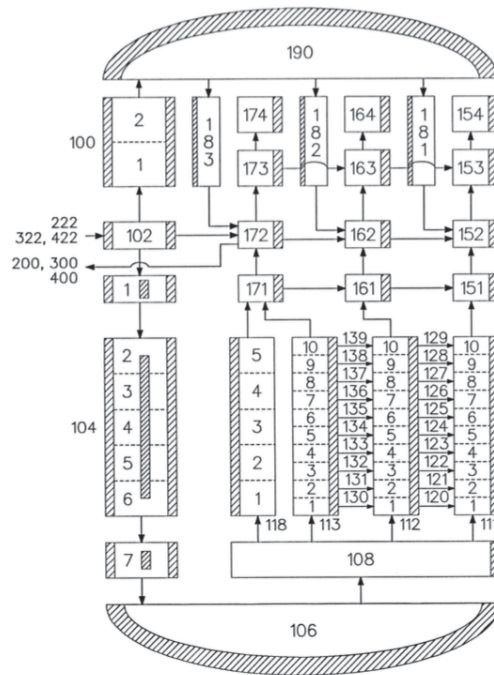
Figure 38 – RELAP5-3D RPV Model.
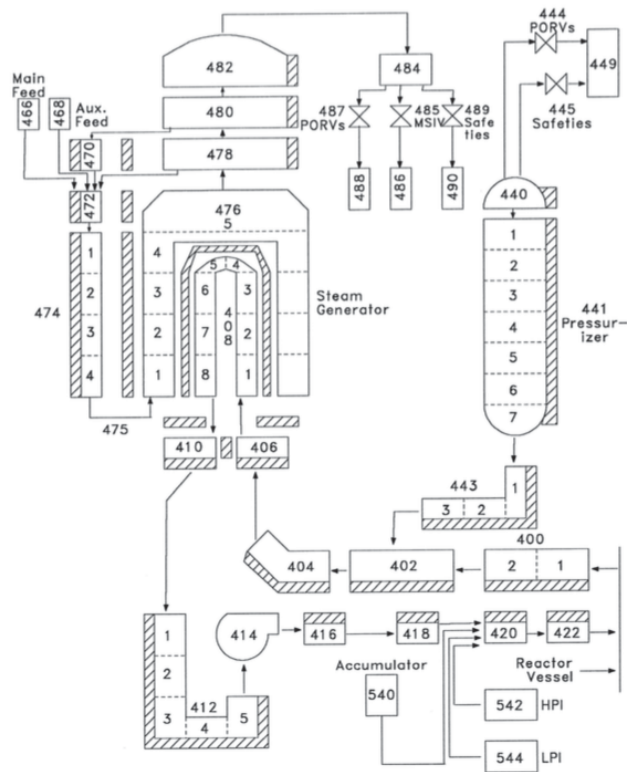
Figure 39 – RELAP5-3D MCC & SG Model.
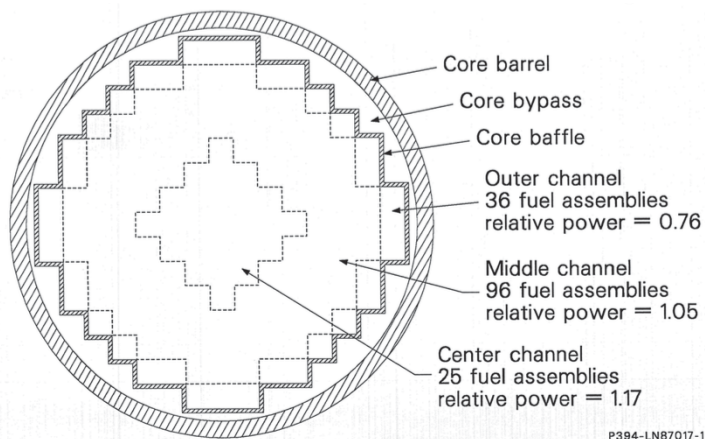
Figure 40 – RELAP5-3D Core Model.

The possible operator actions (SG cool-down, feed and bleed, AFW flow control, etc.) are implemented through the RELAP5-3D control logic. RELAP5-3D control variables calculate the derived parameters for the control logic and for the transients' analyses.

3.4.3 Steady State Analysis

A null-transient of 1000 s was calculated for validating the steady-state solution. Comparison between RELAP5-3D calculated values and IGPWR reference data are provided in Table 6. Deviations of calculated values are negligible, resulting in an excellent agreement. The stability of the trends of the most relevant parameters is shown in Figure 41 to Figure 46. Thus, the achieved RELAP5-3D SS solution constitutes a valid starting point for performing the different SBO analyses.

Table 6 – RELAP5-3D SS calculation of main parameters.

Parameter	Reference Value	RELAP5-3D value	Deviation (%)
Reactor Power (W)	2,546	2,546	imposed
PRZ Pressure (MPa)	15.5	15.5	imposed
Total RCS Coolant Loop Flowrate (Kg/s)	12,738	12,738	0.0
CL Temperature (K)	555.6	557.3	0.3
		557.3	0.3
		557.3	0.3
HL Temperature (K)	591.8	593.1	0.2
		593.1	0.2
		593.1	0.2
Feed-water Temperature (K)	501.5	501.5	imposed
		501.5	imposed
		501.5	imposed
Steam Flowrate per SG (K)	473.	470.1	-0.6
		470.7	-0.5
		471.0	-0.4
Steam Pressure at the Outlet Nozzle (MPa)	5.405	5.405	imposed
		5.405	imposed
		5.405	imposed
Liquid Mass per SG (Kg)	41,639	41,640	0.0
		41,638	0.0
		41,638	0.0
Steam Temperature (K)	542	542	0.0
		542	0.0
		542	0.0
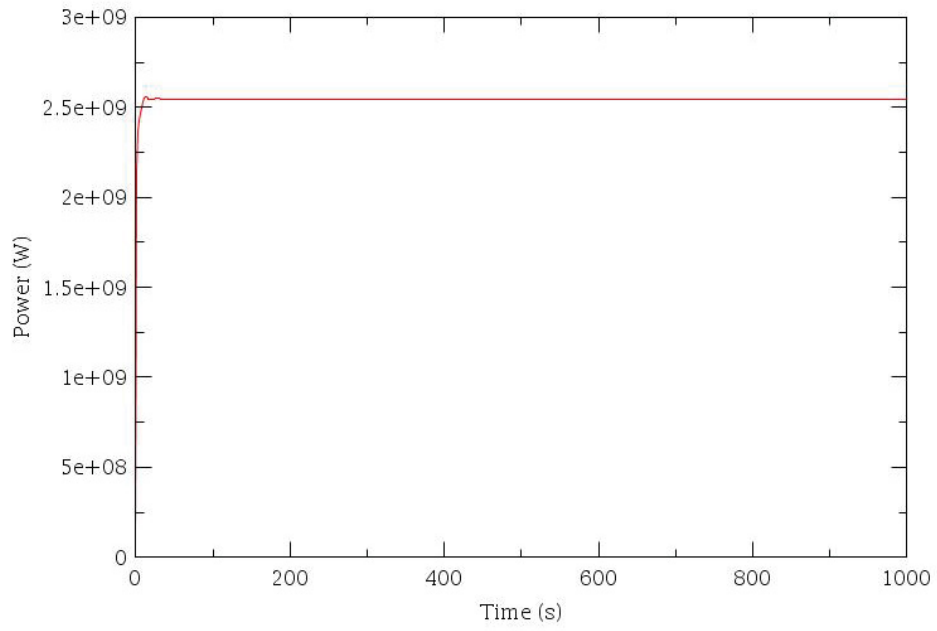
Figure 41 – Core Power.
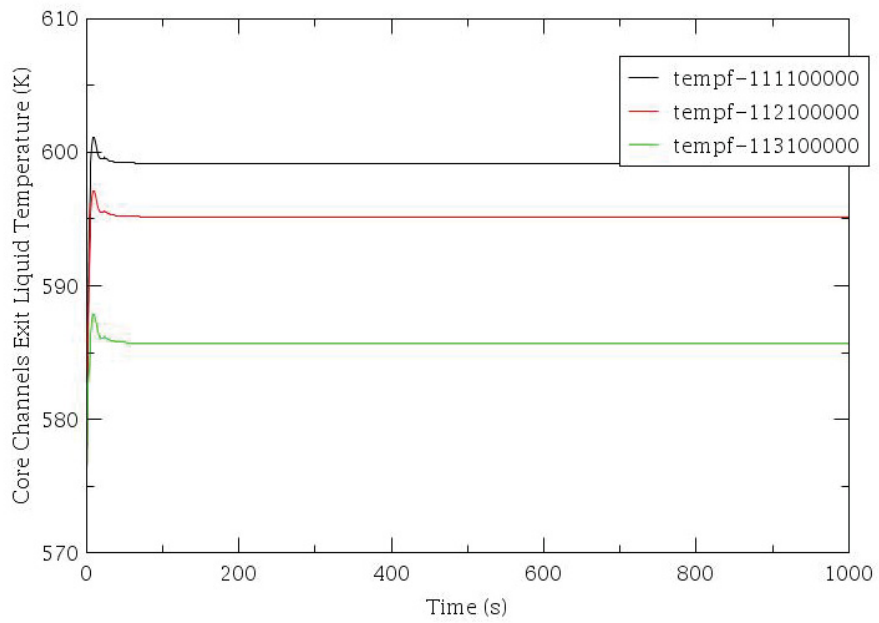
Figure 42 – Core Channel Exit Temperatures.
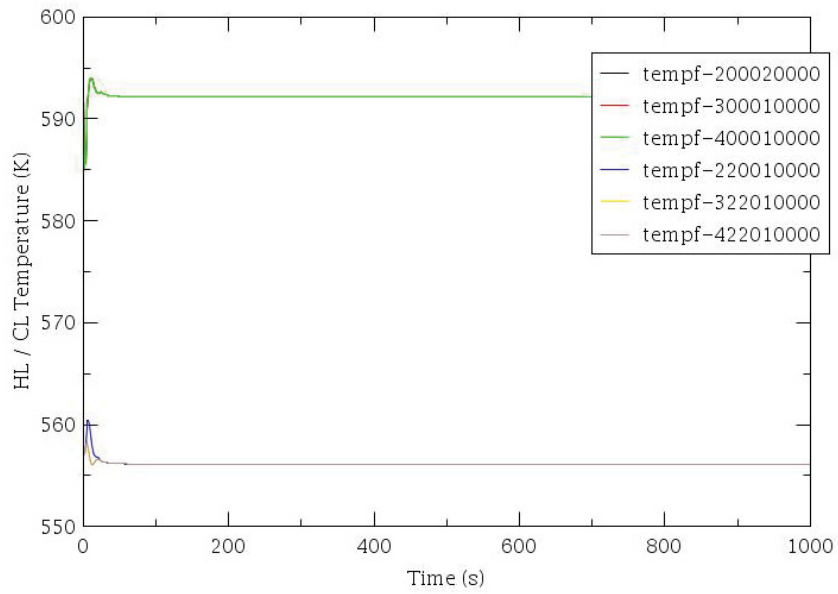
Figure 43 – Hot Leg / Cold Leg Temperatures.
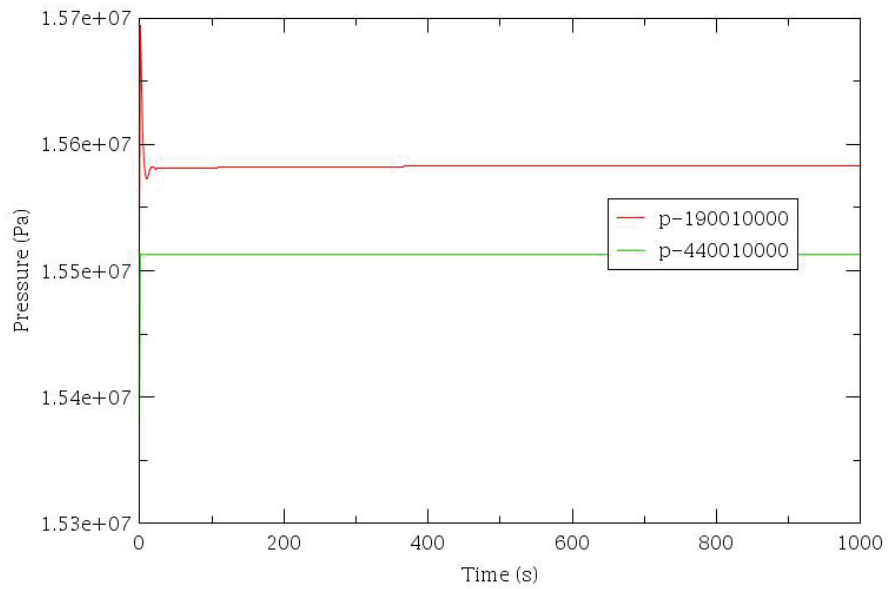
Figure 44 – UP/PRZ Pressure.
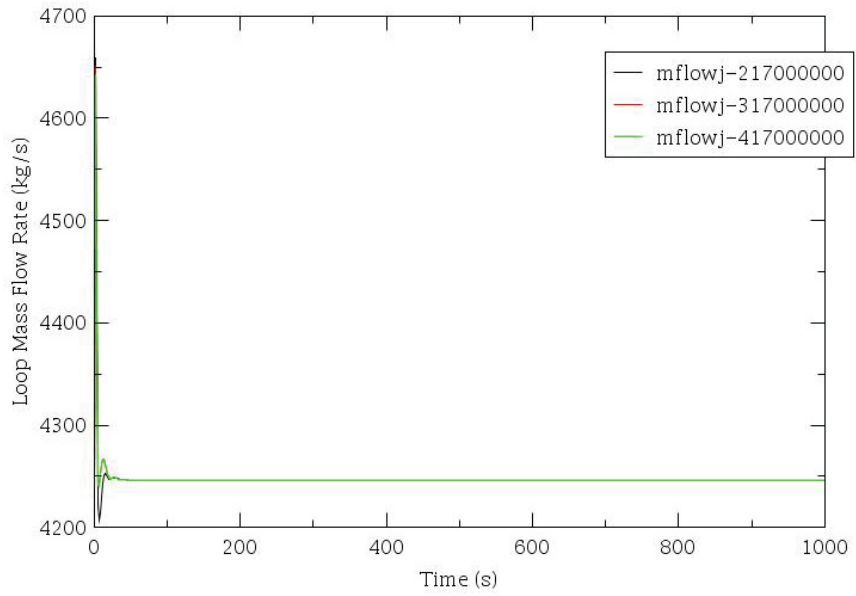
Figure 45 – Primary Side Loops Mass Flow Rates.
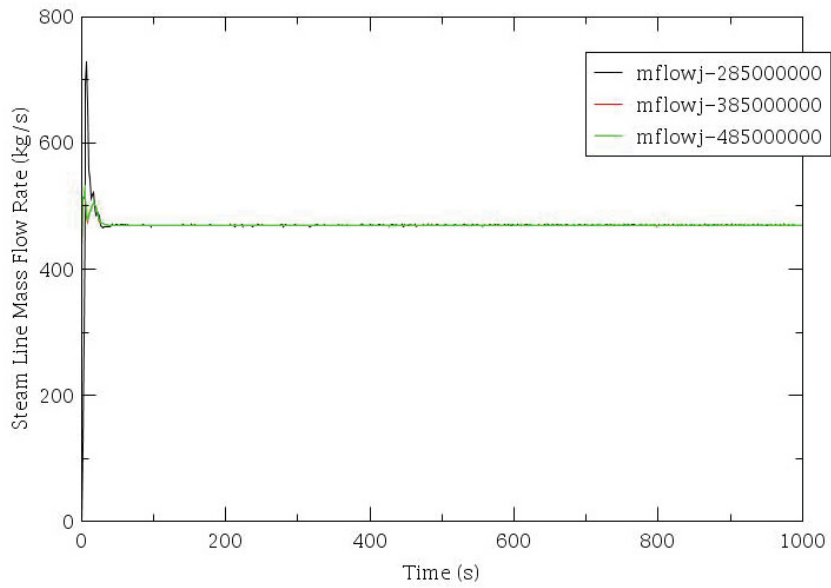
Figure 46 – Steam Line Mass Flow Rates.

3.4.4 Transient Analysis – Reference Calculations

3.4.4.1 *LTSBO results*

A base case for the LTSBO analysis has been performed. The base case is intended to be the reference calculation for the dynamic-PRA and for the Sensitivities & UQ analyses. Standard sequence of events where obtained from [25]. Table 7 reports the sequence of events and Figure 47 to Figure 62 the charts of the transient parameters. For validation purpose, the timing of events calculated by MELCOR code [26] in [25] is also reported. Deviations are minimal and are mainly due to different initial values for the boundary conditions/trip values.

Table 7 – Sequence of events and results for the reference LTSBO case.

EVENT DESCRIPTION	TIME [hh:mm] INL / RELAP5-3D (SOARCA report, [25])
Initiating event – Station blackout loss of all onsite and offsite AC power	00:00
Reactor trip MSIVs close RCP seals initially leak at 21 gpm/pump (~1 Kg/s)	00:00 (00:00)
TD-AFW auto initiates at full flow	00:01 (00:01)
First SG SRV opening	00:15 (00:03)
Operators control TD-AFW to maintain level	00:15 (00:15)
Operators initiate controlled cooldown of secondary at ~100 F/hr (~55.5 C/hr)	01:30 (01:30)
Upper plenum water level starts to decrease	01:40 (01:57)

45

Accumulators begin injecting	02:34 (02:25)
Vessel water level begins to increase	02:35 (02:30)
SG cool-down stopped at 120 psig (9.29 MPa) to maintain TD-AFW flow	03:41 (03:35)
Emergency CST empty	~06:20 (05:00)
DC Batteries Exhausted	08:00
SG PORVs reclose	08:00 (08:00)
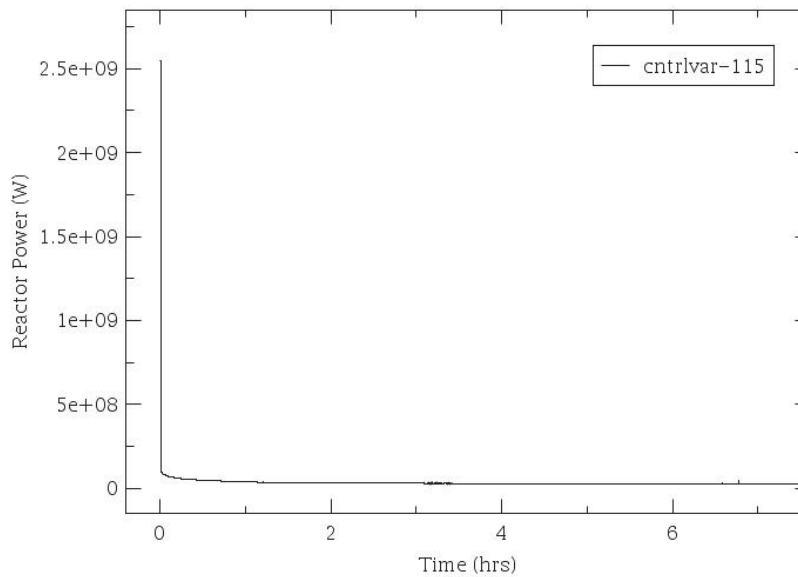
Figure 47 – Reactor Power.
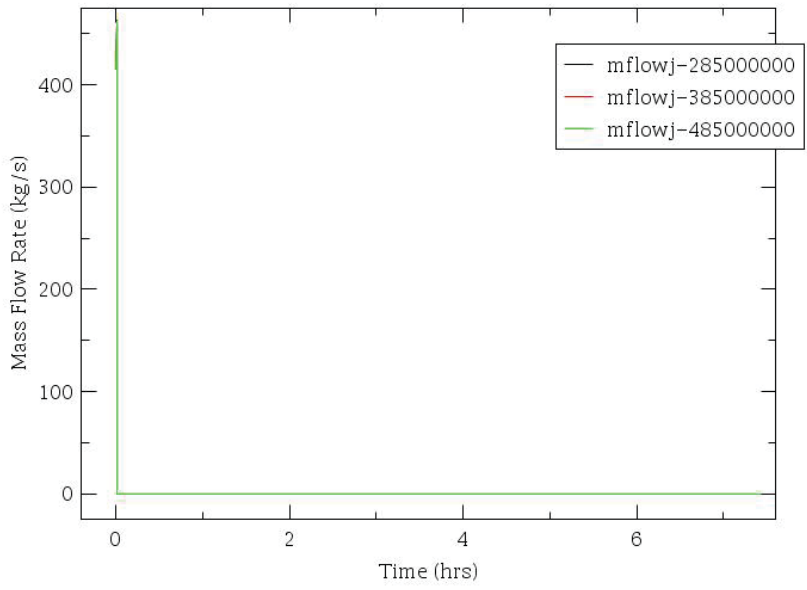
Figure 48 – SG Steam Line Mass Flow.
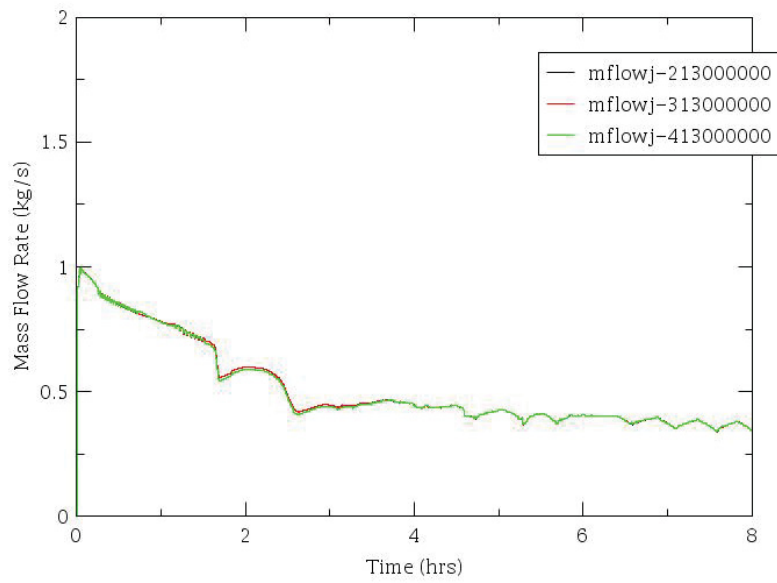
Figure 49 – MCP Seals LOCA.
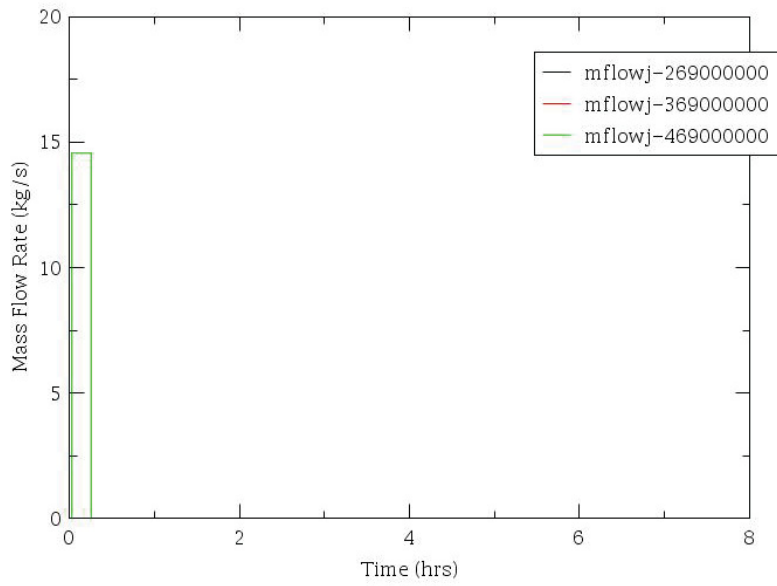
Figure 50 – TD AFW – Auto ON.
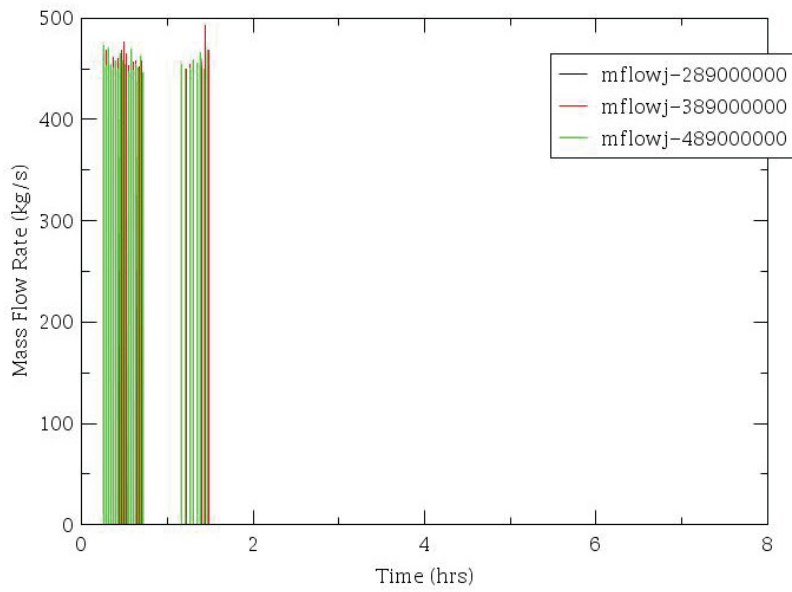
Figure 51 – SRV Mass Flow.
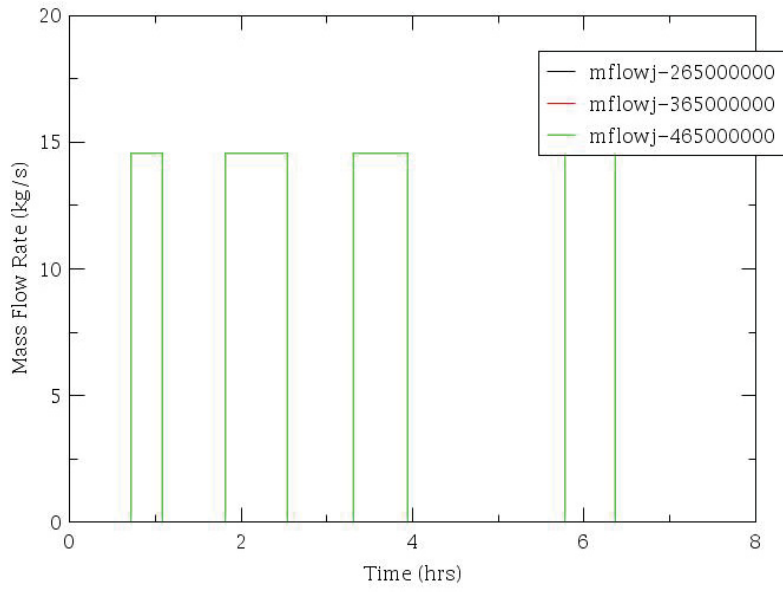
Figure 52 – TD-AFW Mass Flow Operator Control.
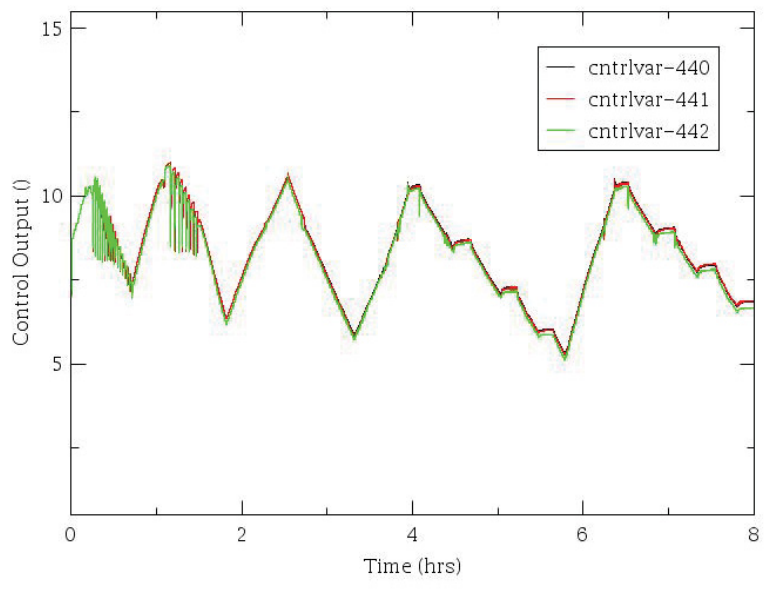
Figure 53 – SG Level Operator Control.
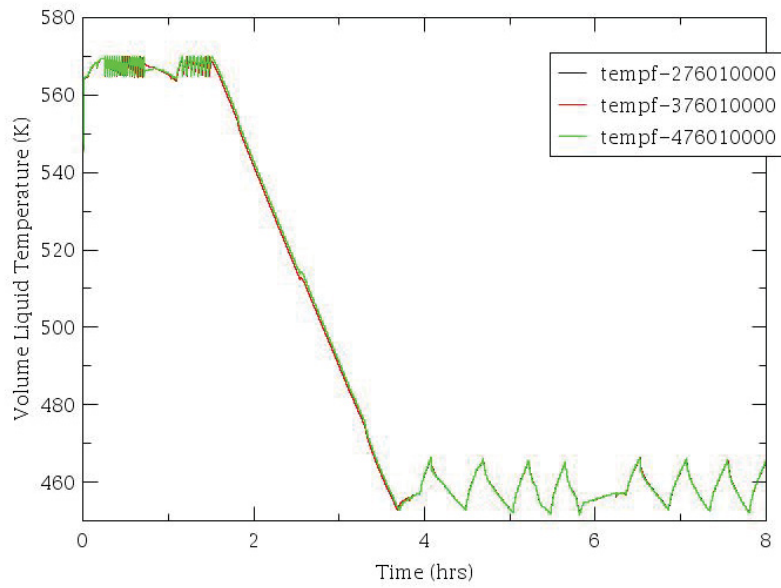
Figure 54 – SGs Temperature – Cooldown by operator.
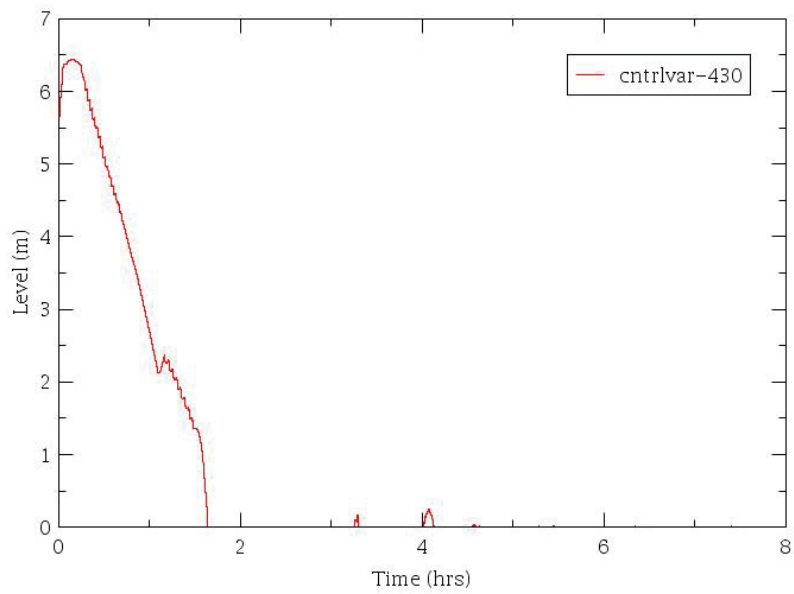
Figure 55 – Pressurizer Level.
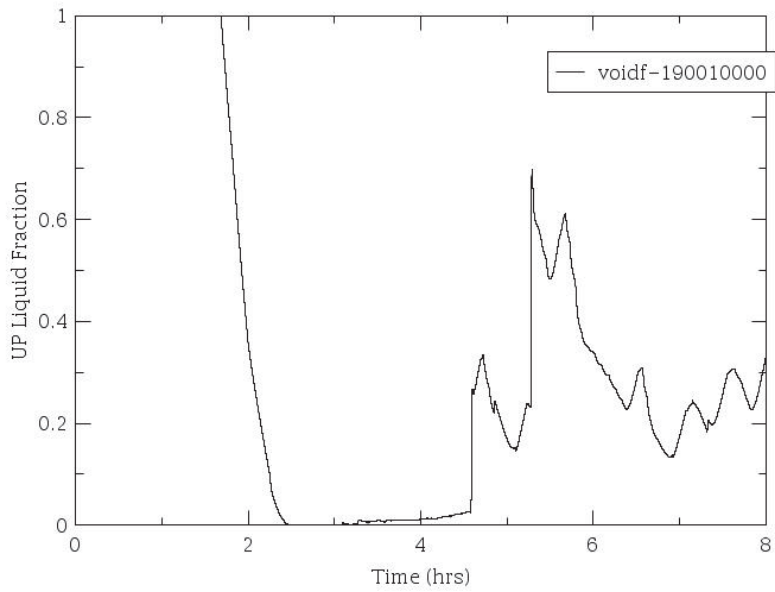
Figure 56 – Upper Plenum Liquid Fraction.
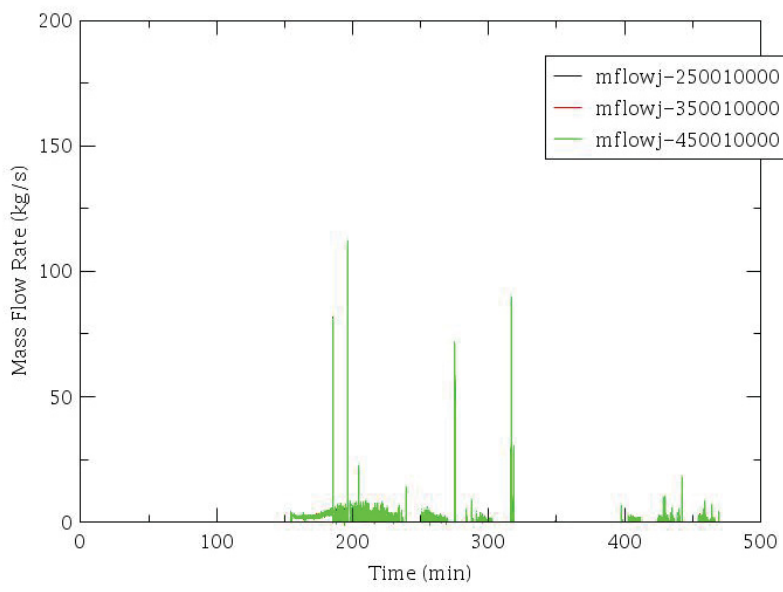
Figure 57 – Accumulators Injection.
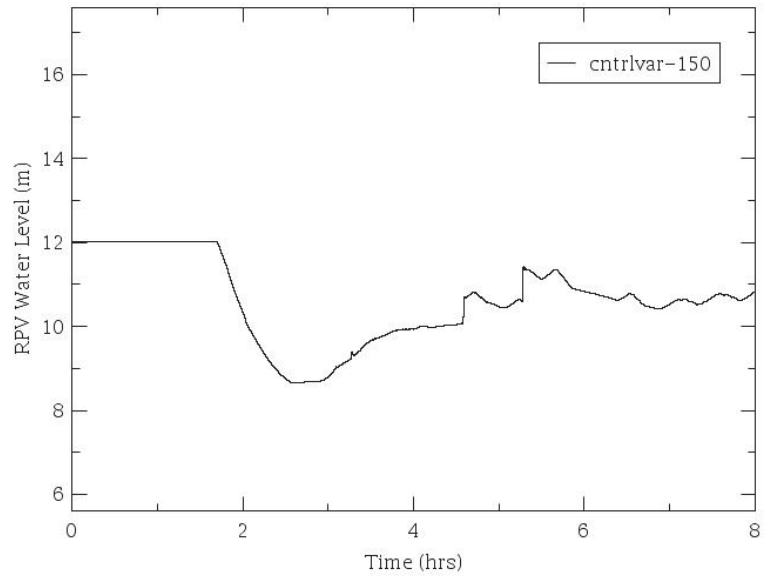
Figure 58 – RPV Water Level (TAF is at 6.722 m).
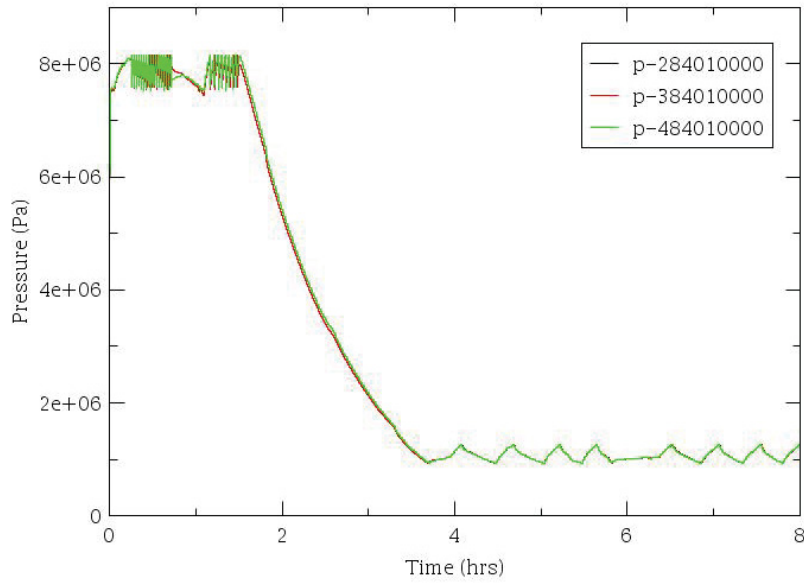
Figure 59 – SG Pressures.
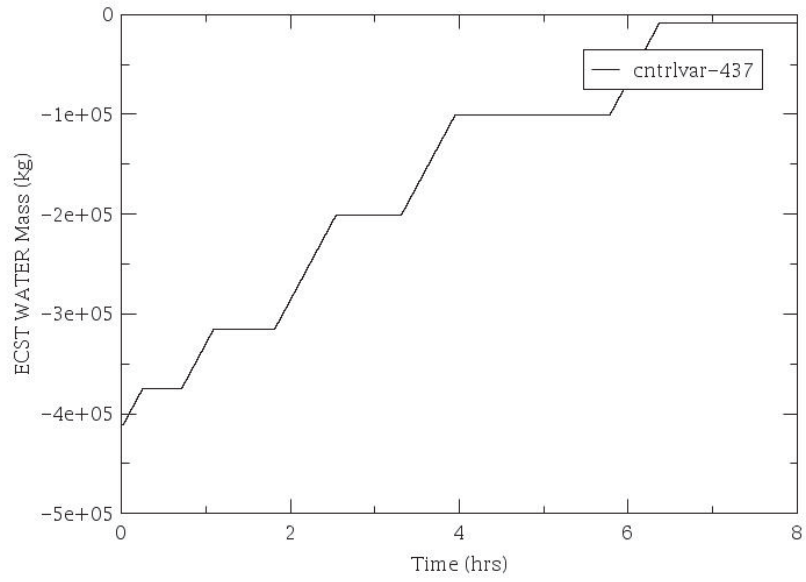
Figure 60 – Emergency Condensate Storage Water Tank Mass.
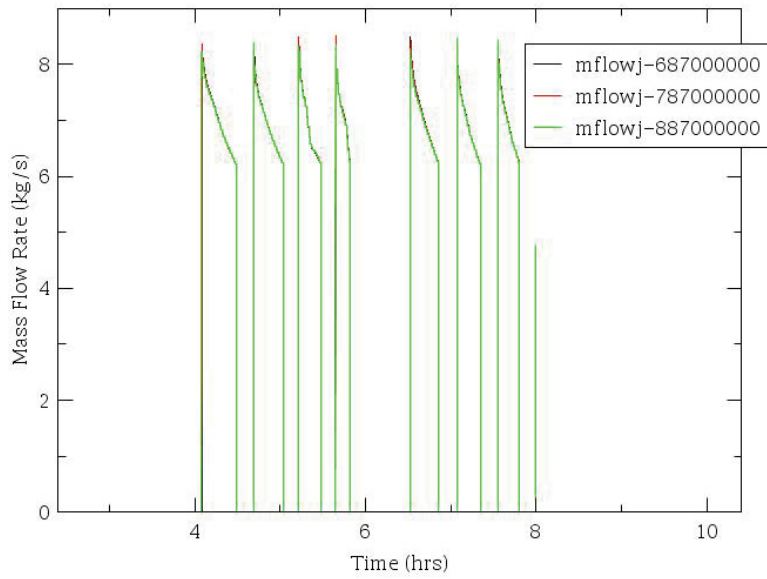
Figure 61 – SG PORV Openings.
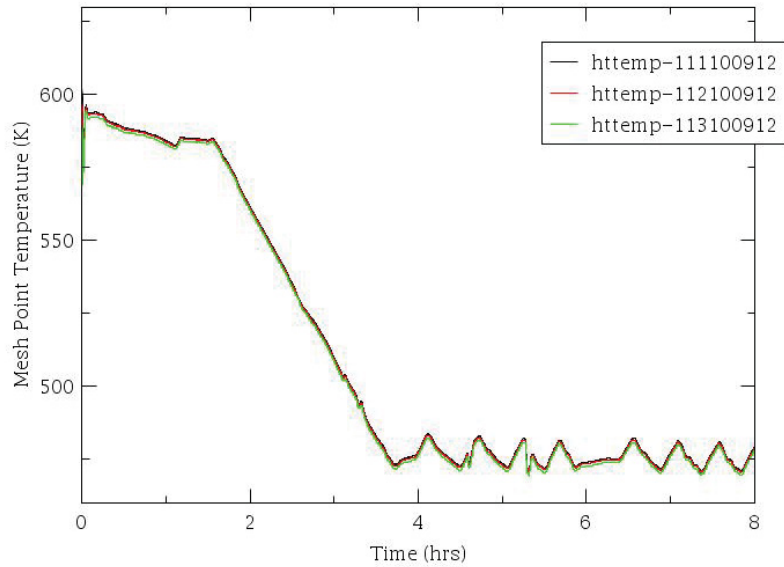
Figure 62 – Core Clad Temperatures.

3.4.4.2   STSBO results

A base case for the STSBO analysis has been also performed. The base case is intended to be the reference calculation for the dynamic-PRA and for the Sensitivities & UQ analyses as well. Standard sequence of events where obtained from [25]. Table 8 reports the sequence of events and Figure 63 to Figure 76 the charts of the transient parameters. For validation purpose, the timing of events calculated by MELCOR code is also reported. Deviations are minimal and are mainly due to different initial values for the boundary conditions/trip values.

Table 8 – Sequence of events and results for the reference STSBO case.

EVENT DESCRIPTION	TIME [hh:mm] INL / RELAP5-3D (SOARCA report, [25])
Initiating event Station blackout onsite and offsite AC power	00:00
Reactor trip MSIVs close RCP seals initially leak at 21 gpm/pump (~1 Kg/s)	00:00 (00:00)
TD-AFW auto initiates at full flow	00:01 (00:01)
EQ damage of ECST and of Auxiliary Buildings Loss of TD-AFW Loss of DC power	00:01.66 (N/A)
First SG SRV opening	00:04 (00:03)
SG Dryout	01:06 (01:16)
Pressurizer SRV open	01:12 (01:30)
Start of fuel heatup	01:58 (01:57)
PCT reaches safety threshold (~1500 K)	02:32
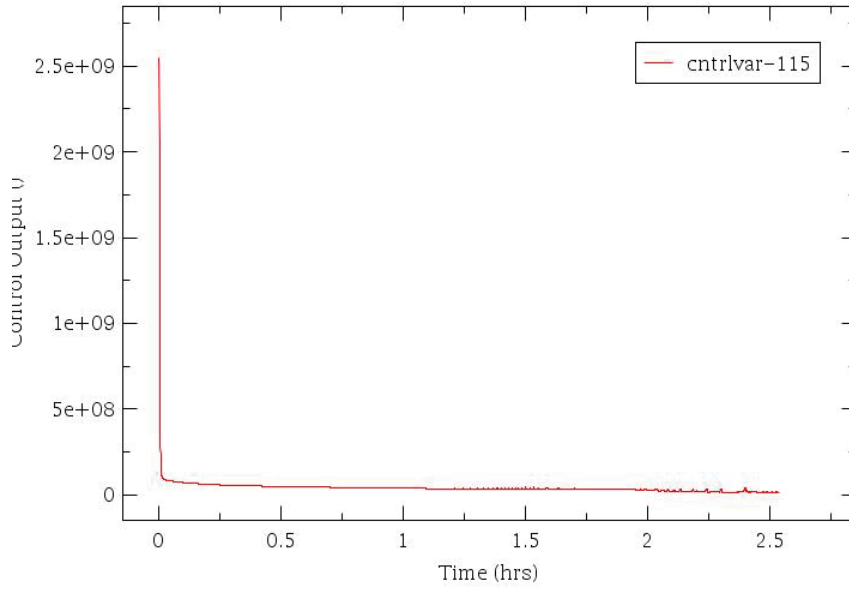
Figure 63 – Reactor Power.
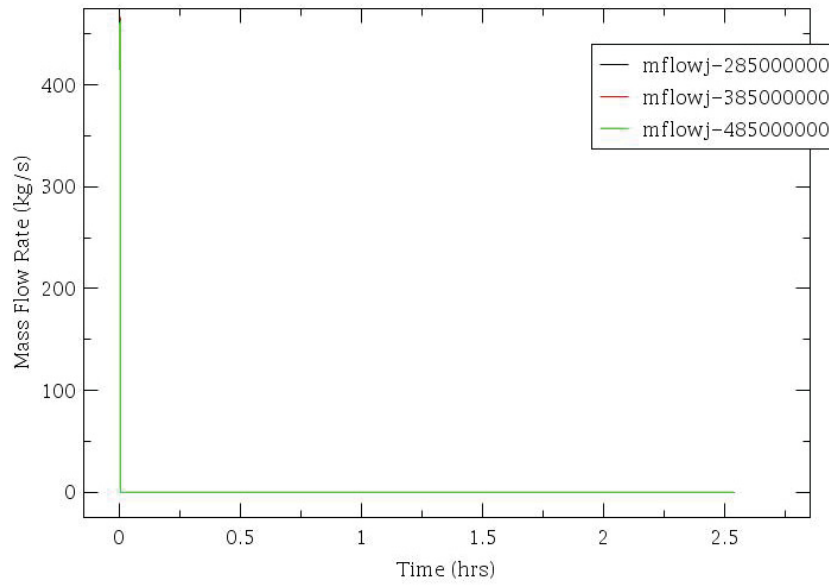
Figure 64 – SG Steam Line Mass Flow.
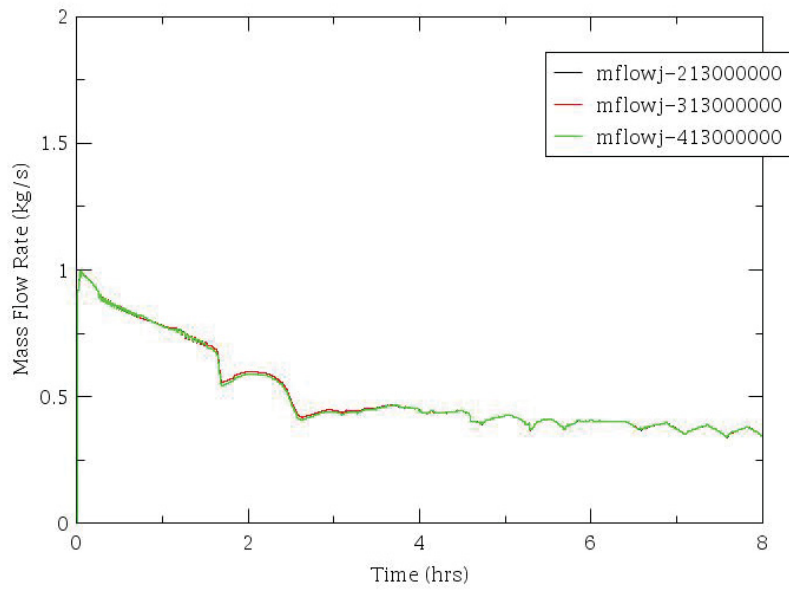
Figure 65 – MCP Seals LOCA.
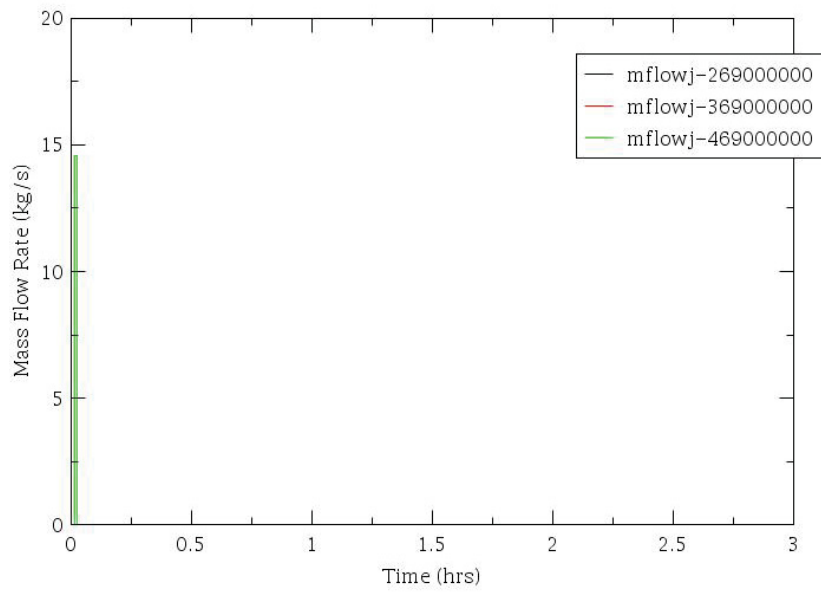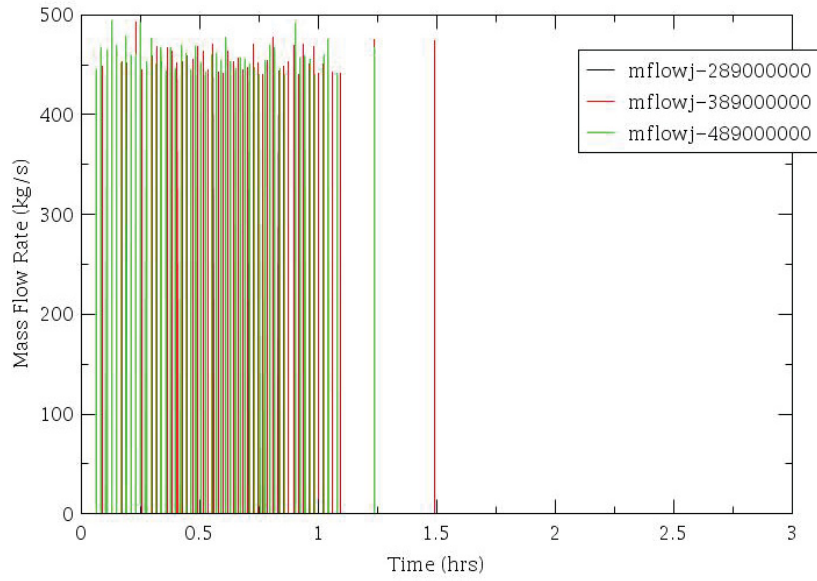

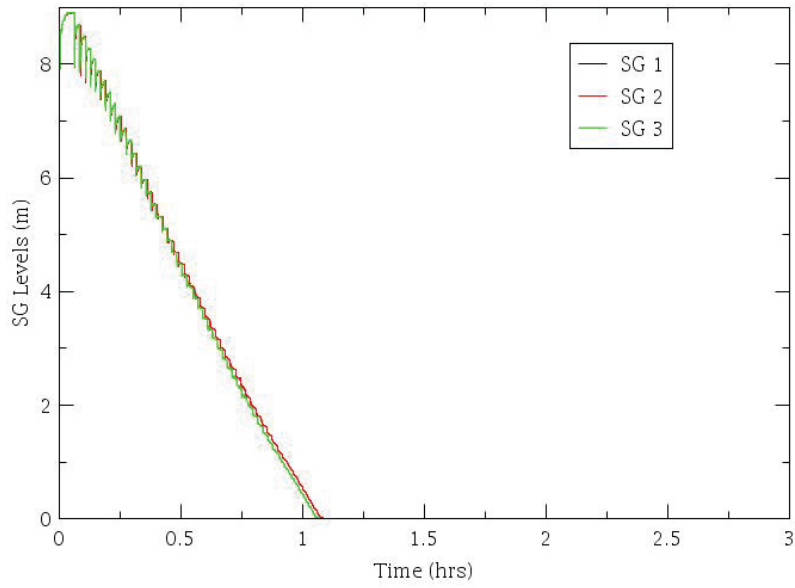Figure 66 – TD AFW – Auto ON.

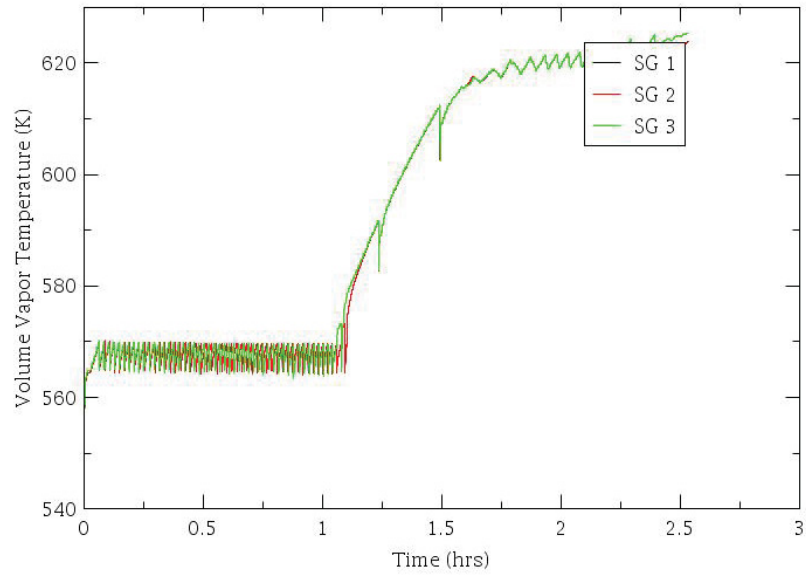Figure 67 – SG SRV Mass Flow.

Figure 68 – SG Level.
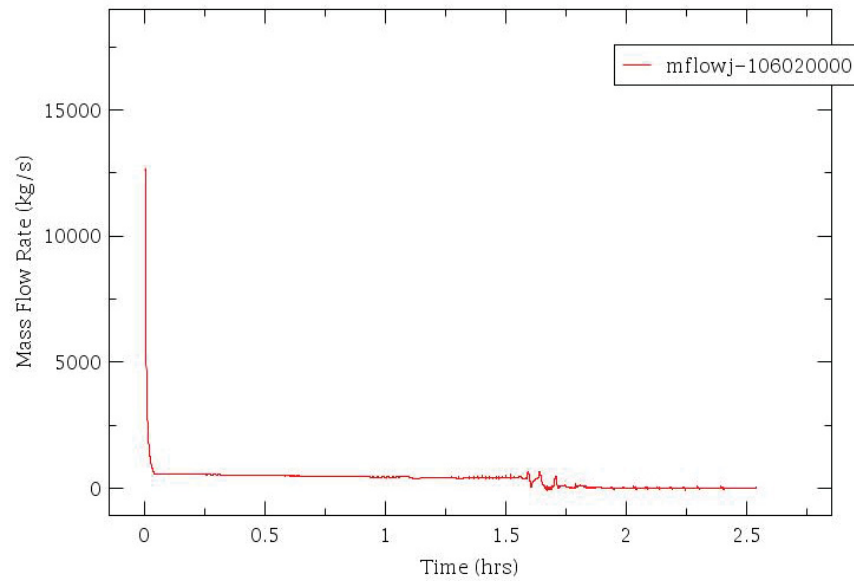
Figure 69 – SGs Temperature.
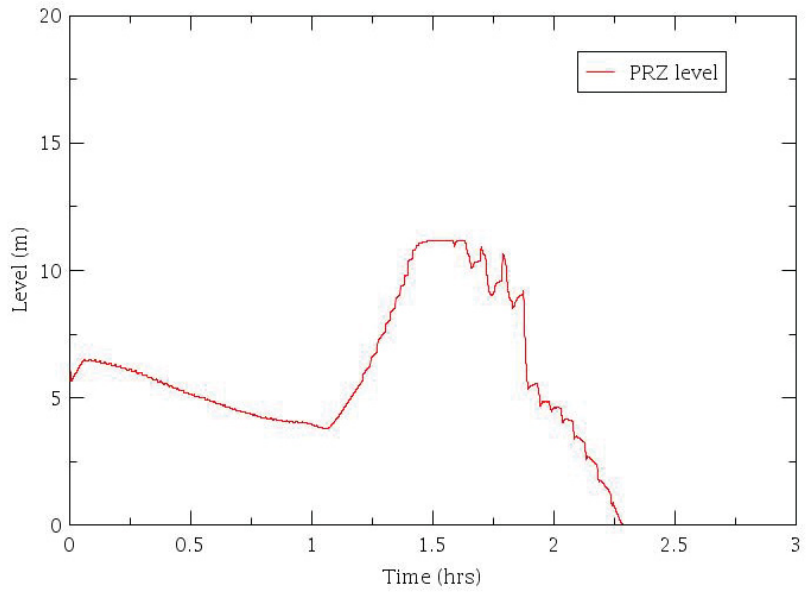

Figure 70 – Primary Side Mass Flow.
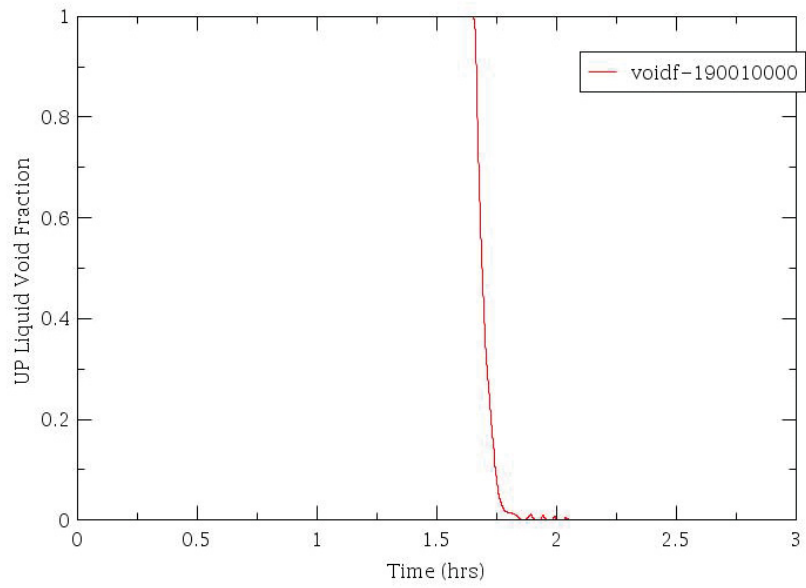
Figure 71 – Pressurizer Level.

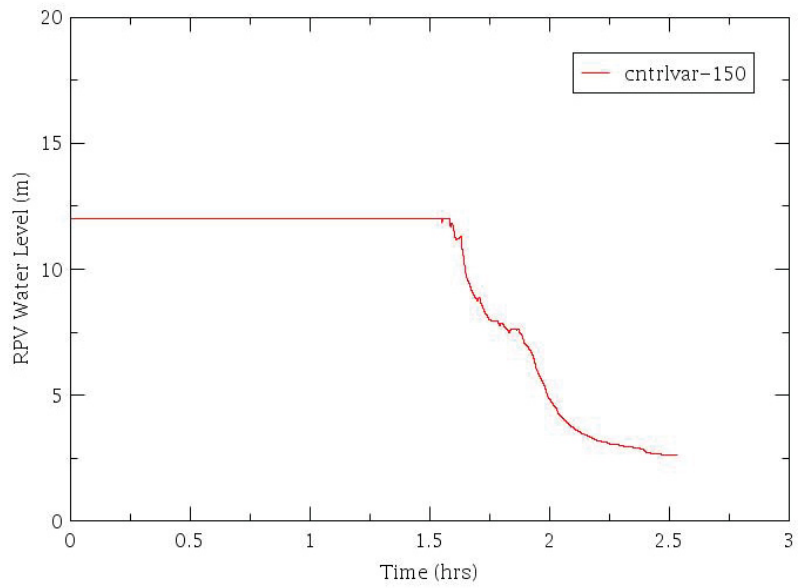Figure 72 – Upper Plenum Liquid Fraction.

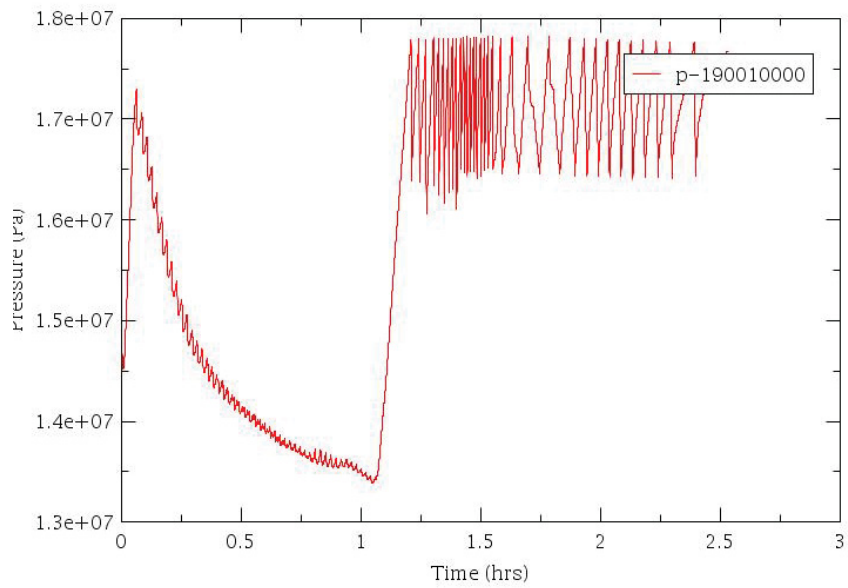Figure 73 – RPV Water Level (TAF is at 6.722 m).

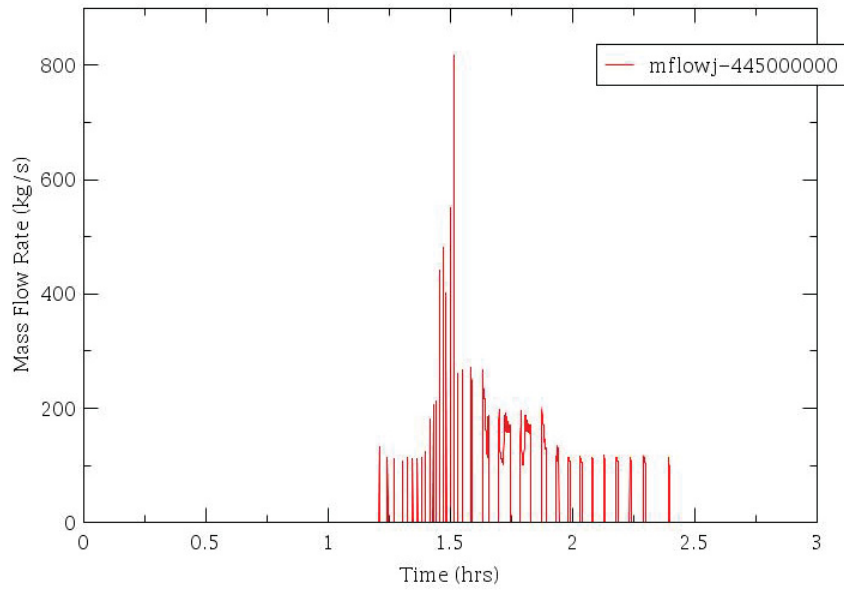Figure 74 – UP Pressure.

61

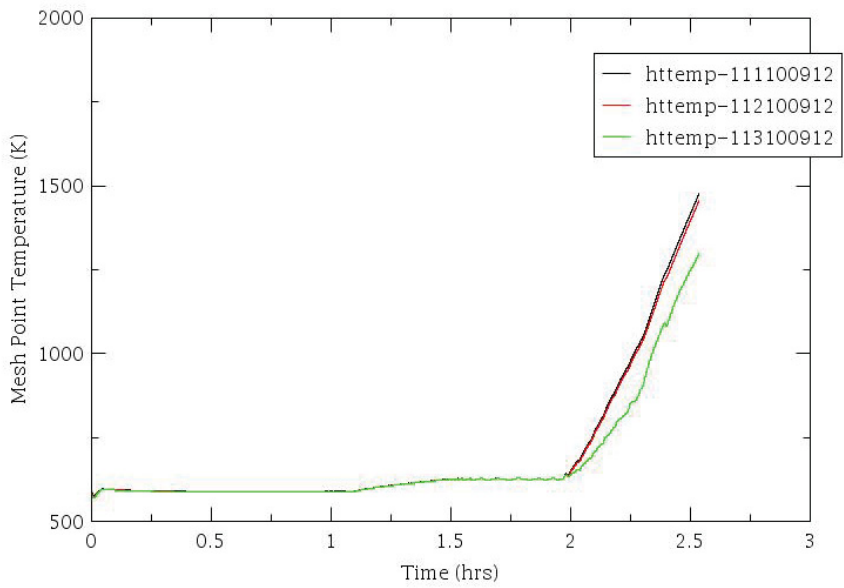Figure 75 – PRZ SRV Openings.

Figure 76 – Core Clad Temperatures.

3.4.5 Sensitivity Analysis & Uncertainty Quantification

The advanced use of Best Estimate tools combined with the PRA implies the quantification of the uncertainties of the calculations (i.e., performing BEPU calculations).

Several methodologies exist for the quantification of the uncertainty, some of them requiring a large amount of human resources [27]. Performing a detailed UQ for a SBO event is beyond the scope of the IA2. Therefore this section will show how one of these methodologies, in particular one requiring the propagation of the input and code uncertainties, could be applied (see Figure 77).
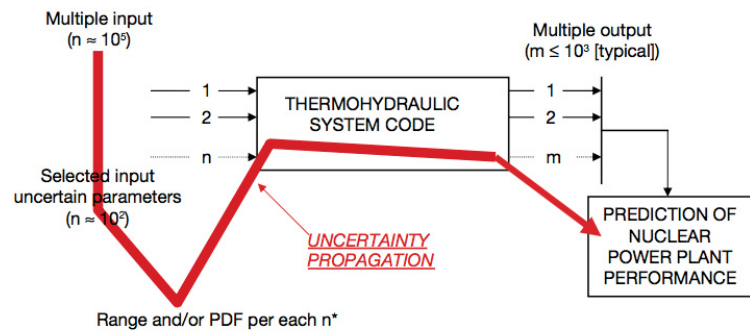

Figure 77 – Input Uncertainty Propagation.

The uncertainties quantification is applied to the RELAP5-3D calculations only. The RAVEN code is applied for the automatic processing of the RELAP5-3D input parameters and for the output data processing.

In general, every UQ method is based on the following steps:

1. Selection of the NPP and scenario
2. Characterization of the scenario and identification of important phenomena
3. Selection of the code
4. Preparation and qualification of the input deck
5. Selection of the uncertainty method
6. Application of the uncertainty method
7. Comparison of the results with the relevant criteria

Points 1, 3 and 4 are addressed by the selection of the IGPWR (paragraph 3.4.2), SBO scenarios (paragraph 3.4.1), RELAP5-3D code and relative SBO input deck qualification (paragraphs 3.4.3 and 3.4.4).

For the characterization of the scenario and the identification of important phenomena, it should be noted that:

- this step is generally performed by means of the Phenomena Identification and Ranking Table (PIRT) development. A PIRT development may require the efforts of several experts and it is beyond the scope of the IA2.

- for the sake of simplicity, a simplified analysis of thermal-hydraulic phenomena is proposed hereafter. In particular, three phases are identified for the LTSBO characterized in paragraph 3.4.1 and paragraph 3.4.3., i.e.:

  o Phase I: from t=0.0 s to t=1.5 hr. Reactor scram, pump run-down, MCP seal LOCA, SG SRV actuation, establish single phase natural circulation (NC), SG at full pressure, primary side depressurization

  o Phase II: from t=1.5 hr to t=3.41 hr. SG depressurization by feed & bleed, secondary and primary side pressure and temperature reduction, single phase NC, SG PORV actuation

  o Phase III: from t=3.41 hr to t=8 hr. SG and primary side at constant pressure and temperature, single phase NC, SG PORV actuation

- Four main phases are instead identified for the STSBO scenario, i.e.:

  o Phase I: from t=0.0 s to t=3.8 min. Reactor scram, pump run-down, MCP seal LOCA, SG SRV actuation, establish single phase natural circulation (NC), SG at full pressure, primary side pressurization

  o Phase II: from t=3.8 min. to t=1.1 hr. SG pressurization and dry-out, primary side pressure reduction, single phase NC, SG SRV actuation

  o Phase III: from t=1.1 hr to t=1.96 hr. Primary side pressure increase, single phase NC, PRZ SRV actuation, RPV water level decreases, SG temperature increases

  o Phase IV: from t=1.96 hr to t=2.5 hr. Core heat-up, PRZ SRV actuation.

- The most important thermal-hydraulic phenomena characterizing the above phases are identified. They are:

  o Single phase NC in the primary loop

  o Secondary side mass inventory loss through the SG SRV and PORV

  o Primary mass inventory loss through the MCP seal

  o Heat transfer between primary and secondary system

- The Figure of Merits (FOMs) selected for the analysis is the coping time (CT), or the time available before the occurrence of fuel damage (PCT = 1500 K), and the PCT itself. This choice is justified by the possibility of having two types of transients: one involving fuel damage (STSBO), the other involving an eventual fuel overheating (LTSBO).

- The following list of the input parameters were selected for the sensitivity analyses and their uncertainty band was specified:

o Core Decay Heat, with a uniform uncertainty distribution of +/-10% of the nominal value. This sensitivity take into account the uncertainty on the decay heat power

o Core Pressure Losses: uniform uncertainty distribution resulting in a variation of +18% and -25% of the mass flow. It takes into account the uncertainties on the vertical and the cross-flows during the natural circulation phase at low flow

o Critical Flow at the SRV/PORV: uniform uncertainty distribution resulting in a variation of +/- 30% of the flow area. It take into account uncertainties in the critical flow prediction and the valves inlet conditions

o Mass Flow through the MCP seal break: a variation of +/- 20 gpm is considered. It takes into account the uncertainty in the seal break area and on its modeling.

Table 9 – Sensitivity Parameters.

Run #	Sensitivity Parameter
Reference Case	Nominal values
1A	Core Decay Heat +10 %
1B	Core Decay Heat -10 %
2A	Reduction of RPV internal circulation mass flow
2B	Increase of RPV internal circulation mass flow
3A	SG PORV and SRV valve flow areas increased by 30%
3B	SG PORV and SRV valve flow areas decreased by 30%
4A	MCP seal LOCA at +20 gpm
4B	MCP seal LOCA at -20 gpm

The demonstration of the propagation of the uncertainties of the four parameters listed above is carried on using the CSAU methodology (point 5).

Preliminary sensitivity calculations are run (see Figure 78 - Figure 85) for assessing the effect of the single uncertainty parameters on the FOMs (CT and PCT).
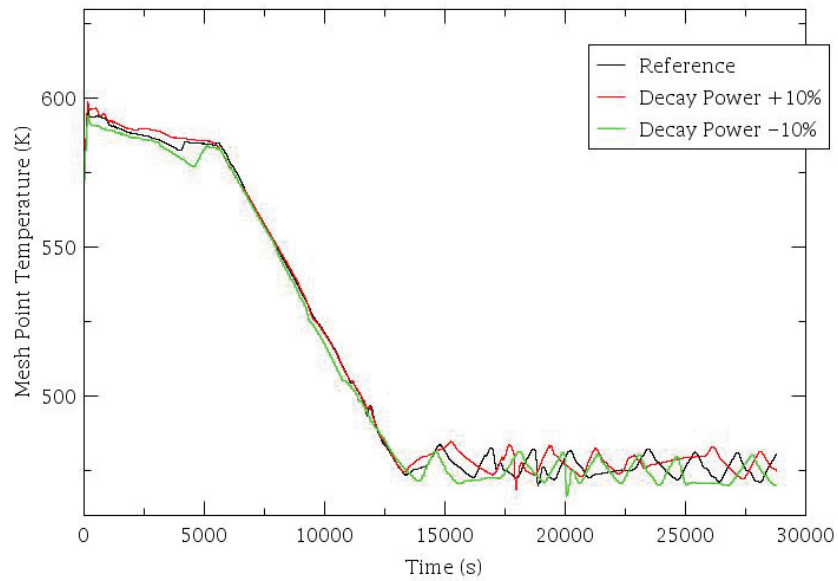
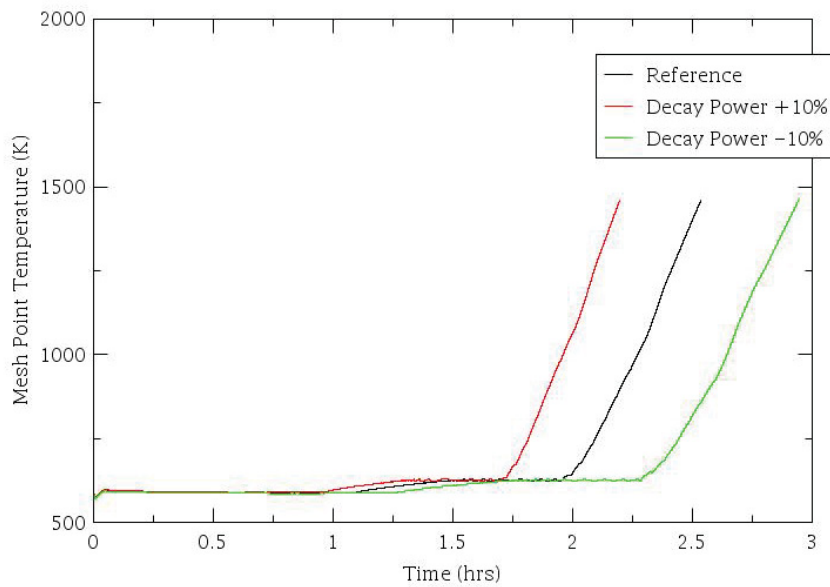Figure 78 – Core Power Sensitivity – LTSBO.

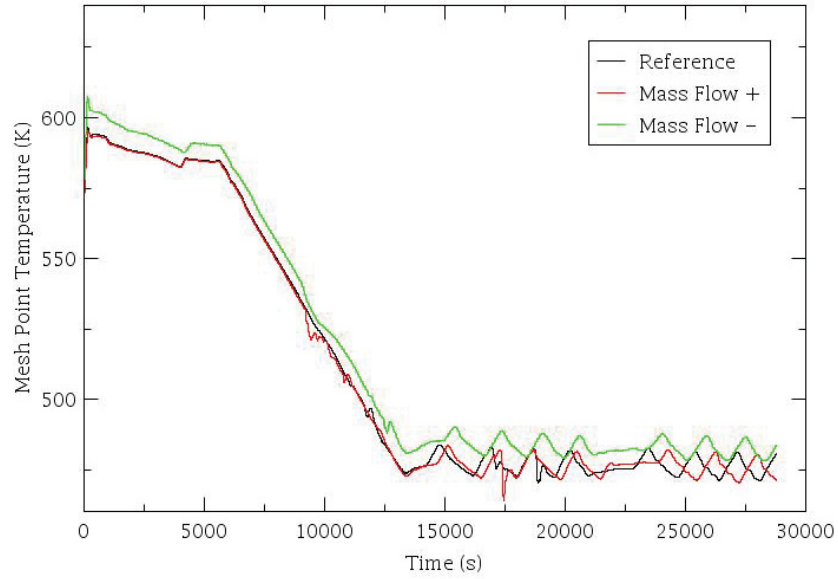Figure 79 – Core Power Sensitivity – STSBO.
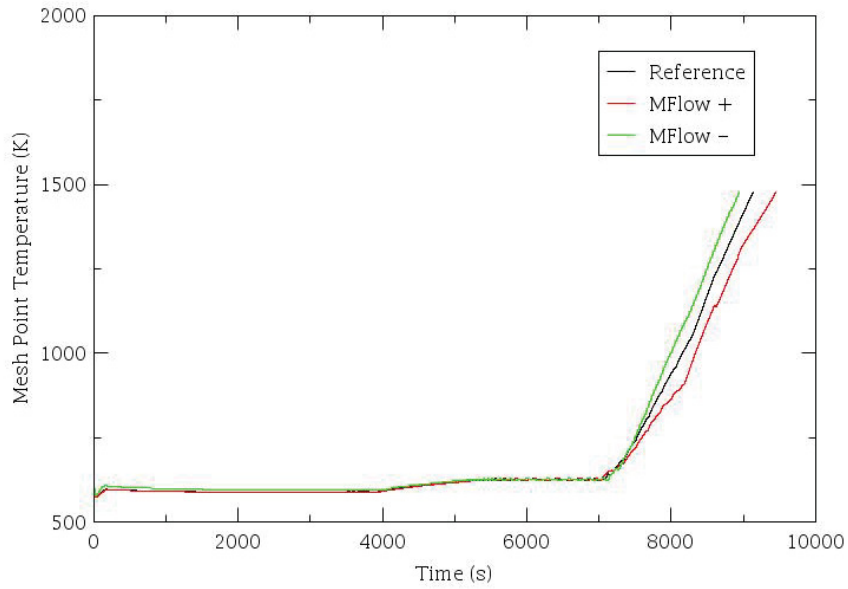
Figure 80 – Core Mass Flow Sensitivity – LTSBO.

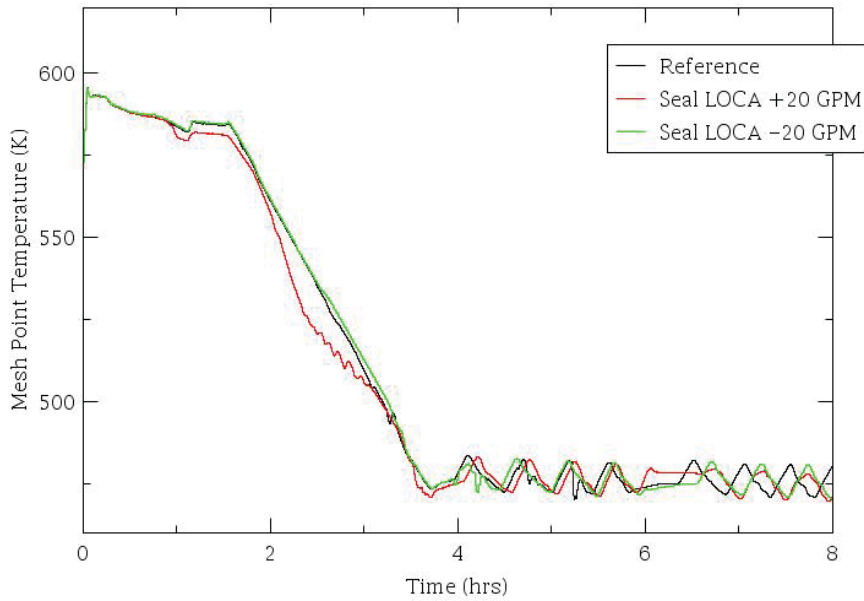Figure 81 – Core Mass Flow Sensitivity – STSBO.

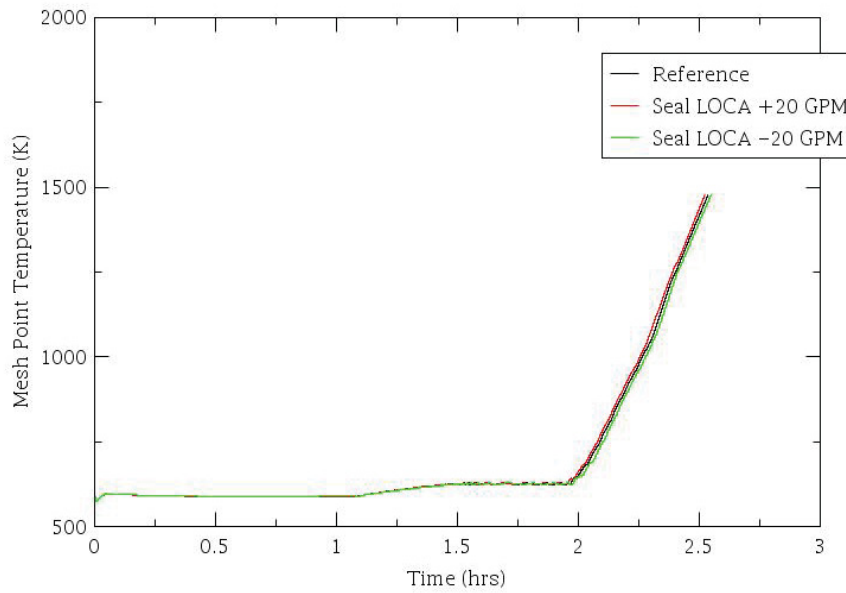Figure 82 – MCP Seal LOCA Sensitivity – LTSBO.

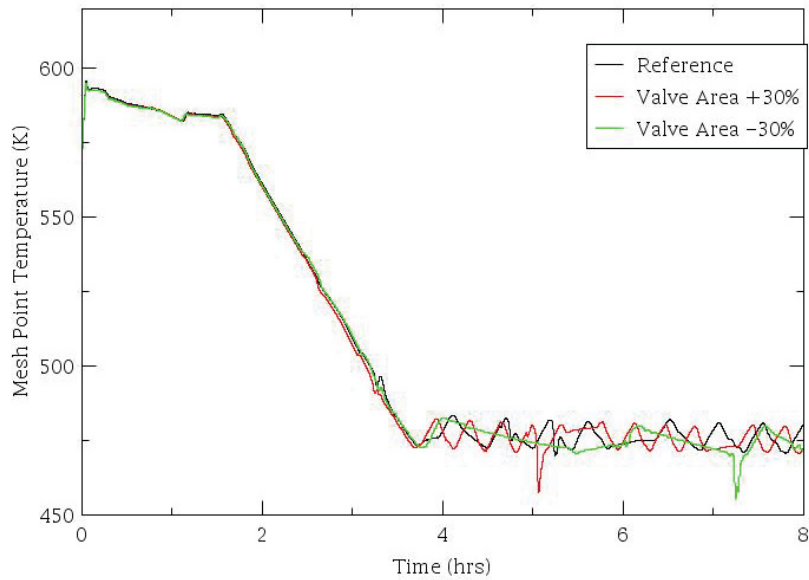Figure 83 – MCP Seal LOCA Sensitivity – STSBO.

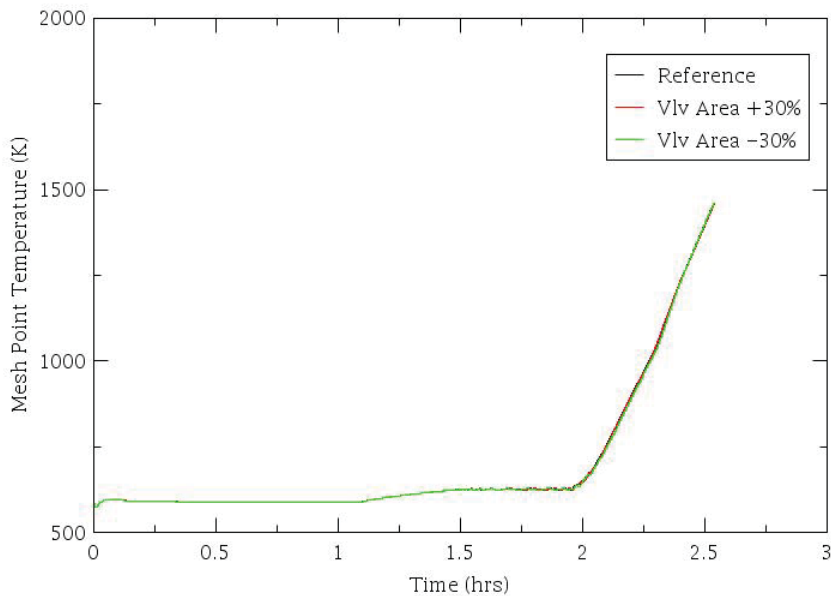Figure 84 – SRV/PORV Area Sensitivity – LTSBO.

Figure 85 – SRV/PORV Area Sensitivity – STSBO.

Then input parameters are simultaneously perturbed by RAVEN code using a Monte Carlo sampler. Wilks' formula [28] is used for achieving a 95% fractile/95% confidence limit on the resulting FOM. 59 calculations are runs (see Figure 86 and Figure 87). Ranking of the input uncertain parameters is also performed 'a posteriori, identifying the correlation coefficients between the FOMs and input uncertainties.
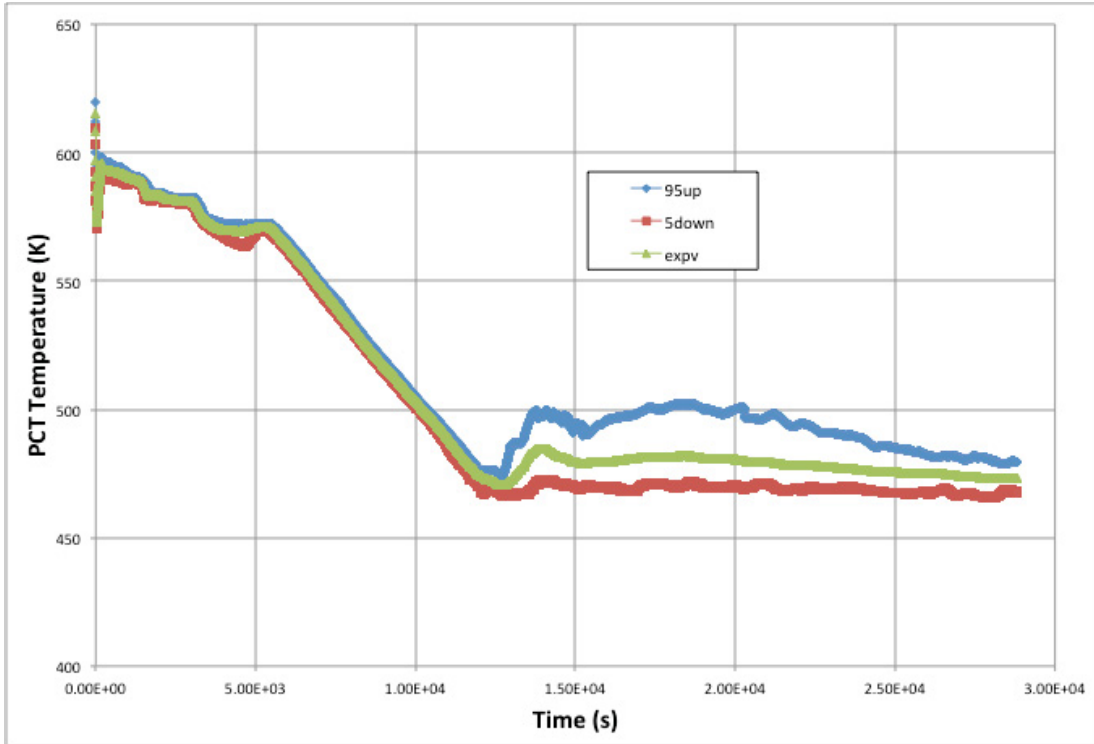
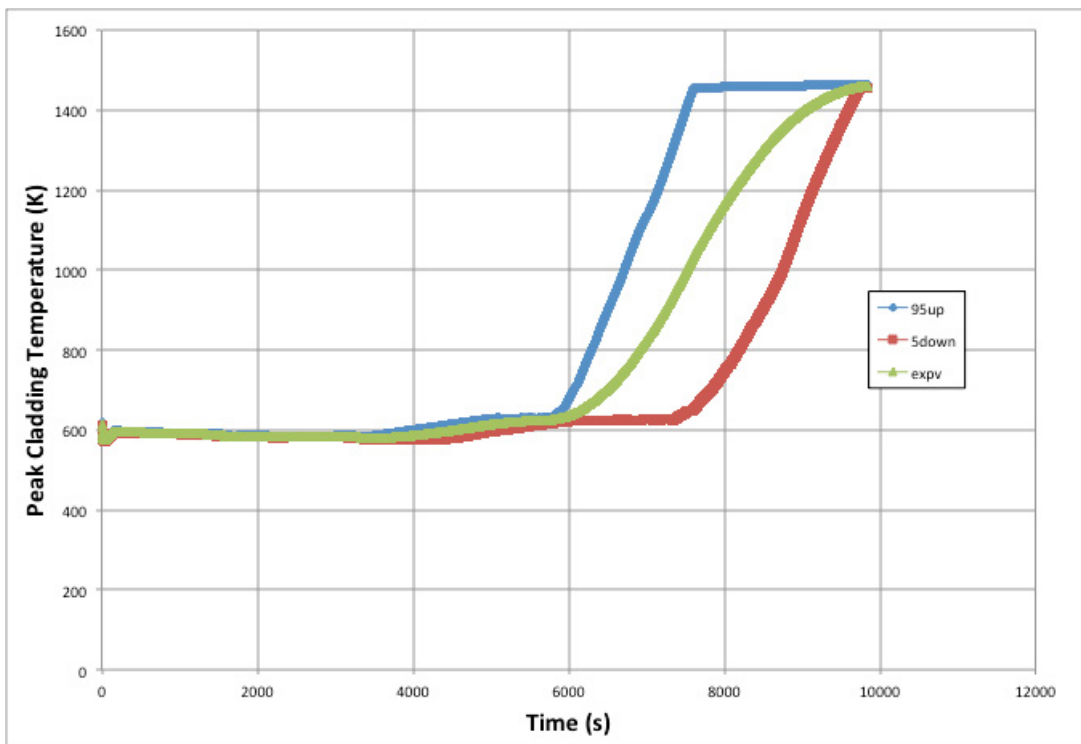Figure 86 – RELAP5-3D/RAVEN 59 Calculations – LTSBO.

Figure 87 – RELAP5-3D/RAVEN 59 Calculations – STSBO.

4. COUPLING

Each of the analysis tools described above provides detailed information for one specific area. Dynamically combining each of these areas provides a more complete picture and result for the defined range of scenarios. Coupling the tools is done using EMRALD code (see Figure 88).
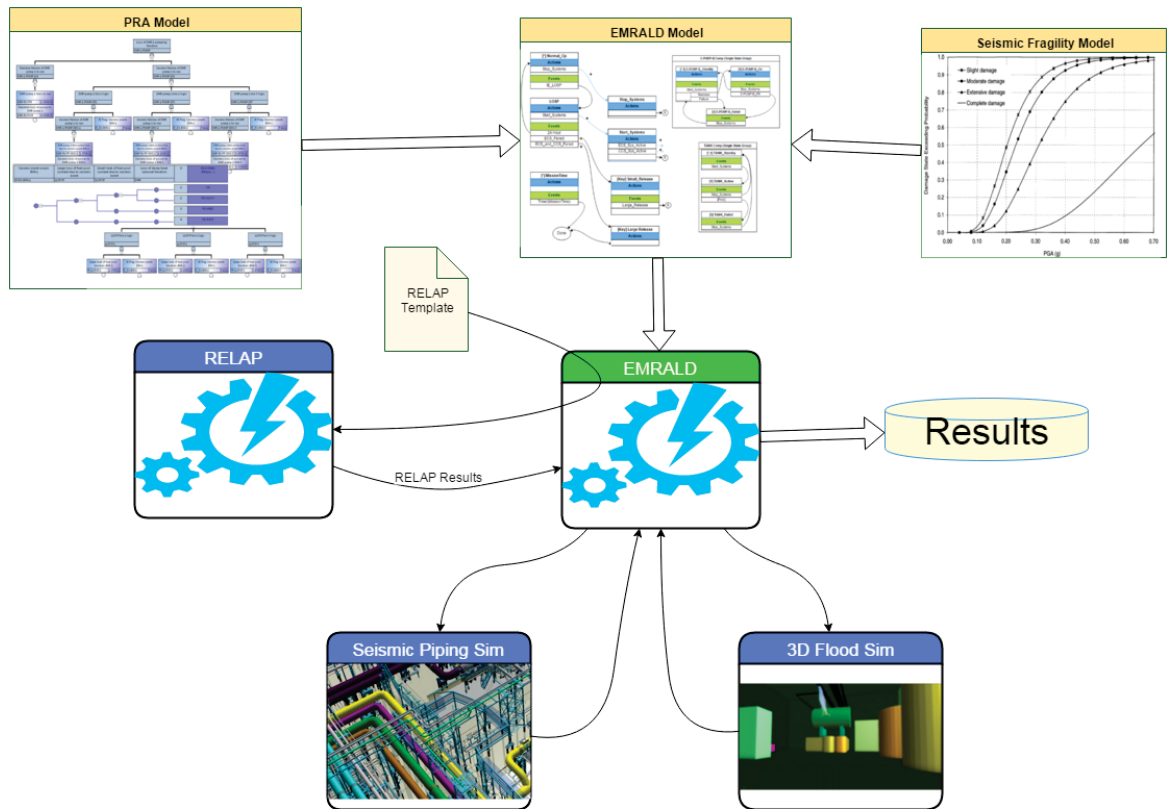

Figure 88 – IA2 tools workflow.

4.1 Steps

This stage of the demonstration consists of running each of the analysis methods for a defined path or events. This has allowed us to test the model for each tool and (if applicable) to test the dynamic execution of the tool and retrieval of result data.

4.1.1 Add seismic data to the plant response diagram

As described in section 3.1 site seismic analysis results were used to generate joint failure probabilities for a given PGA. This data was precompiled and the curves are used in the plant response diagram to dynamically adjusting the failure probability for a given joint according to the sampled seismic event. Although the data used will normally be dynamically chosen, testing

a hard coded seismic event with a given PGA was used. A sampling method to generate the PGA for the seismic event still needs to be developed.
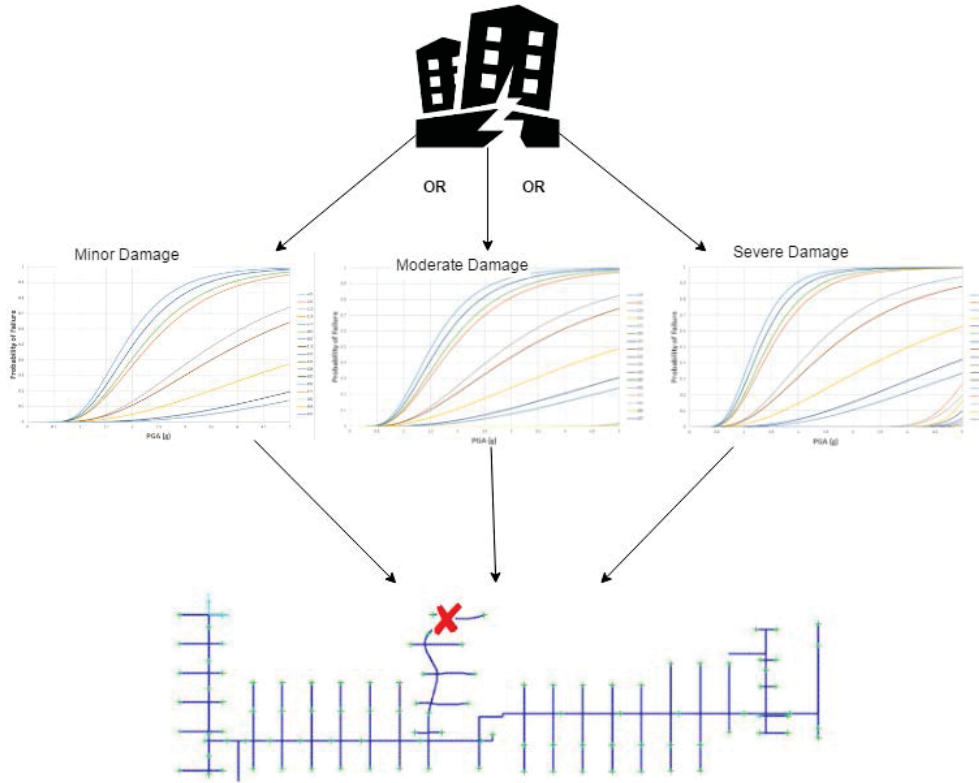

Figure 89 – Mapping of seismic event to piping fragility.

4.1.2   SAPHIRE PRA to Dynamic EMRALD model

DGEN and AFW fault trees from the SAPHIRE model were added and simulated in the EMRALD model. Each sub tree was evaluated to verify the results matched that produced by SAPHIRE. The following table shows result comparisons between SAPHIRE's answer and EMRALD simulation results.

Table 10 – SAPHIRE/EMRLAD comparison.

PARAMETER	SAPHIRE	EMRALD
UDCBAT_1B	4.24E-02	4.24E-02
UDC_CTRLPWR_1	1.90E-03	1.84E-03
UDC_CTRLPWR_1	1.90E-03	1.84E-03
AFW_MDP_P1	4.61E-02	4.59E-02
AFW_MDP_P2	4.61E-02	4.61E-02
AFW_MDP_P3	4.61E-02	4.63E-02
AFW_MDP_P4	4.61E-02	4.62E-02
AFW	1.49E-02	1.30E-02

The EMRALD model can be run without the flooding or RELAP5-3D pieces and a static seismic event to verify it matches the SAPHIRE results. This also provides a baseline for comparing how the flooding analysis and RELAP5-3D results change the overall probability.

4.1.3 3D Flooding Coupling

The 3D flooding simulation was run using EMRALD (see Figure 90). By fixing the probability of a given joint failure to 100%, NEUTRINO was executed and ran with flooding from the failed joint at xyz position (-5.28, 1, 1.3). The spray of water onto the measurement field UDC_125VDC_PNL_1 and sent an event back to EMRALD. This event triggered the movement of component UDC_125VDC_PNL_1 state from "Active" to "Failed".
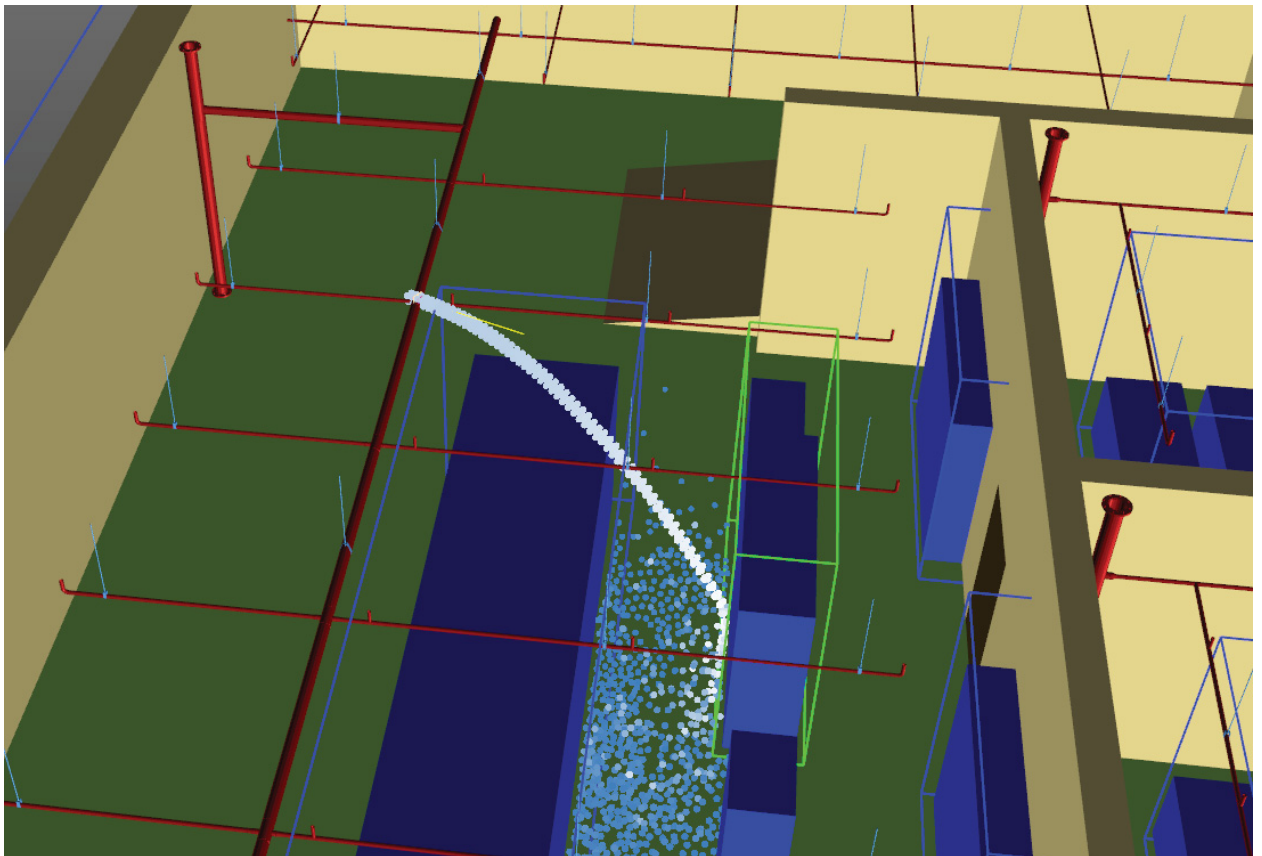

Figure 90 – Pipe rupture causing component failure due to water spray.

4.1.4 RELAP5-3D Execution

The final step is to run RELAP5-3D for the thermal hydraulics analysis if there is the possibility of fuel damage. For this test we use the failure of UDC_125VDC_PNL_1 as that caused by the flooding and forced the failure of UDC_125VDC_PNL_2 due to the seismic event. This causes the failure of DC Power. AC power was gone for more than 8 hours so EMRALD started RELAP5-3D setting DC Power to 1 hr and AFW failure time to 0 hour. The results from RELAP5-3D are then used determine if there is fuel damage.

In the following example the above variables were modified as the following:

- MCP Seal LOCA break area: multiplied by 1
- Battery failure caused by flooding: occurring at time t = 1 hr.
- AFW failure: 0 hr.

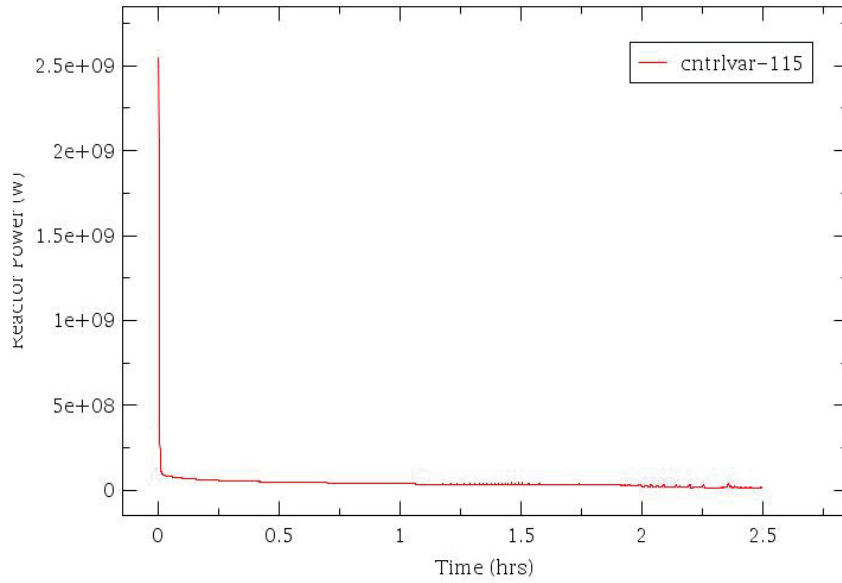The RELAP5-3D/EMRALD results are reported hereafter (see Figure 91 - Figure 96).
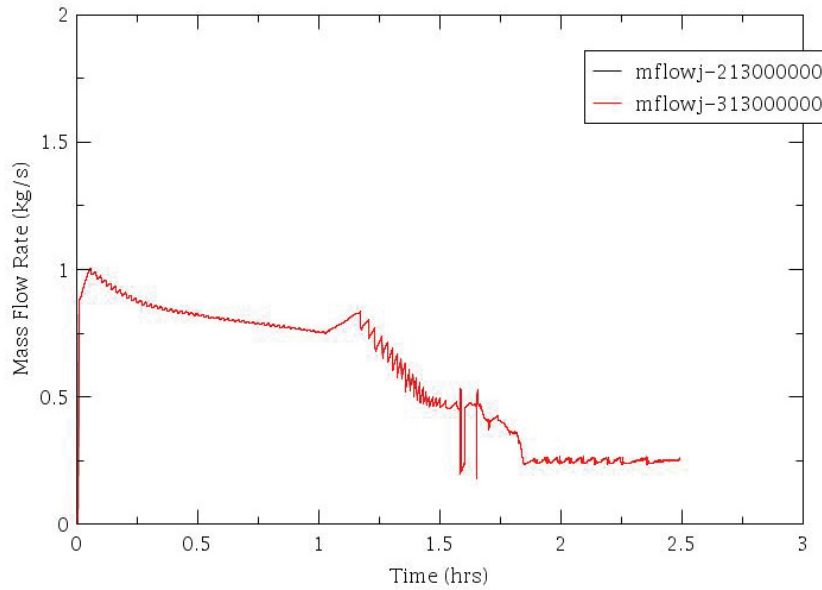

Figure 91 – Reactor Power.
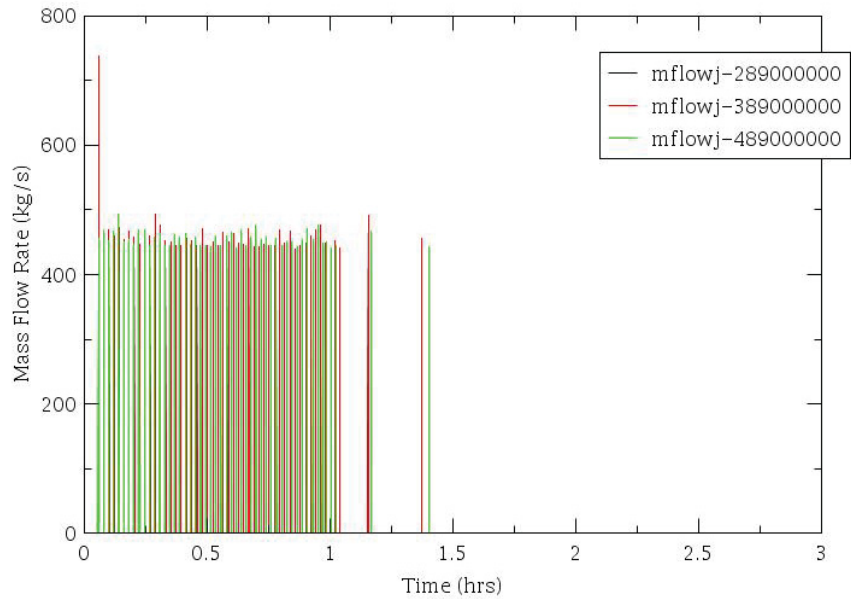

Figure 92 – MCP Seals LOCA.
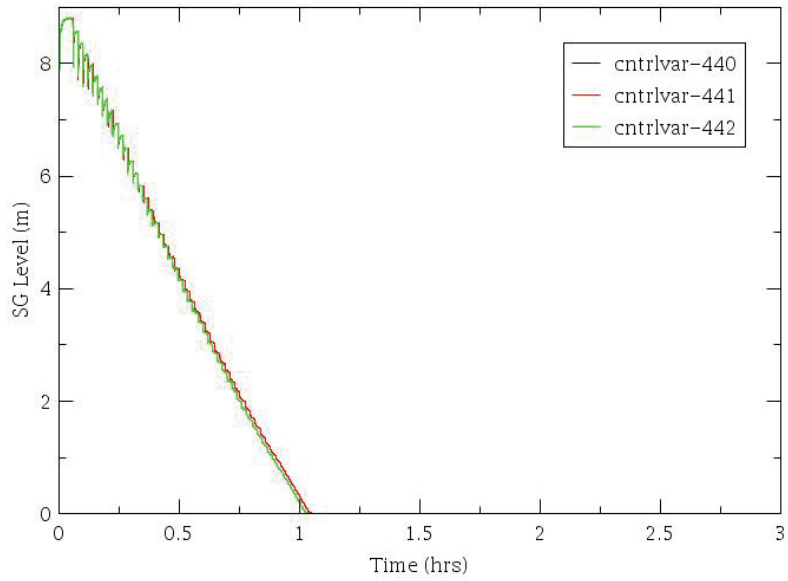
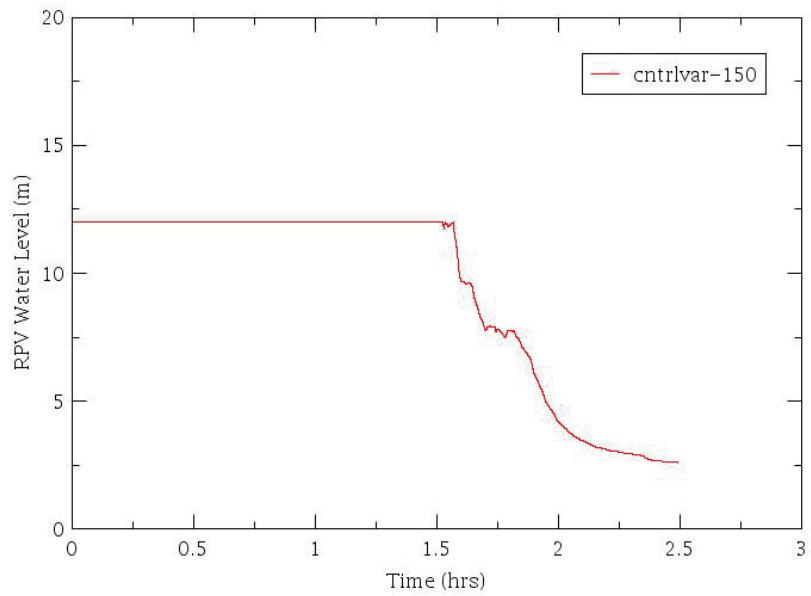Figure 93 – SG SRV Mass Flow.

Figure 94 – SG Level .

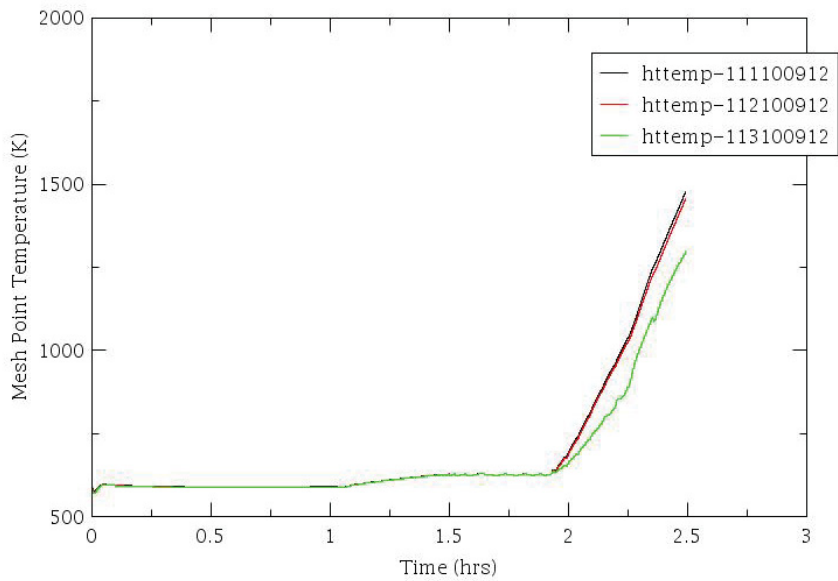Figure 95 – RPV Water Level (TAF is at 6.722 m).

Figure 96 – Core Clad Temperatures.

4.1.5   Results

Initial testing of each analysis tool is successfully executed and a method for coupling these tools is demonstrated. More detailed models are needed before multiple simulation runs can generate more plant-specific results. In particular, piping fragilities are still being developed in order to provide viable failure rates. The EMRALD model needs to handle all piping failure options, estimating different flooding scenarios. Finally the RELAP5-3D model should be adjusted to allow longer event analyses and handle recovery events. When these adjustments are completed, multiple detailed simulations can be run using Monte Carlo sampling.

5. PATH FORWARD

In this document we have presented the rationale for the LWRS/RISMC/IA2 activities, the RISMC methodology and the IA2 baseline toolkit. We have also shown the first results of a combined deterministic-probabilistic analysis of an EQ-induced SBO scenario with internal flooding for a PWR.

Results were obtained by coupling a set of state-of-the-practice tools (LS-DYNA, OPENSEES, NEUTRINO, EMRALD, RELAP5-3D, RAVEN) and by developing realistic models of the NPP and of its SSCs.

The following analyses were performed:

- EQ propagation and Non-Linear Soil-Structure Interaction

- Determination of the Response Spectra for the NPP Auxiliary Building and for the sprinkler system

- Determination of the EQ-induced stresses on the sprinkler system

- Deterministic flooding analysis of the battery rooms

- LTSBO and STSBO system thermal-hydraulic analyses (bounding events)

- UQ for the LTSBO and STSBO scenarios, determination of FOMs and of relevant independent variables

- Integration of the structural mechanics, flooding and system TH calculations in a dynamic PRA model

It should be noted that for the milestone described in this report, only one of the possible PRA-determined SBO scenarios were analyzed. As the modeling development evolves, we will perform a significant larger number of NEUTRINO-EMRALD-RELAP5-3D calculations in order to derive an estimate of CDF.

Comparison with the SAPHIRE-based static PRA calculations will be also performed. The final goal will be to demonstrate the capabilities of the EEVE-B toolkit and to show an enhanced quantification of the safety margins of the analyzed NPP.

For FY2017 and beyond we plan [7]:

- to extend such type of analyses to a more detailed PWR model, using Licensee data on PRA and BOP;

- to analyze BWR systems;

- start using the EEVE-A toolkit, depending on V&V status of the main tools.

Finally, all planned future activities should be coupled to relevant industry stakeholder challenges in long-term operation.

6. REFERENCES

1. U.S. NRC, "Recommendations for Enhancing Reactor Safety in the 21st Century – The Near-Term Task Force Review of Insights from the Fukushima Dai-ichi Accident", July 12 2011. US NRC ADAMS accession no. ML111861807.

2. U.S. NRC, "A proposed Risk Management Regulatory Framework", NUREG-2150, April 2012.

3. R. H. Szilard, C. L. Smith, R. Youngblood, "RISMC Advanced Safety Analysis Project Plan. FY 2015- FY 2019", INL/EXT-14-33186, September 2014.

4. R. H. Szilard, et al. "Industry Application – External Hazard Analyses – Problem Statement", INL/EXT-15-36101, July 2015.

5. US NRC, "Generic Issue 199 (GI-199). Implications of Updated Probabilistic Seismic Hazard Estimates in Central and Eastern United States on Existing Plants. Safety/Risk Assessment", August 2010. US NRC ADAMS accession no. ML100270639.

6. US NRC, "Request for Information Pursuant to Title 10 of the Code of Federal Regulations 50.54(f) regarding Recommendations 2.1, 2.3, and 9.3 of the Near-Term Task Force Review of Insights from the Fukushima Dai-ichi Accident", March 2012. US NRC ADAMS accession no. ML12053A340.

7. R. H. Szilard, et al. "RISMC Toolkit and Methodology Research and Development Plan for External hazards Analysis", March 2016, INL/EXT-16-38089.

8. LS-DYNA Software, Version smp s R7.00, Livermore Software Technology Corporation, Livermore, CA, 2013.

9. *OpenSees version 2.5.0* – http://opensees.berkeley.edu/

10. CentroidLab, "NEUTRINO Dynamics" – http://www.centroidlab.com/neutrinodynamics/

11. Idaho National Laboratory, "RELAP5-3D Code Manual Volume I: Code Structure, System Models and Solution Methods", INEEL-EXT-98-00834, Rev. 4, June 2012.

12. C. Rabiti, A. Alfonsi, J. Cogliati et al., "RAVEN User Manual", INL/EXT-15-34123, Revision 4, October 2015.

13. S. Prescott, C. Smith, R. Samptah, "Incorporating dynamic 3D simulation into PRA", INL/CON-14-33680, 2014.

14. "Beaver Valley, Unit 2, Submittal of the Updated Final Safety Analysis Report," Revision 21, US NRC ADAMS accession no.: ML14339A419, December 15, 2014.

15. R. E. Spears and J. L. Coleman, "Nonlinear Time Domain Seismic Soil-Structure Interaction (SSI) Deep Soil Site Methodology Development," INL/EXT-16-38233, Rev. 0, September 2015.

16. F. C. Filippou, E. P. Popov, V. V. Bertero, "Effects of Bond Deterioration on Hysteretic Behavior of Reinforced Concrete Joints". Report EERC 83-19, Earthquake Engineering Research Center, University of California, Berkeley, 1983.

17. L. Lowes, N. Mitra, A. Altoontash, "A Beam-Column Joint Model for Simulating the Earthquake Response of Reinforced Concrete Frames". PEER Report 2003/10, Pacific Earthquake Engineering Research Center, University of California, Berkeley, 2003.

18. R. Sampath, N. Montanari, N. Akinci, "Large-scale solitary wave simulation with implicit incompressible SPH". Journal of Ocean Engineering and Marine Energy. 2016, 10.1007/s40722-016-0060-8.

19. Virginia Electric and Power Company (Dominion), "Surry Power Station Units 1 and 2. Updated Final Safety Analysis Report. Revision 39". US NRC ADAMS accession no. ML072980795, September 2007.

20. P. D. Bayless "Natural Circulation during a Severe Accident: Surry Station Blackout", EGG-SSRE-7858, September 1987

21. A. Prosek, L. Cizelj, "Long-Term Station Blackout Accident Analyses of a PWR with RELAP5/MOD3.3", Science and Technology of Nuclear Installations, Volume 2013, Article ID 851987, April 2013

22. A. Matev "Analysis of Operator Response to Station Blackout", International RELAP5-3D User Group Meeting (IRUG), 2006.

23. Modular Accident Analysis Program 5 (MAAP5) Applications Guidance: Desktop Reference for Using MAAP5 Software - Phase 2 Report. EPRI, Palo Alto, CA: 2015. 3002005285.

24. C. Allison and J. Hohorst, "Role of RELAP/SCDAPSIM in Nuclear Safety", Science and technology of Nuclear Installations, Volume 2010 (2010), Article ID 425658.

25. U.S. NRC, "State-of-the-Art Reactor Consequence Analyses Project. Volume 2: Surry Integrated Analysis", NUREG/CR-7110, Vol. 2, Rev. 1. August 2013.

26. R. Gauntt, et al., 2005, MELCOR-H2 Computer Code Manuals, Vol. 2: Reference Manuals, Version 1.8.6, Prepared by Sandia National Laboratories for the U.S. Nuclear Regulatory Commission, Office of Nuclear Regulatory Research, NUREG/CR-6119, Vol. 2, Rev. 3, SAND 2005-5713, September 2005.

27. IAEA, "Best Estimate Safety Analysis for Nuclear Power Plants: Uncertainty Evaluation", Safety Reports Series No. 52, Vienna, 2008.

28. S. S. Wilks, "Determination of Sample Sizes for Setting Tolerance Limits," The Annals of Mathematical Statistics, Vol. 12, no. 1, pp. 91-96, 1941.

APPENDIX A

Piping System Leakage Locations

After the completion of the sample runs, the piping system is analyzed for the first 5 time histories provided by INL, both in the X and Y direction. The PGA's are normalized to levels of – 0.3 g, 0.6 g, 0.9 g, 1.2 g and 1.5 g, implying a total of 50 runs, 25 each in X and Y directions.

For the first time history in the X direction, the first damage is observed at a PGA of 0.297 g. The locations of damage are increasing in number with the increasing values of PGA. All the damages are for 1 inch pipes.

For the time history runs in the Y direction, two locations of damage are identified for a PGA level up to 1.5 g. The damages are for 2 inch pipes.

Leakage Locations on Piping System for the First Time History in X Direction

Figure 97 to Figure 101 indicate the location of damage for the increasing values of PGA, for the first time history in the X direction. All the damages are for 1 inch pipes. Figures are in X-Y plane.
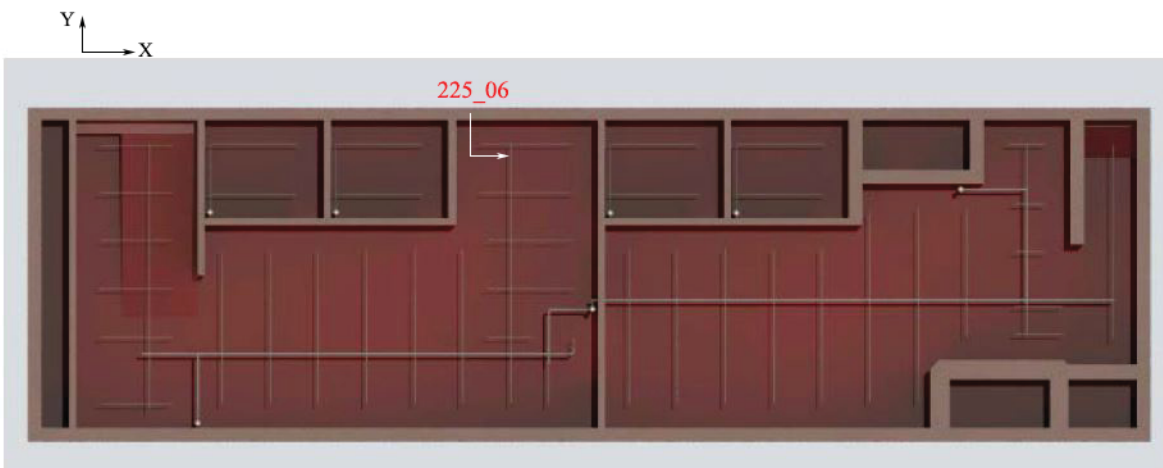
Figure 97 – Leakage Locations for the First Time History in X Direction– 0.297 g.

81
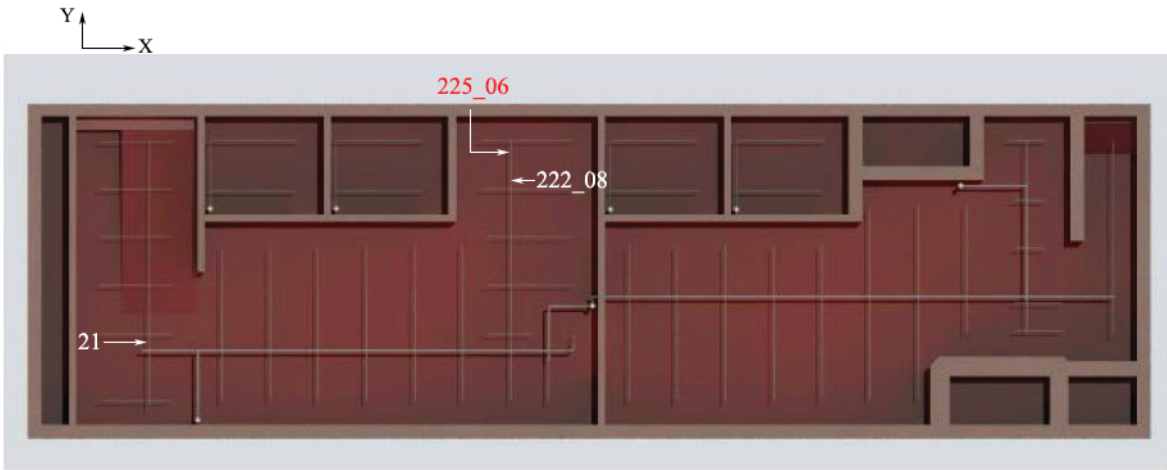
Figure 98 – Leakage Locations for the First Time History in X Direction– PGA normalized to 0.6 g.
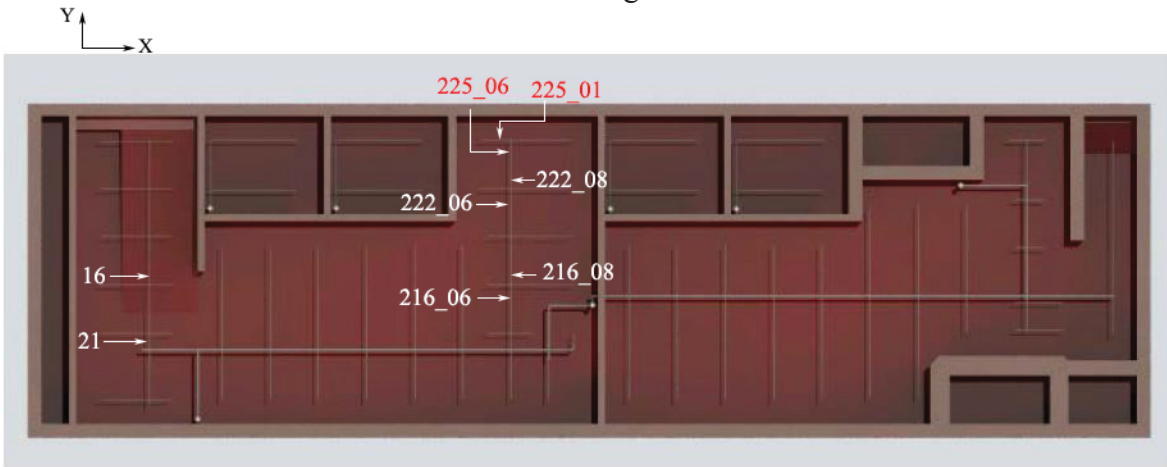
Figure 99 – Leakage Locations for the First Time History in X Direction– PGA normalized to 0.9 g.
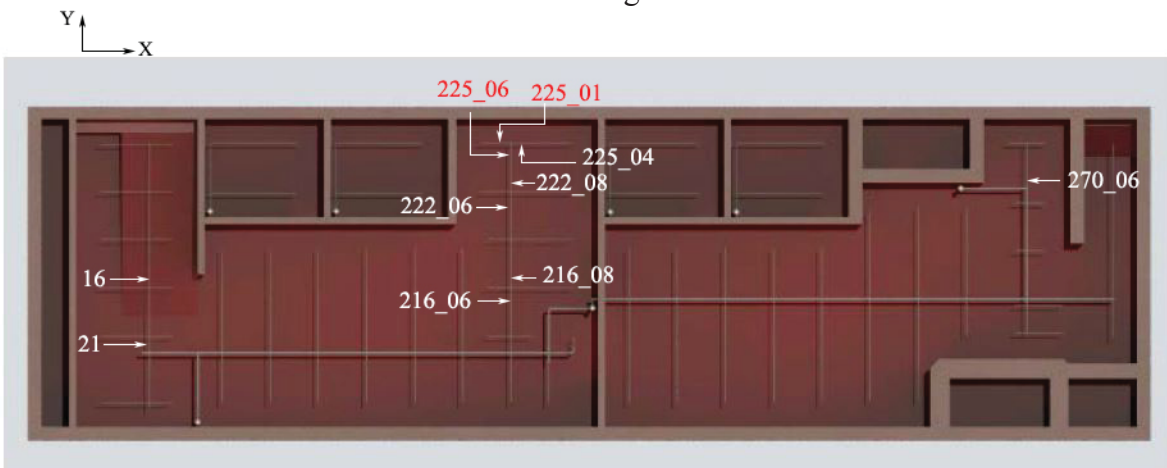

Figure 100 – Leakage Locations for the First Time History in X Direction– PGA normalized to 1.2 g.
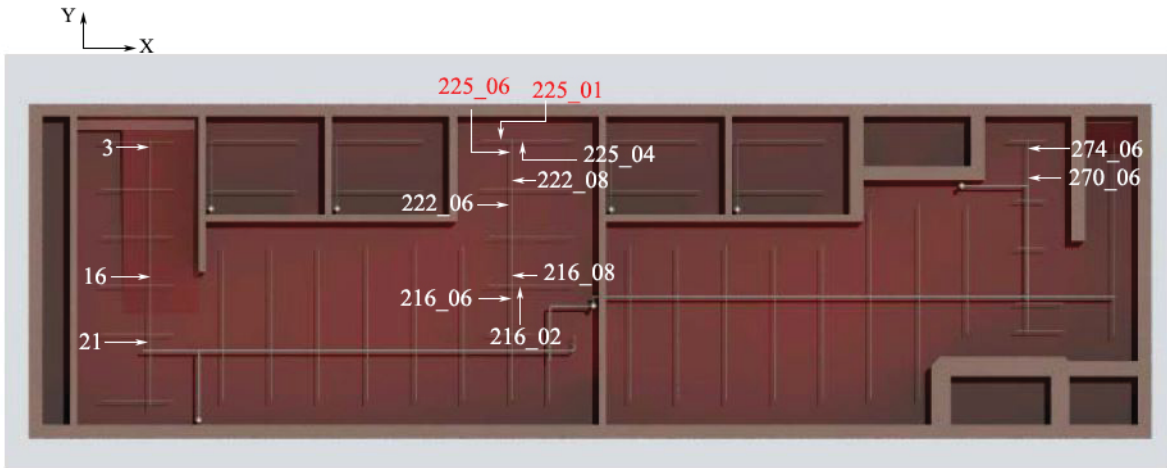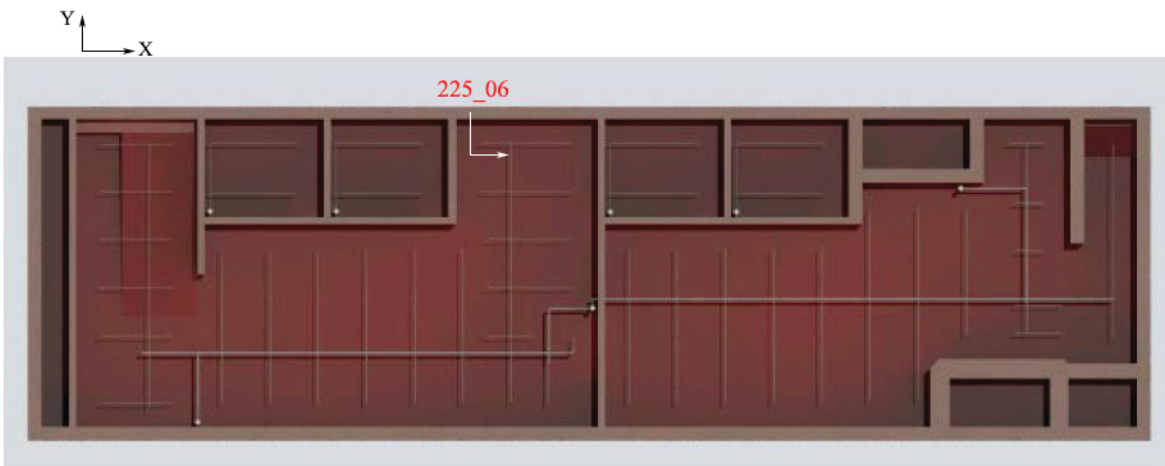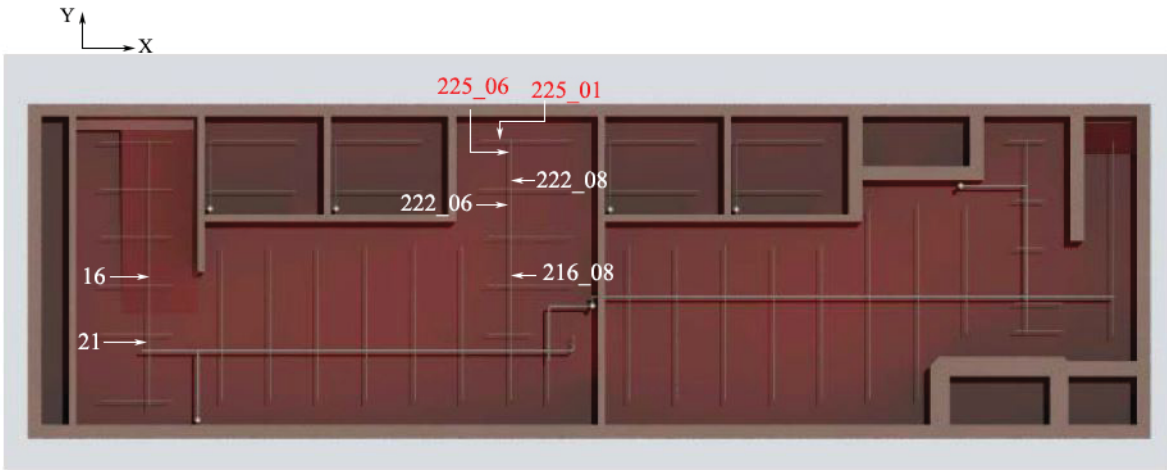
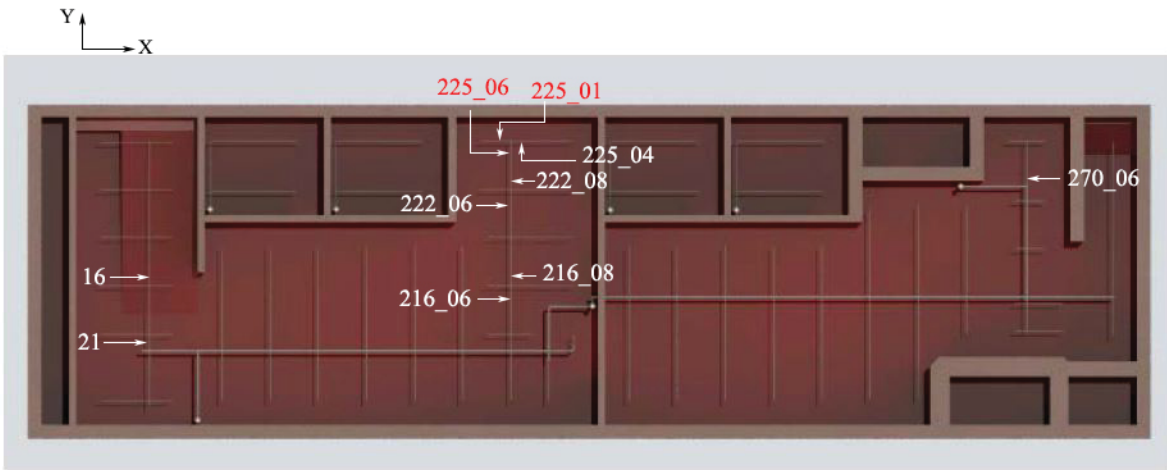Figure 101 – Leakage Locations for the First Time History in X Direction – PGA normalized to 1.5 g.

Leakage Locations on Piping System for the Second Time History in X Direction

Figure 102 to Figure 105 indicate the location of damage for the increasing values of PGA, for the second time history in the X direction. All the damages are for 1 inch pipes. Figures are in X-Y plane.

Figure 102 – Leakage Locations for the Second Time History in X Direction – PGA normalized to 0.6 g.

Figure 103 – Leakage Locations for the Second Time History in X Direction– PGA normalized to 0.9 g.

Figure 104 – Leakage Locations for the Second Time History in X Direction– PGA normalized to 1.2 g.
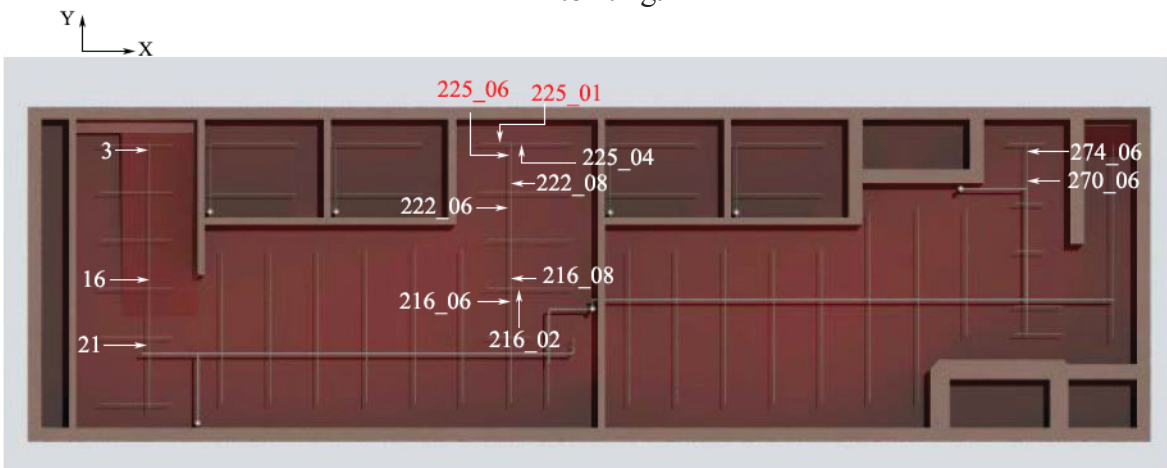

Figure 105 – Leakage Locations for the Second Time History in X Direction– PGA normalized to 1.5 g.

Leakage Locations on Piping System for the Third Time History in X Direction

Figure 106 to Figure 109 indicate the location of damage for the increasing values of PGA, for the third time history in the X direction. All the damages are for 1 inch pipes. Figures are in X-Y plane.

Figure 106 – Leakage Locations for the Third Time History in X Direction– PGA normalized to 0.6 g.
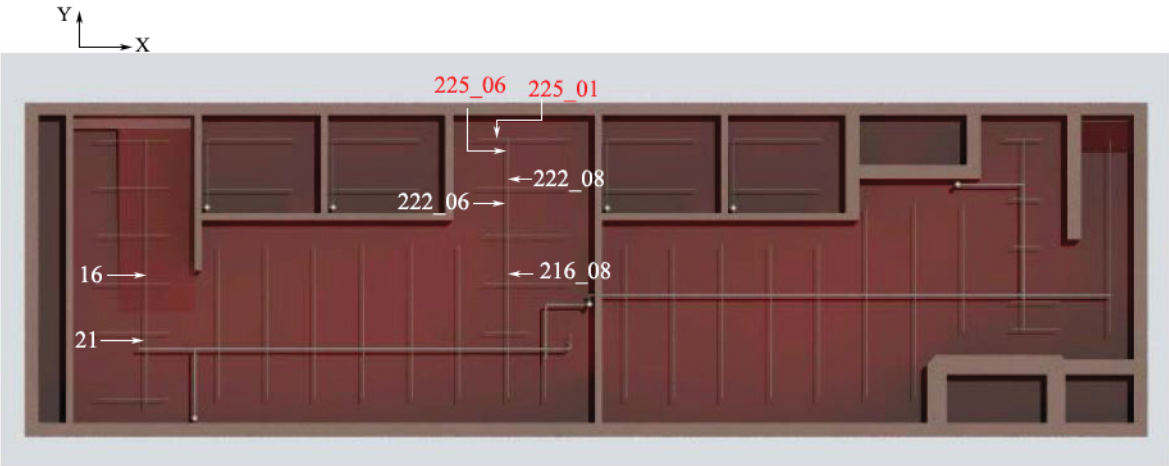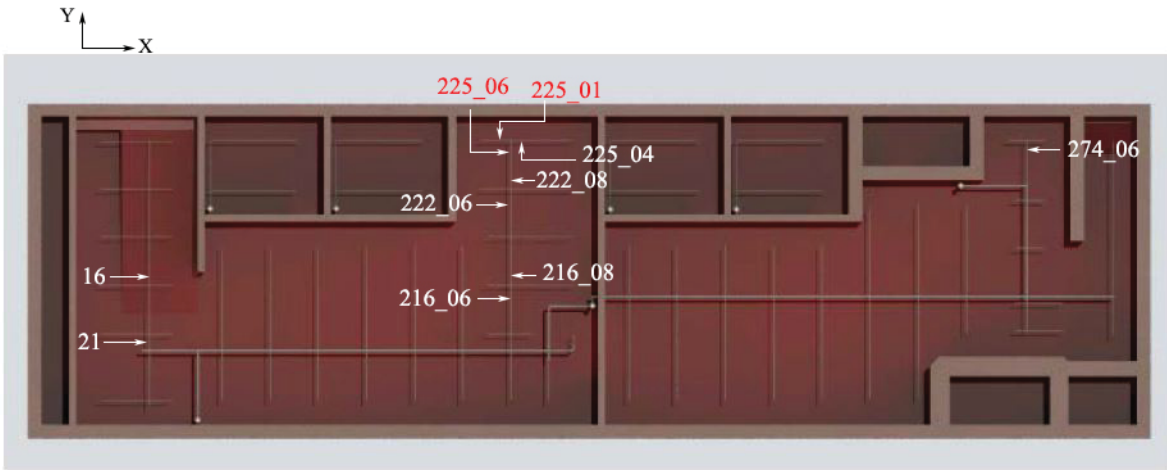

Figure 107 – Leakage Locations for the Third Time History in X Direction– PGA normalized to 0.9 g.

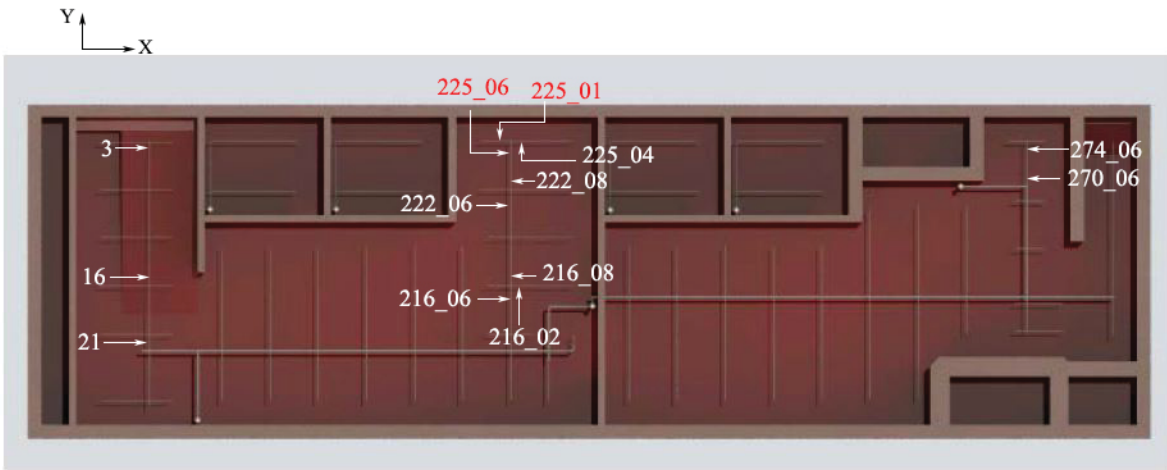Figure 108 – Leakage Locations for the Third Time History in X Direction– PGA normalized to 1.2 g.

Figure 109 – Leakage Locations for the Third Time History in X Direction– PGA normalized to 1.5 g.

Leakage Locations on Piping System for the Fourth Time History in X Direction

Figure 110 to Figure 113 indicate the location of damage for the increasing values of PGA, for the fourth time history in the X direction. All the damages are for 1 inch pipes. Figures are in X-Y plane.
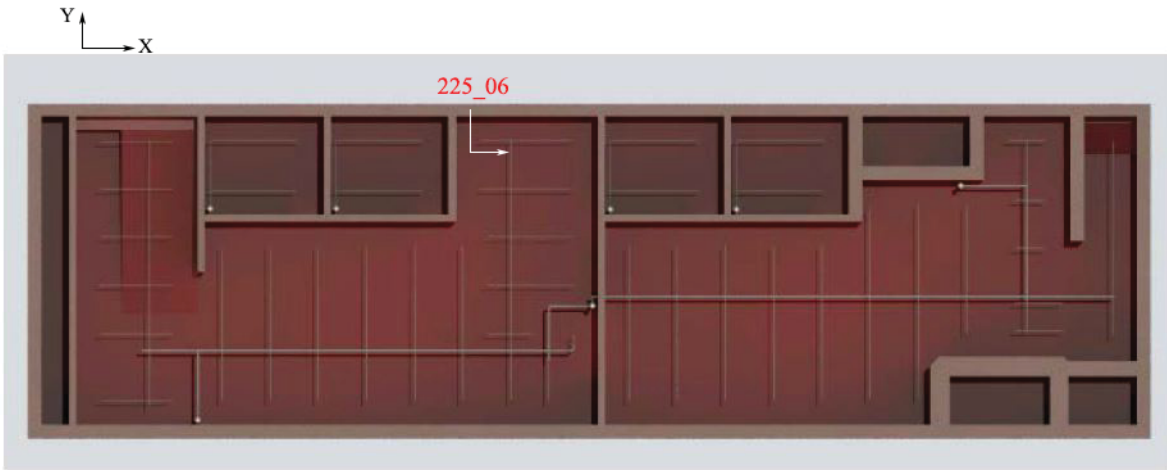
Figure 110 – Leakage Locations for the Fourth Time History in X Direction– PGA normalized to 0.6 g.
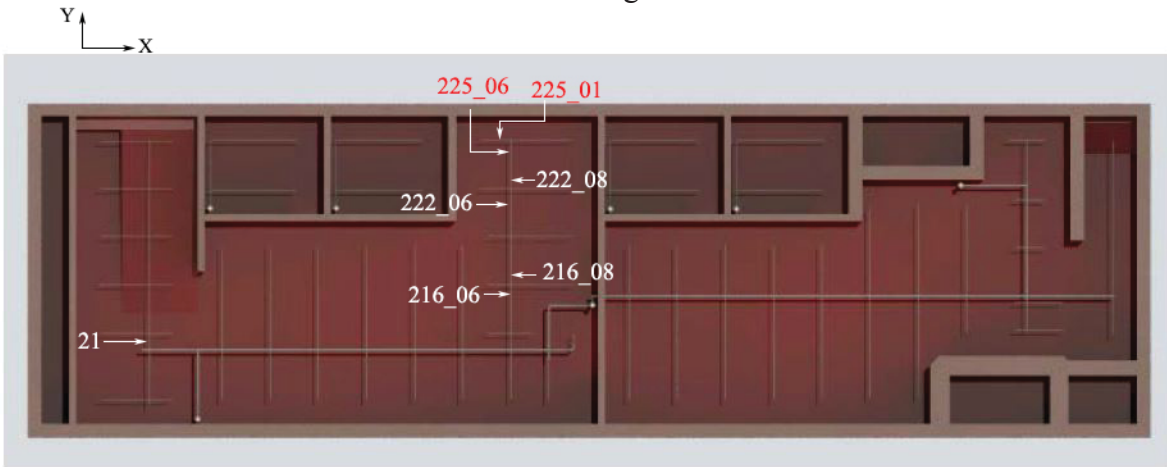

Figure 111 – Leakage Locations for the Fourth Time History in X Direction– PGA normalized to 0.9 g.
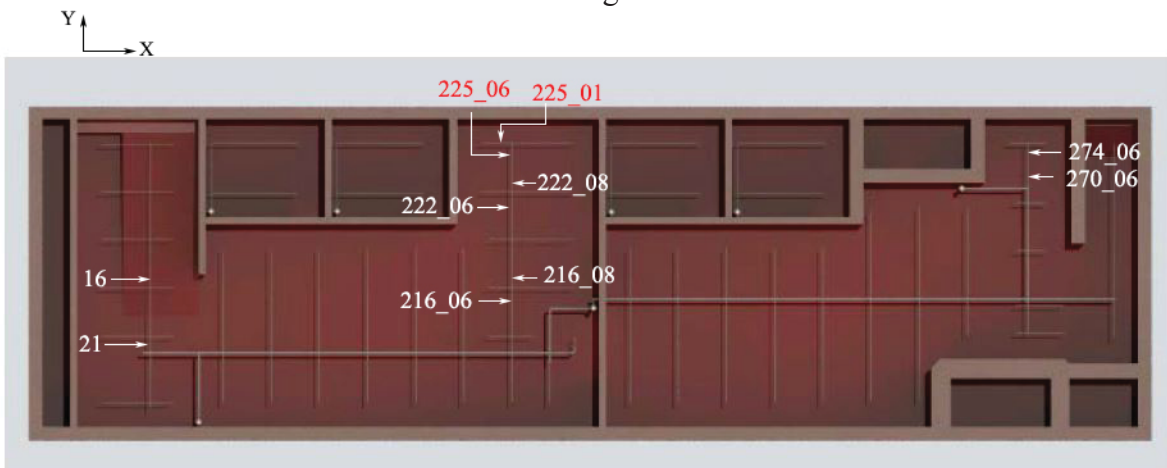

Figure 112 – Leakage Locations for the Fourth Time History in X Direction– PGA normalized to 1.2 g.
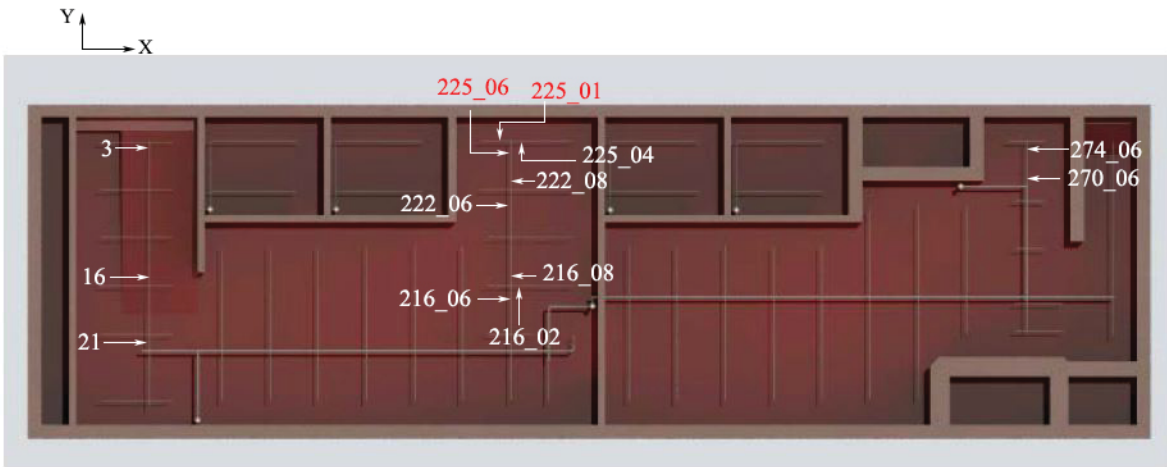
Figure 113 – Leakage Locations for the Fourth Time History in X Direction– PGA normalized to 1.5 g.

Leakage Locations on Piping System for the Fifth Time History in X Direction

Figure 114 to Figure 117 indicate the location of damage for the increasing values of PGA, for the fifth time history in the X direction. All the damages are for 1 inch pipes. Figures are in X-Y plane.

Figure 114 – Leakage Locations for the Fifth Time History in X Direction– PGA normalized to 0.6 g.
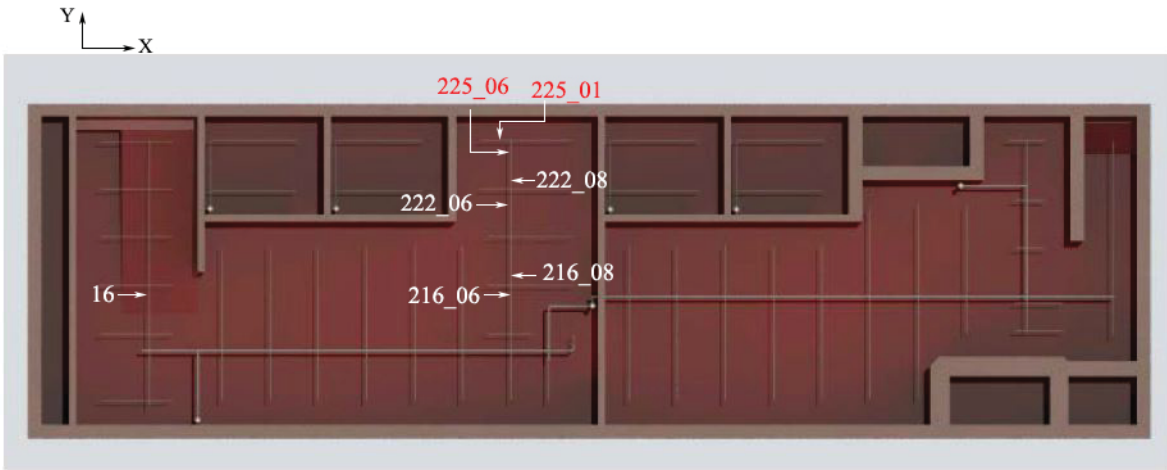
Figure 115 – Leakage Locations for the Fifth Time History in X Direction– PGA normalized to 0.9 g.
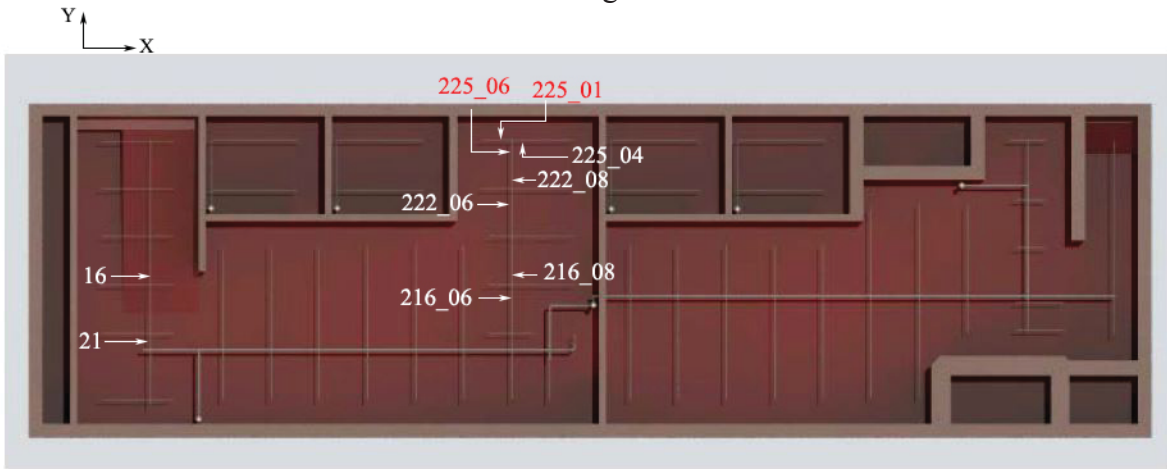

Figure 116 – Leakage Locations for the Fifth Time History in X Direction– PGA normalized to 1.2 g.
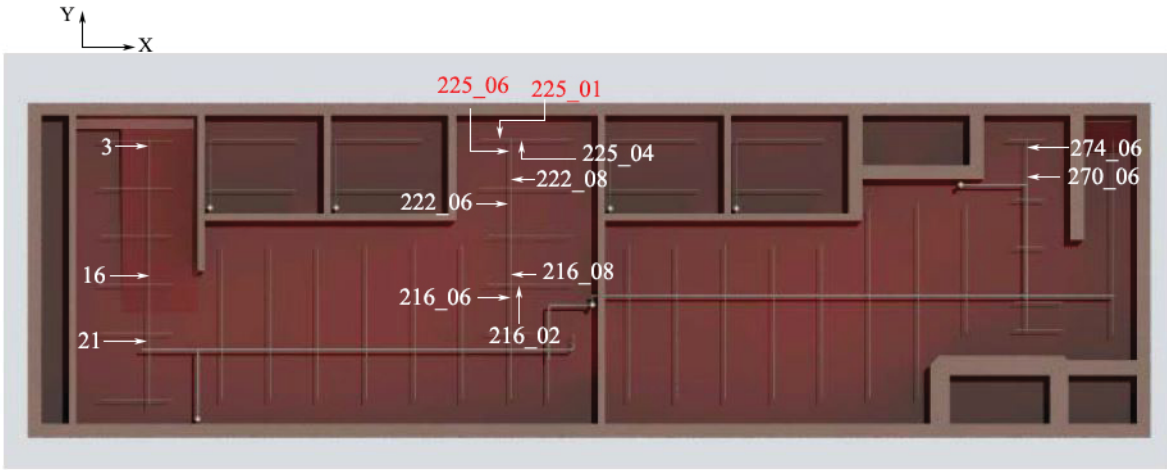

Figure 117 – Leakage Locations for the Fifth Time History in X Direction– PGA normalized to 1.5 g.

Leakage Locations on Piping System for the First Time History in Y Direction

Figure 118 to Figure 120 indicate the location of damage for the increasing values of PGA, for the first time history in the Y direction. All the damages are for 2 inch pipes. Figures are in X-Y plane.

Figure 118 – Leakage Locations for the First Time History in Y Direction– PGA normalized to 0.9 g.

Figure 119 – Leakage Locations for the First Time History in Y Direction– PGA normalized to 1.2 g.

Figure 120 – Leakage Locations for the First Time History in Y Direction– PGA normalized to 1.5 g.

Leakage Locations on Piping System for the Second Time History in Y Direction

Figure 121 to Figure 123 indicate the location of damage for the increasing values of PGA, for the second time history in the Y direction. All the damages are for 2 inch pipes. Figures are in X-Y plane.

Figure 121 – Leakage Locations for the Second Time History in Y Direction– PGA normalized to 0.9 g.

Figure 122 – Leakage Locations for the Second Time History in Y Direction– PGA normalized to 1.2 g.

Figure 123 – Leakage Locations for the Second Time History in Y Direction– PGA normalized to 1.5 g.

It is observed that for time histories 3-5, the location of damages do not change – i.e. they are the same as for the first 2 time histories.